EFFECTIVE DELAYED NEUTRON FRACTION IN SUBCRITICAL STATES

MASAO YAMANAKA

CONTENTS

CHAPTER 1

INTRODUCTION

1.1 Background

The atomic energy utilization was opened mainly for electric generation by operating nuclear power plants under the promise for peaceful purposes by the address of "Atom for peace" by U. S. President Eisenhower in 1953. The International Atomic Energy Agency (IAEA) established in 1957 and member states have fulfilled the commitment by mutual cooperation, including the inspection and the report on the operating progress of the facility. IAEA reports that the number of the operational reactors has saturated around 440 since 1995, while the net electrical power increases from about 246 GW in 1985 to about 383 GW in 2015[1], as shown in Fig. 1-1. The electricity increase has been attained by increase of operation rate of existing power plants. The reason of the electricity increase by the nuclear reactor is considered to ensure the energy security and to suppress the emission of the carbon dioxide (CO_2) for the climate change by taking an advantage of nuclear reactor over much less production CO_2 compared with other major energy, including the petroleum, coal and natural gas. Also, the number of operational reactors is predicted increased especially in Asia and (Central and Eastern) Europe[2]. As increasing the amount of the electric generation by nuclear reactors, a side effect on producing high-level radioactive waste has become into the social problem.

The high-level radioactive waste is accumulated in the spent fuel of power reactors, and should be separated from the human living area, and, for example, should be stored into

geological repository after containment into the canister. The simple storage strategy (Once-through Fuel Cycle: OFC) is the direct disposal of the canister. More than 0.1 million years is required until the radioactive toxicity included in the waste becomes less than that of the same amount of natural uranium for the production of the same number in the original fuel assemblies[3].

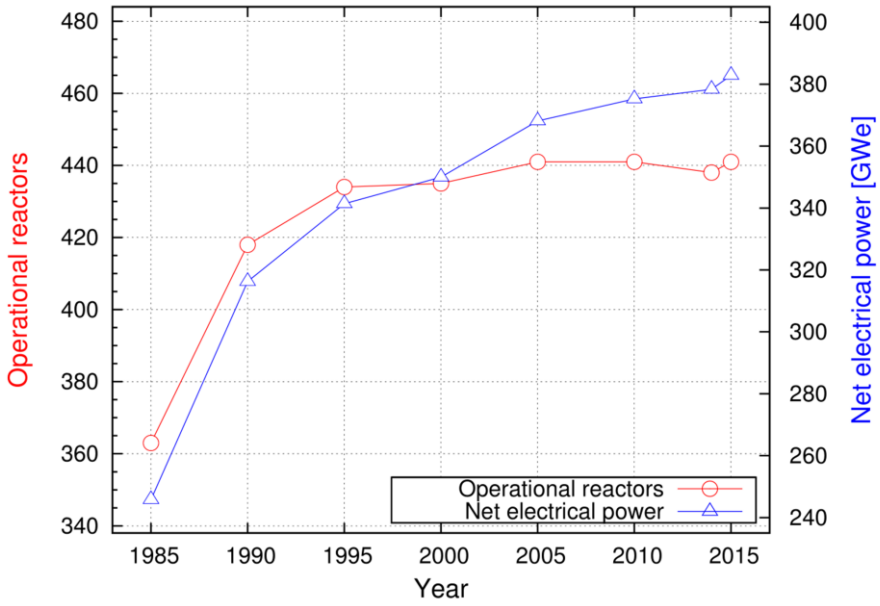

Fig. 1-1 Number of operational reactors and net electrical power in the world[1].

To reduce the volume of the geological repository, the reprocessing of the spent fuel, including group separation, is proposed[4], and spent fuel was separated into individual nuclide, including plutonium (Pu), uranium, minor-actinide (including neptunium (Np), americium (AM) and curium (Cm)) and long-life fission products (LLFP) in terms of their half-life. After the reprocessing, uranium and Pu can be used as the nuclear fuel again. For the utilization of Pu in light water reactor (LWR), the mixed oxide (MOX) fuel has been fabricated by mixing Pu oxide collected from the reprocessing into uranium oxide. The remained nuclides separated by reprocessing are disposed after treatment into a solid state

such as vitrified waste having characteristics of long-life resistance against the damage and the heat by the radiation from the radioactive material[5]. After the reprocessing of the spent fuel incinerated with LWR, the radiotoxicity is dominated by the nuclides of Np and Am over 0.1 million years, as shown in Fig. 1-2. Here, even if the treatment is made by making vitrified waste, the validity of the prudent containment cannot be provided because such a long time promising geological repository for 0.1 million years is not proven. Thus, the problems on the storage of the high-level radioactive waste have been lying on the subject of the nuclear power utilization.

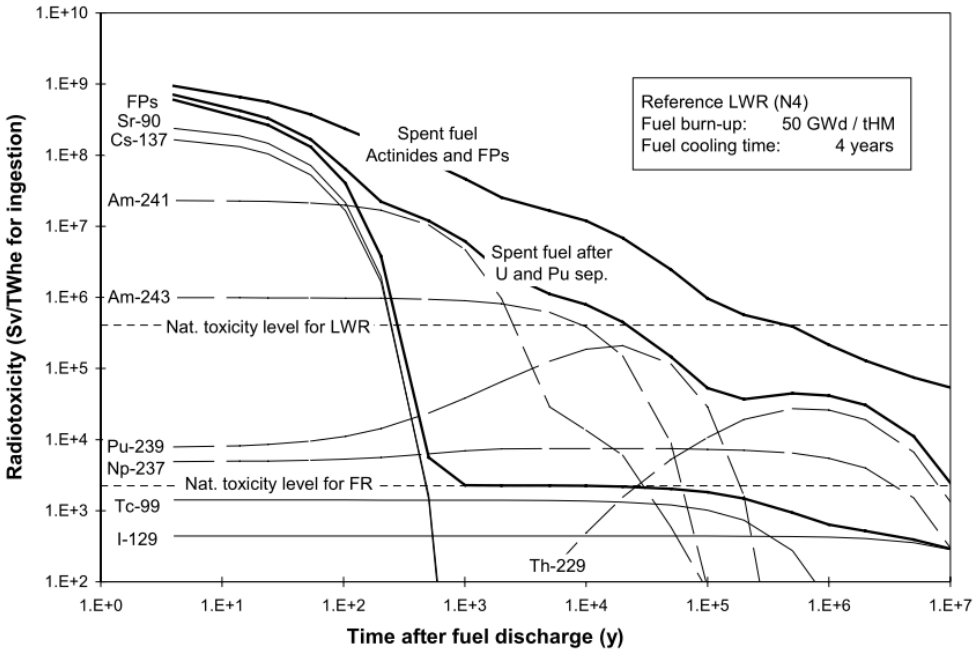

Fig 1-2 Time evolution of radiotoxicity by the nuclides in the spent fuels after incineration with LWR[6].

Further volume reduction of the geological repository can be made with the use of Pu and MA produced in the LWR operations, several transmutation strategies (Pu Burning or TRU Burning in FR strategies) had been proposed with the use of fast reactor (FR) by

reprocessing the spent fuel for the fuel including Pu and MA to attach subsequent stage. Here, the transmutation is attained by the neutron injection into the target nuclide to vary the nuclide for detoxifying the radiotoxicity. The ideal strategy (FR strategy) is considered to establish the closed fuel cycle only FR without LWR to maximize the possibility to achieve the transmutation and to efficiently utilize the natural uranium resources while producing much less amount of MA compared with other strategies. However, the technical issues, including the MOX fuel and PUREX reprocessing technology[5] are still remained on the establishment of the closed fuel cycle for the employment FR strategy[6].

As a solution for the problem in conventional nuclear transmutation using FRs, the accelerator-driven system (ADS) was proposed to operate the reactor in static state by the combination of a subcritical core and the external neutrons generated from an accelerator. ADS has several advantages for nuclear transmutation compared with FR and detail description of ADS is mentioned in the next section. The strategy (Double strata strategy), which ADS is attached for the transmutation and Pu burner after usage of uranium fuel in the commercial LWRs, has been proceeded by Japan[7], Europe[8] and USA[9] for the achievement of the efficient transmutation and the utilization of the Pu resources. ADS has advantages where the safety margin till prompt critical state is large because of operating the reactor in the subcritical state. Also, ADS can transmute MA efficiently by loading a large amount of MA. However, since the accuracy of nuclear data of MA is considered to be low compared with other fissile nuclides such as uranium and Pu, the subcriticality evaluation is not accurate enough in the design and the operating stages of ADS, and the designed subcriticality, namely the margin to criticality, should be confirmed by the accurate subcriticality measurement.

1.2 Accelerator-Driven System

The technique was proposed to decrease the radiotoxicity of the radioactive waste in spent fuels and to shorten the isolation time from living sphere by injecting neutrons into radioactive isotopes in the high-level radioactive waste to induce its amount after group separation of the spent fuel for partitioning, which is called transmutation (P&T). This method has been considered effective to process the high-radioactive waste effectively. Recent years, the research is conducted to promote effective transmutation with the use of ADS, and the storage period becomes about 100 years until the radiotoxicity decays the same level as natural uranium by loading the isotope having larger atomic number than uranium in the waste as the nuclear fuel containing MA[10]. The fission reactions of MA are intended with high-energy neutrons, and then, the efficient transmutation is expected by loading them to FR. In the case of the use of FR which contain Pu and MA in high-concentration without uranium for transmutation, however, another problem arises by low values of delayed neutron fraction of MA and Pu compared with that in uranium-based fuel. The delayed neutron fraction which contributes to the neutron multiplication becomes half value of about 0.2% compared to that in the typical FR of about 0.4%. Thus, when the positive reactivity induced to the reactor accidentally, the safe margin upto prompt critical state is low compared with typical FR loaded with MOX fuel without MA. Further, the positive reactivity by void coefficient of coolant becomes larger when the MA is largely loaded in the reactor[11].

The new type reactor concept of ADS offers the advantages to be specialized as the MA and Pu burner, minimizing the number of the facility for the transmutation of MAs and LLFPs. ADS can load a large amount of MA for the transmutation compared with FR because the margin for the reactivity insertion is taken by setting appropriate subcriticality

through ADS operation. Also, the subcritical reactor is able to stop its operation by the shutdown of the accelerator operation in principle. At the Kyoto University Critical Assembly, the fundamental study on ADS has been conducted in static and kinetic experiments with the use of different external neutron sources: americium-beryllium neutron sources, 14 MeV neutrons by D-T reactions and neutrons having wide energy range through proton reactions bombarded by a tungsten target. Also, for acquisition of the operation experience of combination with the subcritical core and the external neutrons with the accelerator, the Multiplication avec Source Externe experiments (MUSE experiments) was launched a series of experiments since 1995 at the MASURCA facility of CEA in Cadarache[12, 13]. The purpose of these experiments has to separate the effects of the source and of multiplication in the subcritical core. In the MUSE-4 experiments, the neutron source study was conducted by surrounding a 14 MeV neutron source (called GENEPI) in lead or lead-bismuth targets, investigating the validity of the neutron transport calculation. Also, the measurements were conducted in the static experiments for the reaction rate distribution, the spectrum index, and neutron source index, and in the kinetic experiments for neutron behavior in time after the injection of the pulsed neutron source. Further, the subcriticality measurements were conducted not only by the control rod calibration experiments, but also by the neutron source multiplication method. Additionally, in the preliminary analysis for the reactivity insertion and the loss-of coolant-flow accidents of ADS, the choice of the subcriticality level was indicated to influence the reactor power behaver after the reactivity insertion into the subcritical core[14, 15].

Here, measured subcriticality, in general, is obtained in dollar units against calculated one in $\Delta k/k$ units, and the effective delayed neutron fraction is required to convert the measured subcriticality into calculated one to ensure the validity of the subcriticality evaluations. In these MUSE experiments, the analyses were conducted for the kinetic

experiments and the subcriticality measurements, however, the variation of the kinetic parameters and the effective delayed neutron fraction as the conversion constant were not discussed on the subcriticality. Also, the future subject was extracted to improve the accuracy of the experimental analysis, especially in the kinetic experiments, including the choice of the nuclear data and the calculation methodology.

From an economic perspective, since the accelerator consumes the electricity for the ADS operation to control the power of ADS, the level of the subcriticality is preferred to be set close to the critical state to minimize the necessity of the source neutrons. Conversely, when the priority was placed on the safety margin against the accident by setting the deep subcriticality in ADS, the behavior of the reactivity insertion accident becomes mild, however, the power of the accelerator should be increased to maintain the high output power of the reactor core, namely high transmutation efficiency of MA. Thus, to continue the operation of ADS by reconciling economic and safe stand points, accuracy of the preliminary analysis should be improved in the design stage of ADS. Further, the subcriticality should be measured in good accuracy in the reactor physics test in operation stage for the assessment of the safe margin of ADS.

1.3 Subcriticality Estimation

The eigenvalue calculations play a main role in the nuclear design calculations even in subcritical system for the determination of the criticality criteria with neutron flux distribution in the fundamental mode. In general, the calculations with nuclear data involve the calculation bias originated in the uncertainty of the nuclear data. Here, the uncertainty of calculated k_{eff} value is considered significant for the shallow subcritical system to prevent the criticality accidents (further reactivity insertion accident by prompt critical) in design or prediction calculations. In the preliminary analysis of the ADS designed by the Japan Atomic Energy Agency (JAEA), the uncertainty was estimated for the criticality, the void reactivity and Doppler reactivity of about 1.7%, 9.2% and 7% respectively[16].

To examine the impact to be involved by the uncertainty, sensitivity and uncertainty analyses are generally performed, and identify the impact caused by each isotope, kinds of its nuclear reactions and neutron energy of the reactions. Further, the uncertainty in subcriticality can be reduced by the bias factor method with the use of experimental results (benchmark) under a condition: precisely approximated neutron characteristics between the reference (critical) and target (subcritical) cores. To take into account plural critical experiments, the cross-section adjustment methods were proposed by Dragt et al.[17] and Takeda et al.[18] for the reduction of the uncertainty. In these methods, neutronic characteristics parameters such as the neutron flux are made consistent with the experimental results including the experimental error through the sensitivity analysis for the nuclear data. However, the cross-section adjustment is not performed by taking into account the neutronics of the target core. Sano et al. and Kugo et al. proposed the generalized bias factor method[19] and the extended bias factor method[20], respectively, to adjust the cross sections taking into account plural critical experiments for the uncertainty reduction of one

designed parameter. The applicability of the generalized bias factor method was confirmed through the demonstration of uncertainty reduction for erbia-bearing fuel with the cross-section adjustment method[21]. Also, the effectiveness of the extended bias factor method was demonstrated by the improvement of prediction accuracy with the use of FCA-XXII-1 critical experiments[22]. Further, Yokoyama et al. developed the extended cross-section adjustment method focusing on target core parameters including criticality, power distribution, central control rod worth, sodium void reactivity, doppler reactivity coefficient and burnup reactivity coefficient, and verified the applicability with the improvement of their prediction accuracy[23]. Here, an emphasis should be placed where the bias factor and the cross-section adjustment methods had been successfully applied to the target core in the critical state with benchmark experiments conducted in the critical state. Thus, beside the reduction of the uncertainty in designed subcriticality, the verification of the prediction accuracy should be requisite by subcriticality measurements of the target core.

In the operation stage of the reactor such as the reactor physics test, in the case of the system which is possible to attain critical state, the subcriticality is able to be obtained by dropping an absorber such as the control rod into the critical system. This method, called as the integral counting method in the control rod drop method, is carried out by measuring the count rate n_0 before dropping the control rod and counting the neutron signals, after the drop until the count rate could be regarded as considerably decreased, as follows:

$$\rho_{\$} = \frac{\rho}{\beta_{\mathrm{eff}}} = \frac{n_0 \sum_i \frac{\beta_{\mathrm{i,eff}}}{\lambda_i}}{\beta_{\mathrm{eff}} \int_0^{\infty} n(t)\, dt} \quad , \tag{1-1}$$

where $\rho_{\$}$ is the subcriticality in dollar units, ρ the subcriticality calculated by $(1-k_{\mathrm{eff}})/k_{\mathrm{eff}}$, β_{eff} the effective delayed neutron fraction, $\beta_{\mathrm{i,eff}}$ i-th group effective delayed neutron fraction, λ_{i} the decay constant of i-th group effective delayed neutron fraction, $\int_0^\infty n(t)\,dt$ the infinite count after dropping the control rod. To estimate the subcriticality by this method, the kinetic parameters related to effective delayed neutron fraction are requisite to be prepared beforehand. The kinetic parameters can be easily obtained by the eigenvalue (critical) calculations.

In the case of subcritical system which is impossible to attain critical states, the subcriticality can be deduced with the use of an external neutron source. Sjostrand proposed the area ratio method[24] with the use of pulsed neutron source in the pulsed neutron source method (PNS method) to measure the subcriticality in dollar units by counting the neutron signals related to prompt and delayed neutrons separately, as follows:

$$\rho_{\$} = \frac{\int_0^T X_{\mathrm{p}}(t)\,dt}{\int_0^T X_{\mathrm{d}}(t)\,dt} \quad , \tag{1-2}$$

where X_{p} and X_{d} are the areas of the decay curves by prompt and delayed neutrons in PNS histogram, respectively, and T is the pulsed repetition period. By the external neutron source, the excitation of the higher-mode components is predicted in the neutron flux, affecting the subcriticality measurements because the neutron flux in the fundamental mode is assumed in the derivation of the area ratio method. To decrease the effect of higher-mode components, Gozani proposed the extrapolation area ratio method[25], as follows:

$$\rho_{\$} = e^{\alpha t_{\mathrm{w}}} \frac{\int_{t_{\mathrm{w}}}^T X_{\mathrm{p}}(t)\,dt}{\int_0^T X_{\mathrm{d}}(t)\,dt} \quad , \tag{1-3}$$

where α is the prompt neutron decay constant and t_w the waiting time of decreasing higher-mode components. In the subcritical estimation by the measurements, subcriticality is obtained in dollar units, and should be converted into $\Delta k/k$ units to compare the calculated and measured subcriticalities. For the conversion of the subcriticality, the accurate estimation of β_{eff} is required in the calculation or the measurement.

1.4 Effective Delayed Neutron Fraction

The total neutrons, emitted from the fission reactions, can be classified into two neutrons: prompt neutrons immediately emitted from fission fragments after the fission reaction and delayed neutrons emitted from the specified fission products (after a several interval from the fission reaction) called as delayed neutron precursor. Further, the delayed neutrons were divided into 6 groups, proposed by Keepin[26], depending on the half time to be emitted from the delayed neutron precursor. The both neutrons induce next fission, resulting in the neutron multiplication in the reactor. However, the attributable fraction to the multiplication is varied by the energy spectrum of the prompt and the delayed neutrons. On the basis of the contribution of delayed neutrons attributed to the soft energy spectrum compared with energy spectrum of prompt neutrons, the delayed neutron fraction is defined as effective delayed neutron fraction β_{eff} when specifying the actual fraction of delayed neutron in the neutron multiplication. In this section, the present status is described on the calculation and the measurement methodologies; the research issues are discussed on the estimation of β_{eff} in the existence of the external neutron source in the subcritical system.

1.4.1 Estimation Methodology

The calculation methodology of β_{eff} was firstly defined by Keepin with the use of the forward and adjoint fluxes ϕ and ϕ^{+}, respectively, as follows:

$$\beta_{\text{eff}} = \frac{\int d\mathbf{r} \int \phi^{+}(\mathbf{r},E)\,\chi_{\text{d}}(\mathbf{r},E)dE \int \nu_{\text{d}}(\mathbf{r})\,\Sigma_{\text{f}}(\mathbf{r},E')\,\phi(\mathbf{r},E')\,dE}{\int d\mathbf{r} \int \phi^{+}(\mathbf{r},E)\,\chi(\mathbf{r},E)dE \int \nu(\mathbf{r})\,\Sigma_{\text{f}}(\mathbf{r},E')\,\phi(\mathbf{r},E')\,dE} \quad , \tag{1-4}$$

where χ and χ_d are the neutron energy spectra of total and delayed neutrons, respectively, ν and ν_d the neutron yield of total and delayed neutrons, respectively, E and E' the neutron energy, Σ_f the macroscopic fission cross section, and **r** the spatial position. In general, β_{eff} has been evaluated by performing the forward and the adjoint calculations in eigenvalue calculations by the deterministic methodology, and widely used in the reactor core analysis. However, the estimation by the deterministic methodology involves the approximations in the procedure of the calculation: homogenization of the core regions and discretization of the neutron energy and the phase space. To decrease the negative impact by the approximation, β_{eff} by the stochastic methodology had been evaluated approximately by the k-ratio method[27] with the ratio of the effective multiplication factor k_{eff} and the prompt multiplication factor k_p because the adjoint flux was not able to be obtained by the stochastic methodology. In the k-ratio method, assuming that the difference can be negligible between the neutron fluxes considering total neutrons and only prompt neutrons, estimation accuracy in the comparison with β_{eff} calculated with Eq. (1-4) can be verified by the deterministic methodology. By the improvement in the stochastic methodology, on the basis of the concept of the iterated probability proposed by Hurwitz[28], the weighting function corresponding to the adjoint flux has been obtained with the calculation of the next fission probability[30] proposed by Meulekamp et al. or the iterated fission probability[25] proposed by Nauchi et al., instead of solving the adjoint transport equation in stochastic methodology. Further, Chiba et al. analytically proved the relationship between the next fission probability and the iterated fission probability, concluding that the iterated fission probability is appropriate for the use to estimate the adjoint flux[31]. Thus, β_{eff} is able to be evaluated by the Monte Carlo method without the approximations in the homogenization and discretization of energy and phase space.

As for the evaluation of β_{eff} by measurements, the experiments have been carried out to validate the differential cross sections related to the delayed neutrons. The measurement of β_{eff} was firstly conducted with the use of the relationship between calculated reactivity in $\Delta k/k$ units and measured reactivity in dollar units. On the basis of this measurement concept, Perez-Belles et al. evaluated β_{eff} for the Bulk Shielding Reactor-I with the acquisition of the reactivity by replacing the fuel plates to the poisoned ones[32]. The measurement was conducted in the critical states by moving the control rod to attain criticality with the load of both fuel plates and was deduced by the combination of the calculated and the measured reactivity. Also, Carpenter et al.[33] developed ^{252}Cf method to obtain β_{eff} for fast critical assemblies with the use of the measured absolute fission rate, reactivity worth of ^{252}Cf neutron source obtained by changing the location of the neutron source adjusting the control rod to keep the same power during the substitutions and a correction factor by the ratio with the importance of ^{252}Cf and that of fuel plates. With the use of the Feynman-α method[34], McCulloch proposed the measurement methodology of β_{eff} called as the covariance-to-mean method[35]. In this method, however, the detector efficiency, which is difficult to measure or calculate, is requisite to measure β_{eff}. Bennett developed the methodology by the cross-correlation noise technique[36] with needless of the detection effeciency[37, 38]. Further, the covariance method was proposed by Bennett with the use of two detectors to determine the absolute fission rate. To suppress the drift of average count, Yamane et al. [39] modified the Bennett method with the use of the linear difference filter technique developed by Hashimoto et al[40]. In the measurement methodologies with the noise analysis above, the measurement is requisite to acquire the parameters beforehand: the central fission rate of the core material and the relative fission integral. Spriggs developed the Nelson number method[41] with the Rossi-α method. Also, in the measurement of β_{eff} by these methodologies, a factor determined by the calculations is requisite to correct

the neutron flux in subcritical states to that in critical states for the comparison with β_{eff} by the eigenvalue calculation. The measurements involve the calculations. However, the measured β_{eff} value is considered validated and to be ensured by applying different measurement methodologies.

Thus, the estimation methodology of β_{eff} is considered fully prepared with good accuracy in the Monte Carlo calculations which are not relevant to the approximation of the energy group and discretization of phase space in the eigenvalue calculation. Also, the measurement methodologies have been developed to complement the accuracy of nuclear data of delayed neutrons.

1.4.2 Research Issue

The estimation of β_{eff} is considered accurately obtained by the calculations as discussed in Sec. 1.4.1. For the current approach, to evaluate the subcriticality, β_{eff} obtained by the eigenvalue calculation had been assumed that the neutron flux can be approximated by that in the critical core. Further, β_{eff} had been measured to validate the calculation accuracy in the critical state.

Here, β_{eff} has been measured in the core having very shallow subcriticality and stable neutron source which the neutron spectrum placed at the core center can be regard as the fission neutron spectrum. For the cores, in which the components are unclear such as the meltdown core and the uncertainty of the nuclear data largely influences the prediction accuracy of the subcriticality such as ADS, the measurements of β_{eff} is considered to support the validity of subcriticality and β_{eff} estimated by the eigenvalue calculations. In the case of the meltdown core, the neutron source is predicted difficult to install inside the core. Further, ADS is scheduled that the subcriticality measurement is conducted with the use of

pulsed neutron source. To complement the accuracy of subcriticality measurement with β_{eff} obtained by the calculations, the measurement methodology of β_{eff} is requisite to be developed for a wide range of the subcriticality with various kinds of stable and pulsed neutron sources located outside the core.

Further, β_{eff} estimated by the eigenvalue calculations shown in Eq. (1-4) can be considered approximately applicable to the subcriticality measurement for the target core having shallow subcriticality. This approximation is assumed that the neutron flux in the subcritical core can be regarded as that in the critical core. A problem, however, arises when the subcritical core has deep subcriticality and the neutron source placed outside the core. In these cases, the influence of the neutron source is predicted impossible to be negligible, resulting in the excitation of the higher-mode components in the neutron flux. Thus, β_{eff} is requisite to be evaluated by the fixed-source calculation considering the position and the neutron energy of the neutron source. The adjoint neutron flux, however, is not defined in the fixed-source calculations, and then the proposal of the evaluation methodology is necessary to define β_{eff} under the existence of the external neutron source.

1.5 Purposes of the Present Thesis

In the subcritical state, β_{eff} of the reactor core is considered to be varied by the type of the nuclear fuel because of the difference of the delayed neutron fraction. Also, since the β_{eff} is relevant to ratio of the prompt and the delayed neutron leakages, the value depends on the reactor configuration including a full withdrawal or a full insertion of the control rods and replacements of fuel rods into another materials. In this dissertation, the variation of the β_{eff} value is revealed in terms of the subcriticality for the reactor configuration. Further, in the subcritical core with the external neutron source, β_{eff} is predicted to be varied by the energy and the position of the external neutron source. Thus, in this dissertation, for the various subcritical cores with an external neutron source such as ADS which is maintained at the steady state, the accurate evaluations of β_{eff} by experiments and calculations are mainly aimed to improve the measurement accuracy of the subcriticality, used in the safety assessment, with the consideration of the spectrum and the position of the external neutron source.

For the preparation of the discussion about β_{eff} in the subcritical state, basic ADS experiments were carried out at the Kyoto University Critical Assembly (KUCA) with the variation of subcriticality and the kinds of external neutron sources. The ADS experiments were aimed to acquire the neutronic characteristics of the subcritical cores, and to investigate the experimental accuracy of those characteristics by the conventional experimental analysis method with the use of two kinds of external neutron sources of different energy spectrum, through the measurements: (1) the reaction rate distribution which is closely related with neutron flux distribution to investigate the neutron leakage from the core caused by initial energy of the neutron source, (2) the prompt neutron decay constant to investigate the dependency of the kinetic parameters on the external neutron

source, (3) the subcriticality to obtain the subcriticality in dollar and (4) the subcritical multiplication factor that is measure of the actual multiplication in subcritical cores to reveal the influence of the external neutron source on the multiplication in the subcritical core.

On the basis of the results which indicated dependency of β_{eff} on the subcriticality in the basic ADS experiments, in order to provide the measurement methodology of β_{eff} in reactor physics experiments of ADS, the focus was aimed to verify β_{eff} for the ADS experiments having stable or pulsed external neutron sources. Since conventional measurements of β_{eff} had been conducted for the core in shallow subcritical states with the stable neutron source at the core center, in order to investigate the capability of the β_{eff} measurement methodology with external neutron source, the measurement was carried out with stable neutron source outside the core by varying the subcriticality. Based on the experimental method using a stable neutron source, attempt was made to develop the measurement methodology of β_{eff} with a pulsed external neutron source in the subcritical range during down to $k_{\mathrm{eff}} = 0.93$, because the pulsed neutron source is one of the candidates for the accelerator neutron in ADS. Through a comparison with the calculated β_{eff} in the eigenvalue calculations, these topics were emphasized as follows: (1) the development of the measurement methodology in the ADS experiments, (2) the investigation of the applicability of the proposed methodology, and (3) revealing the dependency of β_{eff} values in the subcriticality.

In the basic ADS experiments, the conventional experimental analysis was examined for the accurate subcritical estimation with the use of β_{eff} by the eigenvalue calculation. Here, development of new calculation methodology of β_{eff} by the fixed-source calculation was aimed to accurately evaluate β_{eff} in the subcritical system. In this method, neutron multiplication factor that is equivalent with k_{eff} value in the eigenvalue calculation was

proposed in the fixed-source calculations and to obtain β_{eff} in consideration of the rector conditions, such as the energy and the position of the external neutron source, the subcriticality, and the reactor configuration. Finally, the applicability of β_{eff} estimated by the fixed-source calculations was investigated through the subcriticality measurement in the ADS experiments varying the subcriticality and external neutron source.

1.6 Composition of the Present Thesis

This thesis addresses the issues in the β_{eff} evaluation under the existence of the external neutron in subcritical states. The ADS experiments by varying the subcriticality or the energy of the external neutron source are described in Chapter 2. The measurement methodology of β_{eff} and the validation evaluation by the experiments conducted with the use of a stable and a pulsed neutron sources are explained in Chapter 3. The β_{eff} evaluation methodology by the fixed-source calculations was proposed, and the subcriticality measured with the β_{eff} compared with another measured or calculated ones are shown in Chapter 4. Finally, conclusions are summarized in Chapter 5.

CHAPTER 2

KINETIC AND STATIC EXPERIMENTS OF ACCELRATOR-DRIVEN SYSTEM AT KYOTO UNIVERSITY CRITICAL ASSEMBLY

2.1 Introduction

The accelerator-driven system (ADS) composed of a subcritical reactor and an external neutron source has been proposed as a new type reactor under the concept of energy amplifier system [1-2]. An inherent advantage gained by the ADS operation at subcritical states could contribute to decreasing the risk on reactivity insertion accident, and loading various fuel material could be accomplished to expand energy resources. As other research activities, experimental and numerical studies had been conducted to establish the ADS facility for an experimental proof of nuclear transmutation of minor actinides and long-lived fission products [3-6].

At the Kyoto University Critical Assembly (KUCA), preliminary studies on thorium-loaded ADS had been conducted with the use of 14 MeV neutrons generated by deuterium-tritium (D-T) reactions or spallation neutrons generated by injecting 100 MeV protons onto a heavy metal target [7-12]. In a series of ADS experiments, neutron characteristics of reactor physics parameters were preliminarily examined, including reaction rate distributions, subcriticality (in dollar units) and neutron multiplication, through the experimental analyses in a deep subcritical core.

Previous thorium-loaded ADS experiments temporarily suggested the influence of the external neutron source on the reactor physics parameters[12], however, a further

multiplication system was required to examine a significant impact of the external neutron source on the neutron characteristics in ADS. In the present study, to resolve all the remaining issues, ADS experiments were carried out in the multiplying system over $k_{eff} \simeq$ 0.854 with the variation of external neutron source through the experimental analyses and in the subcritical system with the variation of the subcriticality ranged between 1300 and 7500 pcm to examine neutron characteristics

The objective of this study was to investigate the dependence of the subcriticality and the external neutron source on the kinetic parameter with the use of reactor physics parameters, including reaction rate distributions, prompt neutron decay constants, subcriticality and subcritical multiplication factors, by varying the external neutron source and the subcriticality in ADS experiments.

2.2 Experimental Settings

Of three cores designated A, B and C at KUCA, A and B are polyethylene solid-moderated and -reflected core, and C is a light water-moderated and -reflected one. The three cores are operated at a low mW power in the normal operation. Both ADS experiments with the variation of the subcritifcality and the external neutron source were carried out at the A-core as shown in Fig. 2-1(a). At the KUCA A-core, two external neutron sources, including 14 MeV neutrons by the D-T reactions and spallation neutrons by injection of 100 MeV protons onto a tungsten target, are installed outside the core, and can be injected separately into the core.

2.2.1 Uranium-Loaded ADS Core

The critical 1/8”P60EU-EU(3) core (reference core) was assembled at the Kyoto University Critical Assembly (KUCA) A-core, and was made up by 25 fuel rods surrounded by polyethylene reflectors as shown in Fig. 2-1(a). Each fuel rod (1/8”P60EU-EU) was composed of highly-enriched uranium (HEU; 2” × 2” and 1/16” thick) and a polyethylene moderator (PE; 2” × 2” and 1/4” thick) as shown in Fig. 2-1(b). This core was selected for considering the variation of β_{eff} along the subcriticality level. For the measurement of subcriticality, protons accelerated to 100 MeV were injected onto a disk-type tungsten (W) target in order to generate spallation neutrons. The accelerator was operated in pulsed mode and the repetition rate of the pulse was 20 Hz. The time width of the pulsed proton beam was 100 ns. The averaged proton current was 50 pA. The target was located at (15, H) grid in Fig. 1(a). The diameter and the thickness of the target were 50 mm and 12 mm, respectively. The thickness of tungsten target was determined to stop the 100 MeV protons

in the target, on the basis of a previous target study [13].

The neutron signals were obtained with the use of a BF_3 detector inserted diagonally at (10, U; Fig. 2-1(a)) to the core for the measurements of the subcriticality. For the reference core in the critical experiment, excess reactivity and control rod worth (C1, C2 and C3) were measured by the positive period method and the rod drop method, respectively. Experimental analyses were available to examine the precision of eigenvalue calculations by the Monte Carlo method and the accuracy of measured subcriticality. To achieve deep subcriticality, some of the fuel rods "F" (Fig. 2-1(a)) were substituted for polyethylene reflectors and configured as shown in Figs. 2-1(c) and 2-1(d), and the subcriticality level then ranged between about 1300 and 7500 pcm.

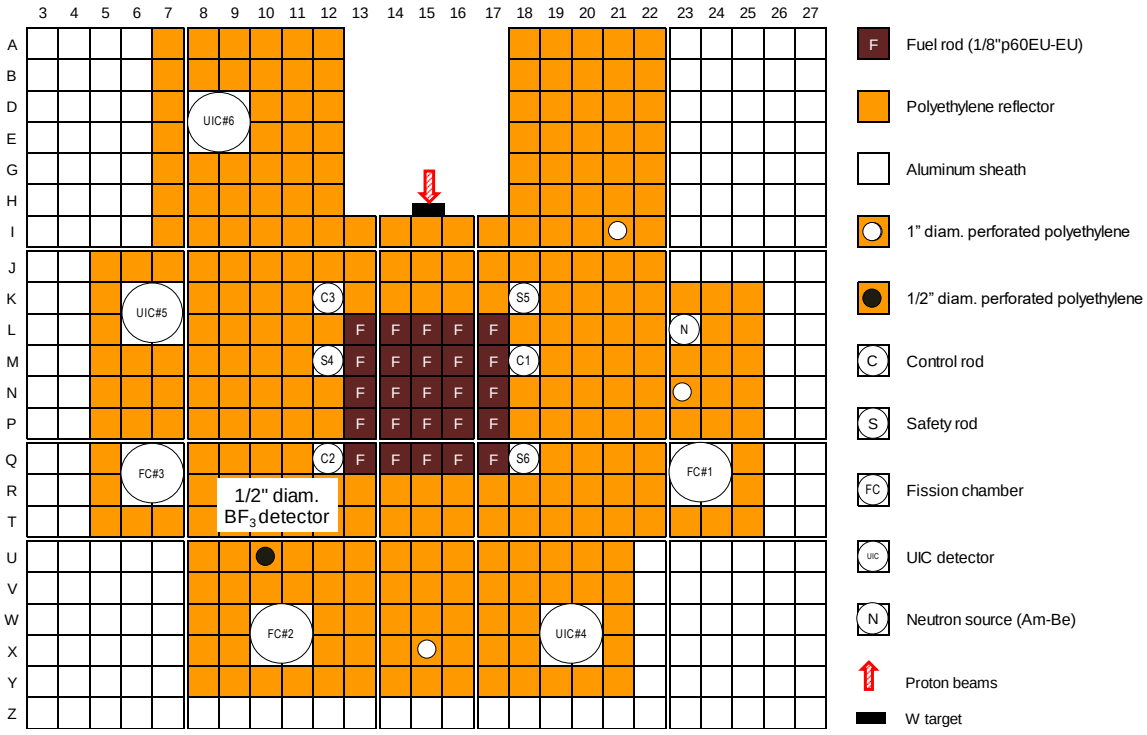

Fig. 2-1(a) Top view of 1/8"P60EU-EU(3) core (reference core).

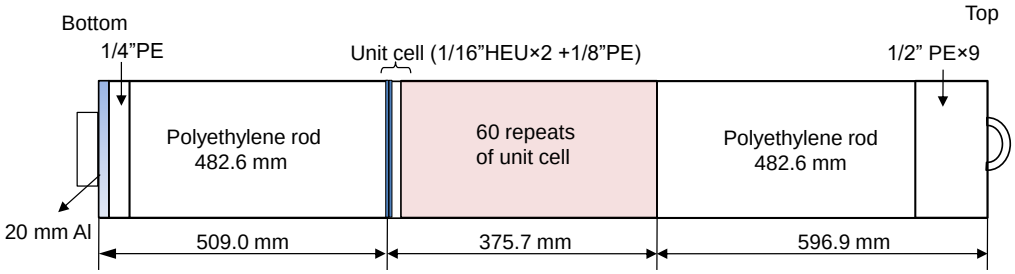

Fig. 2-1(b) Schematic diagram of fuel rod for 1/8”P60EU-EU(3) core shown in Fig. 2-1(a).

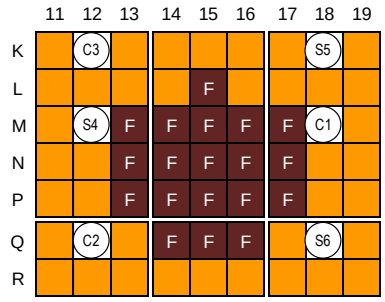

Fig. 2-1(c)
Fuel substitution pattern I in 1/8”P60EU-EU(3) core.

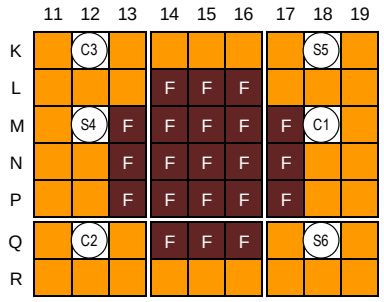

Fig. 2-1(d)
Fuel substitution pattern II in 1/8”P60EU-EU(3) core.

2.2.2 Thorium-loaded ADS core

To investigate the ADS neutronics, including reaction rate distributions, prompt neutron decay constants, subcriticality and subcritical multiplication factors, subcritical core (Th-HEU-5PE core) was provided in the KUCA A-core for the ADS experiments with the variation of external neutron source, as shown in Figs. 2-2(a) and 2-2(b). In the ADS experiments, fuel rods were surrounded by the polyethylene moderator (reflector) rods, and

were composed of thorium, HEU, and PE as shown in Fig. 2-2(c). 14 MeV neutrons were generated by the injection of deuteron beams onto the tritium target, and spallation neutrons were generated by the injection of 100 MeV protons onto the tungsten target (50 mm diameter and 12 mm thick). The both external neutron sources were operated in the pulsed mode through the thorium-loaded ADS experiments.

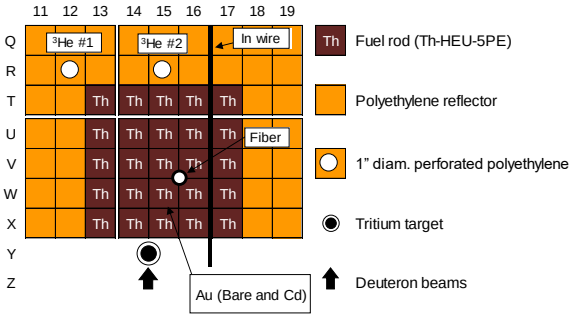

Fig. 2-2(a)
Top view of central part of core configuration in the ADS experiments (14 MeV neutrons).

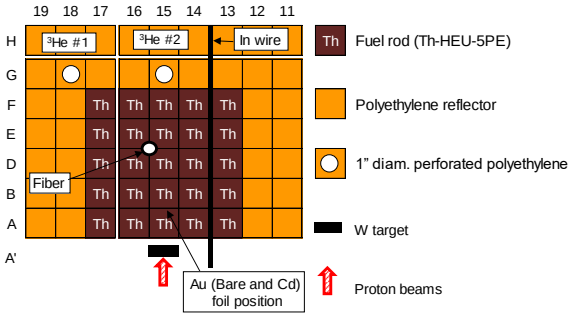

Fig. 2-2(b)
Top view of central part of core configuration in the ADS experiments (100 MeV protons).

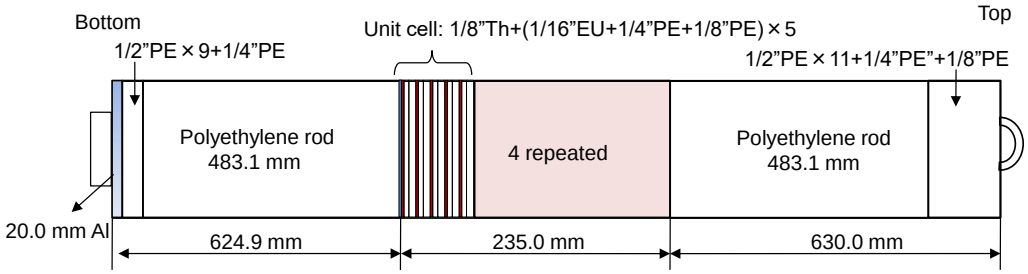

Fig. 2-2(c) Schematic detail of fuel rod "Th" (Th-HEU-5PE core) shown in Figs. 2-2(a) and 2-2(b).

Time evolution of the behaviors of prompt and delayed neutrons was obtained from the signals of two ^{3}He detectors (20 mm diam. and 200 mm long) installed around the core and an optical fiber detector[14] at the time sampling of 100 ns. The optical fiber was coated

with a powdered mixture of ^{6}LiF (95% enrichment) for detection of thermal neutrons based on ^{6}Li(n, t)^{4}He reactions and ZnS(Ag) for scintillation (1 mm diam. and 200 mm long) in the core shown in Figs. 2-2(a) and 2-2(b). In the kinetic experiments, 14 MeV neutrons were produced by a 0.4 mA deuteron beam, 10 Hz pulsed frequency and 10 μs pulsed width; 100 MeV protons were of 50 mm spot size, 10 pA intensity, 20 Hz pulsed frequency and 100 ns pulsed width. The prompt neutron decay constant was deduced by the least-square fitting on the basis of the pulsed neutron method (referred to PNS) to an exponential function, and by the Feynman-α method (referred to Noise) for the delayed neutron region (detailed on its application in Refs. 15-16).

The specifications of the foils and wire used in static experiments are shown in Table 2-1. Indium (In) wire was used for acquiring ^{115}In (n, γ) ^{116m}In reaction rates and was set on a radial axis at core mid-plane, in cases of 14 MeV neutrons and 100 MeV protons shown in Figs. 2-2(a) and 2-2(b), respectively. To normalize the reaction rate distribution, the niobium (Nb) and indium foils were attached to tritium and tungsten targets to obtain the source intensity from the reaction rates based on ^{93}Nb(n, $2n$)^{92m}Nb and ^{115}In(n, n')^{115m}In threshold reactions of 9 MeV and 0.3 MeV, respectively. Further, Bare and Cd covered gold foils were set at (W, 15; Fig. 2-2(a)) for 14 MeV neutrons and at (B, 15; Fig. 2-2(b)) for 100 MeV protons to obtain the thermal neutron flux experimentally. In the static experiments, deuterons were at 0.4 mA intensity, 400 Hz pulsed frequency, 10 μs pulsed width, and produced around 10^{6} n/s; 100 MeV protons were of 50 mm spot size, around 0.8 nA intensity, 20 Hz pulsed frequency, 100 ns pulsed width and produced around 10^{7} n/s. The irradiation time was about 2.5 hours and one hour for 14 MeV neutrons and 100 MeV protons, respectively.

Table 2-1
Specification of irradiation foils in ADS experiments.

Reactions	Dimension (mm)	Half-life	γ-ray energy (keV)	Emission rate (%)	Threshold (MeV)
^{197}Au(n, γ) ^{198}Au	10 diam. and 0.05 thick (Foil)	2.698 d	411.9	95.51	-
^{115}In(n, γ) ^{116m}In	1.5 diam. and 500 long (Wire)	54.12 m	1097.3 1293.54	55.7 85	-
^{93}Nb(n, 2n) ^{92m}Nb (14 MeV neutrons)	10×10×1 (Foil)	10.15 d	834.3	99.22	8.9
^{115}In(n, n') ^{115m}In (100 MeV protons)	10×10×1 (Foil)	4.486 h	336.2	45.08	0.3

2.3 Kinetic Analysis

Kinetic experiments were carried out by varying the kind of external neutron source and the measurement methodology. Prompt neutron decay constants were deduced from the exponential function fitting of the PNS measurements shown in Fig. 2-3(a) as follows:

$$Count\,rate = C \cdot \exp(-\alpha t) + B \quad , \tag{2-1}$$

where, α is the prompt neutron decay constant, C and B are constant values. In the Fig. 2-3(a), the double peaking was found in the time spectrum for 100 MeV protons. This peaking is considered to result from the count loss due to the pile up by extreme high count rate. The PNS fitting was achieved in the region from 1.5 to 5.0 ms to obtain the sloop in the time spectrum avoiding the contribution of the count loss. Also, the reactor noise analyses were conducted by the Feynman-α method regarding the delayed neutron region in the time spectrum from 50 ms for 14 MeV neutrons and 20 ms for 100 MeV protons as the stable neutron level[16]. And, the α was deduced by the Feynman-α method shown in Fig. 2-3(b), from the least square fitting for Y-value with the gate width t_{gw} as follows:

$$Y = C\left\{1 - \frac{1-\exp(-\alpha t_{gw})}{\alpha t_{gw}}\right\} - B \quad . \tag{2-2}$$

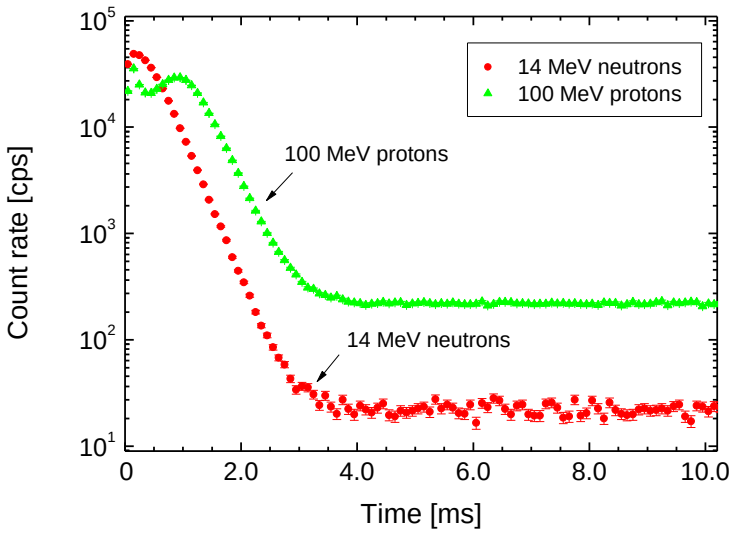

Fig. 2-3 (a)　Time spectrum of ^{3}He #1 detector response to a PNS measurement.

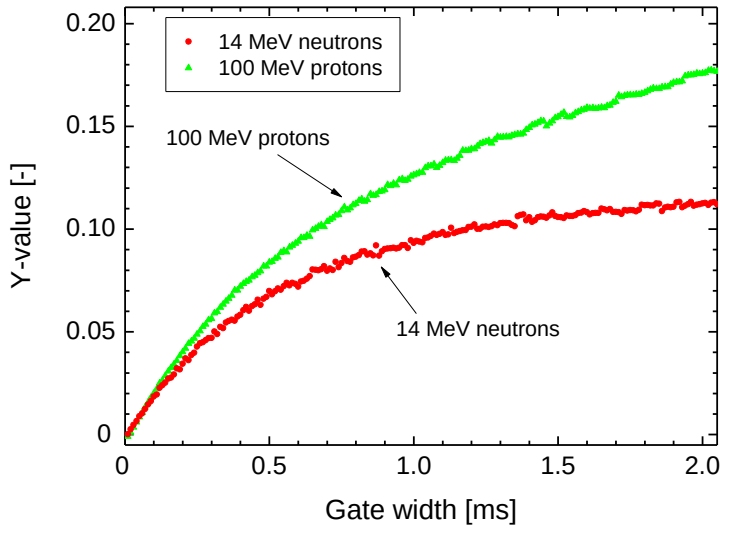

Fig. 2-3 (b)　Covariance-to-mean ratio (^{3}He #1) against gate width in Feynman-α method.

The results of the analyses by Feynman-α method were remarkably differed with the external neutron source as shown in Fig. 2-3(b). The α values deduced by the Feynman-α method were expected to resolve the dependence of detector positions, since the higher-mode components of neutron flux distributions were not dominant in the delayed neutron region, regardless of the locations of detectors. The dependence on detector positions was, however, found in the α values by the Noise method as well as the dependence in fitting method presented in Fig. 2-4. Also, the dependence on the spectrum of the external neutron source was observed in the α values when varying the external neutron source. In general, the values of kinetic parameters have been considered independent of the external neutron source in the core system. However, the dependence on the external neutron source suggested a significant impact of changing in not only the α values but also the kinetic parameters, including the effective delayed neutron fraction β_{eff} and generation time Λ, under the existence of the external neutron source.

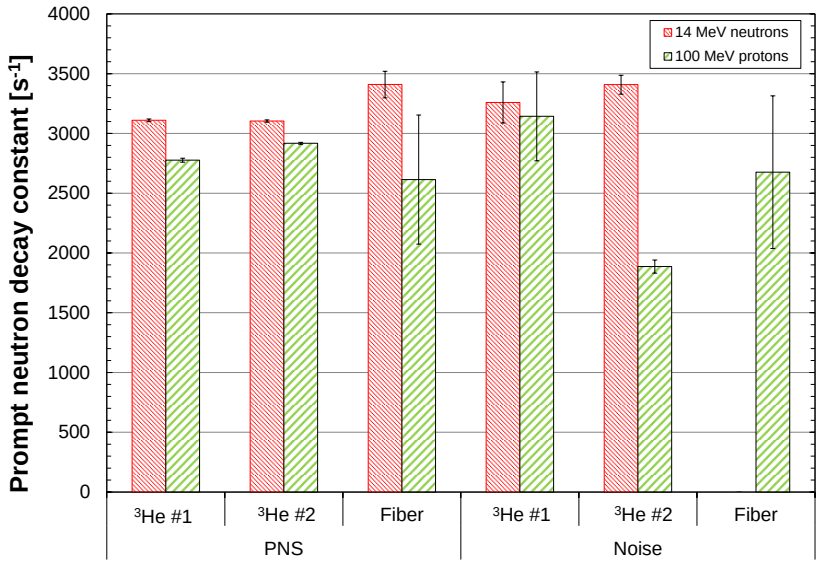

Fig. 2-4 Measured results of the prompt neutron decay constant α 1/s by the PNS fitting method and the Feynman-α method.

To investigate the probability of the variation in β_{eff} under existence of the external neutron source and the subcriticality, subcriticality was measured by the extrapolated area ratio method[21] applied to the BF_3 and the optical fiber detectors with the use of β_{eff} approximately estimated by k-ratio method[22] with the ratio of two effective multiplication factors involving total (prompt and delayed) and only prompt neutrons.

In the case of the variation of the subcriticality for 1/8"P60EU-EU(3) core, the measured subcriticality obtained by PNS method was compared with the measured one obtained by the combined use of the excess reactivity and the control rod for reference core, and the calculated one obtained by MCNP2.5.0 together with ENDF/B-VII.0 for the substituted cores shown in Figs. 2-1(c) and 2-2(d), respectively. The MCNPX eigenvalue calculations were performed in a total of 1E+08 histories (10^3 active cycles of 10^5 each); the statistical errors were less than 9 pcm. In the comparison between β_{eff} by varying the subcriticality shown in Table 2-2, β_{eff} values showed the tendency to be increased caused by the control rod insertion (Cases I to III, Cases IV to V, and Cases VI to VII, respectively). The reason is considered in the increase of the leakage of prompt neutrons, having high energy compared with that of delayed neutrons, caused by the drastic variation of the buckling of the neutron flux. In the subcriticality measurement, the discrepancy was found about 10% in the relative difference between the measurements obtained by the area ratio method and the combination of the excess reactivity and the control rod worth. Further, the comparison in deep subcriticality of Cases IV to VII showed the discrepancy about 10% between measured and calculated subcriticality.

Table 2-2
Results of subcriticality on the basis of effective delayed neutron fractions estimated by k-ratio method.

Case	Reference subcriticality (pcm)	β_{eff} by k-ratio method	Measured subcriticality (pcm)
I	1200 ± 36	797 ± 9	1119 ± 15 (1.07 ± 0.01)
II	2012 ± 60	801 ± 9	1863 ± 23 (1.08 ± 0.01)
III	2657 ± 80	811 ± 9	2410 ± 30 (1.10 ± 0.01)
IV	2722 ± 32	810 ± 9	2692 ± 33 (1.02 ± 0.01)
V	4891 ± 50	825 ± 9	5044 ± 68 (0.97 ± 0.01)
VI	5291 ± 54	795 ± 9	5.401 ± 73 (0.98 ± 0.01)
VII	7474 ± 75	802 ± 9	8147 ± 117 (0.92 ± 0.01)

*Quantities in parentheses indicate C/E.

In the case of the variation of external neutron source for Th-HEU-5PE core, the measured subcriticality was compared with the calculated one by MCNPX-2.5.0 with ENDF/B-VII.0 in a total number of 10^8 histories (10^3 active cycles of 10^5 each). Here, since measured subcriticality by the area ratio method is considered to have the influence of spatial effects, the optical fiber detector at the core center, which indicated less spatial effects and good agreements with eigenvalue calculation in the previous study[7], was used for the measurements. The measured subcriticality in dollar unit was remarkably differed with the external neutron source as shown in Table 2-3. Although the measured k_{eff} of 100 MeV protons agreed with the calculated one within the relative difference of 5% through the C/E value, the difference of k_{eff} between the measurement and the calculation was within 1% in case of 14 MeV neutrons, as shown in Table 2-3. The significant difference between two external neutron sources was considered to be caused by employing β_{eff} deduced by the neutron flux distributions in fundamental-mode, although a proper value of β_{eff} should be obtained by taking into account the influence of external neutron source.

Table 2-3
Comparison between effective multiplication factors k_{eff} from measurements (Area ratio method) and calculations (MCNPX-2.5.0), and measured subcriticality in dollar unit (ρ($)).

Source	Calculation	Experiment*	C/E
14 MeV neutrons	0.84924 ± 0.00008	0.84516 ± 0.03614 (22.850 ± 4.490)	1.00 ± 0.03
100 MeV protons	0.86397 ± 0.00008	0.89775 ± 0.00397 (14.201 ± 0.563)	0.96 ± 0.01

*:β_{eff} = 802 ± 14 pcm (k-ratio method calculated by MCNPX-2.5.0 together with ENDF/B-VII.0)

From the discussion on kinetic parameters, not only the investigation on difference of α values between the PNS method and Feynman-α method, but also accurate estimation of kinetic parameters were required to get a special treatment for the external neutron source with the use of MCNP calculations. A reliable determination of β_{eff} and Λ is crucial to be able to measure the reactivity of an ADS.

2.4 Static Analysis

2.4.1 Reaction Rate Distribution

Reaction rates of irradiated foils were measured by the saturated activities D_∞ ($s^{-1}\cdot cm^{-3}$) deduced from γ-ray measurements with the use of the highly-purified germanium detector (ORTEC, GEM60P) as follows:

$$D_\infty = \frac{\lambda T_C C \rho}{\varepsilon_D \varepsilon_E \{1-\exp(-\lambda T_i)\}\cdot\exp(-\lambda T_w)\cdot\{1-\exp(-\lambda T_C)\}\cdot M} \quad , \tag{2-3}$$

where λ indicates the decay constant, T_c the counting time, C the count rate, ε_D the detection efficiency, ε_E the emission rate, T_i the irradiation time, T_w the waiting time before the start of the decay measurement, ρ the density, and M the mass of the foil, respectively.

Reaction rate traverses were obtained by the saturated activities D_∞ ($s^{-1}\cdot cm^{-3}$) in Eq. (2-3) as reaction rates on the basis of ^{115}In (n, γ) ^{116m}In reactions, with the use of the same method as those of thorium capture and fission reaction rates. The fixed-source calculations were performed by MCNPX with the nuclear data libraries shown in Table 2-4, in a total number of 10^9 histories within a statistical error of 3% in the reaction rates.

Table 2-4
List of nuclear data libraries in numerical simulations of the ADS experiments.

	Particle transport		Reaction rate
	Neutrons	Protons	Neutrons
14 MeV neutrons	ENDF/B-VII.0	-	JENDL/D-99
100 MeV protons	JENDL/HE-2007 ENDF/B-VII.0 (for Th only)	JENDL/HE-2007	JENDL/D-99

As shown in Fig. 2-5, measured ^{115}In (n, γ) ^{116m}In reaction rate distributions were compared with calculated ones normalized per source neutron thanks to the ^{93}Nb(n, $2n$)^{92m}Nb and ^{115}In(n, n')^{115m}In reaction rates, for 14 MeV neutrons and 100 MeV protons, respectively. Regardless of the external neutron source in fixed-source calculations and the neutron spectrum in the core shown in Fig. 2-6, the calculated reaction rate traverses showed good agreement with the measured ones. The reaction rate distributions differed with the variation of the external neutron source, demonstrating that spallation neutrons induced by 100 MeV protons were contributing significantly to the neutron multiplication compared with 14 MeV neutrons. In the 100 MeV protons, distorted distribution could express the fission reaction distribution, resulting in the variation of the contributions of prompt neutrons and delayed neutrons to the multiplication. Since the prompt neutrons are considered leak out from the core easier than delayed neutrons due to their high energy spectrum, β_{eff} is considered to vary by the spectrum of the external neutron source.

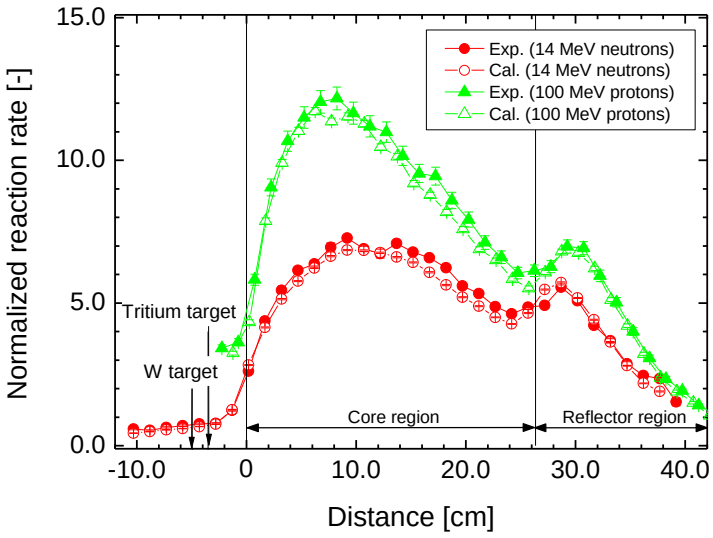

Fig. 2-5 Comparison between measured and calculated In capture reaction rate distributions on axial traverse.

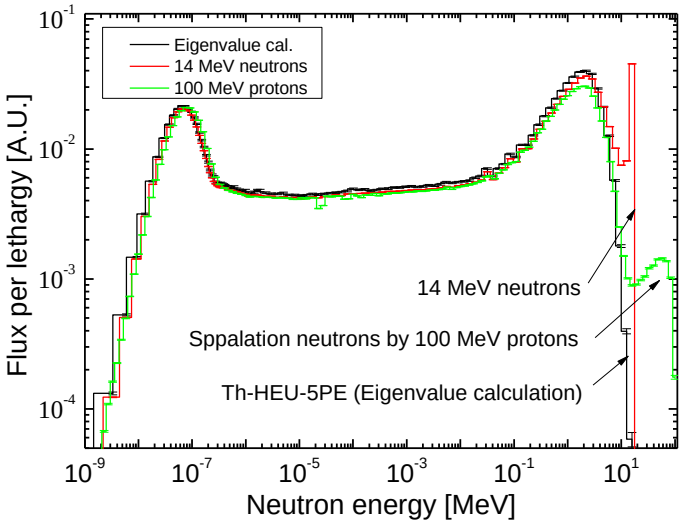

Fig. 2-6 Comparison between neutron energy spectra for the external neutron sources at the core center of TH-HEU-5PE core.

2.4.2 Subcritical Multiplication Factor

Among neutronic parameters of ADS, subcritical multiplication factor k_s has been introduced as an alternative to the effective multiplication factor k_{eff} by taking into account the change of neutron multiplication in the subcritical system[3]. Here, the effective multiplication factor k_{eff} is given as follows:

$$k_{eff} = \frac{\langle \mathbf{P}\phi_0(\mathbf{r}, E) \rangle}{\langle \mathbf{L}\phi_0(\mathbf{r}, E) \rangle} \quad , \tag{2-4}$$

where ϕ_0 represents the neutron flux in critical state, **L** the loss operator, **P** the production operator, and < > the integration over space and energy. In the same manner, k_s is written in the existence of the external neutron source *s* as follows:

$$k_s = \frac{\langle \mathbf{P}\phi_s(\mathbf{r}, E) \rangle}{\langle \mathbf{L}\phi_s(\mathbf{r}, E) \rangle} \quad , \tag{2-5}$$

where ϕ_s is the neutron flux under in the existence of external neutron source. The neutron flux ϕ_s is determined with the use of the term *s* of external neutron source as follows:

$$\mathbf{L}\phi_s(\mathbf{r}, E) = \mathbf{P}\phi_s(\mathbf{r}, E) + s(\mathbf{r}, E) \ . \tag{2-6}$$

From Eqs. (2-4) and (2-5), k_s can be rewritten with both total number of fission neutrons *F* and that of external source neutrons *S* as follows:

$$k_s = \frac{\langle \mathbf{P}\phi_s(\mathbf{r},E) \rangle}{\langle \mathbf{P}\phi_s(\mathbf{r},E) \rangle + \langle s(\mathbf{r},E) \rangle} = \frac{F}{F+S} \quad . \tag{2-7}$$

k_s has been deduced under two assumptions. First, total number of fission neutrons F and external source neutrons S are represented by the indium reaction rates of the wire in the core and the foil at the target by introducing coefficients of C_f and C_s, as shown in Eqs. (2-8) and (2-9), respectively. This assumption had been validated that the indium capture reaction rates can be expressed by the fission reaction neutrons through C_f, and C_f can be treated as a constant from a proportional relation between indium capture and uranium fission cross sections in the thermal neutron energy region, as shown in Fig. 2-7. Second, one-dimensional reaction rates were assumed to extend to three-dimensional ones using a constant of variable separation A, as shown in Eq. (2-8). The validity of the assumptions had been demonstrated by its application in Ref. 11.

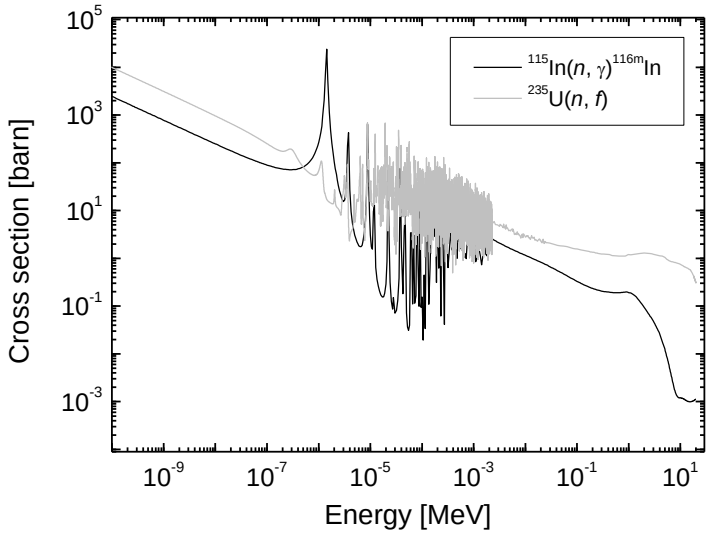

Fig. 2-7 Microscopic cross sections of ^{115}In(n, γ) ^{116m}In and ^{235}U(n, f) reactions.

Numbers of fission reaction neutrons F and external neutron source neutrons S were deduced with the use of the indium capture reaction rate distributions and reaction rates of the attached foils in the core and at the external neutron sources, respectively, as follows:

$$F \approx A \cdot C_{\mathrm{f}} \int_0^{T_{\mathrm{i}}} \int R_{\mathrm{In}}(x, y_0, z_0, t)\, dx\, dt \quad , \tag{2-8}$$

$$S \approx C_{\mathrm{s}} \int_0^{T_{\mathrm{i}}} R_{\mathrm{s}}(\mathbf{r}_{\mathrm{s}}, t)\, dt \quad , \tag{2-9}$$

where, R_{In} and R_{s} indicate reaction rates of indium wire at positions x, y_0, and z_0, and those of niobium (14 MeV neutrons) and indium (100 MeV protons) foils attached at position $\underline{\mathbf{r}}_{\mathrm{s}}$, respectively, T_{i} the irradiation time during experiments. A, C_{f} and C_{S} were determined from ratios of the reaction rates between MCNPX and the experiments. Consequently, subcritical multiplication factor k_{s} can be deduced approximately as follows:

$$k_{\mathrm{S}} = \frac{F}{F+S} \approx \frac{A \cdot C_{\mathrm{f}} \int_0^{T_{\mathrm{i}}} \int R_{\mathrm{In}}(x, y_0, z_0, t)\, dx\, dt}{A \cdot C_{\mathrm{f}} \int_0^{T_i} \int R_{\mathrm{In}}(x, y_0, z_0, t)\, dx\, dt + C_{\mathrm{s}} \int_0^{T_i} R_{\mathrm{S}}(\mathbf{r}_{\mathrm{s}}, t)\, dt} \quad . \tag{2-10}$$

A comparison between the experiments and the calculations of k_{s} revealed good agreement within the relative difference of 5% as shown in Table 2-5. By comparing between k_{eff} and k_{s} in Th-HEU-5PE core, the values of k_{s} were found to be much lower than the value of k_{eff}, resulting from the low contribution of the source neutrons S to the multiplication due to the external neutron source placed outside the core. The value of k_{s} was observed to be compared with 14 MeV neutrons and 100 MeV protons, demonstrating that they were varied by the external neutron source. From the results, a significant impact of the spectrum external neutron source was found in the comparison between k_{s} values in

14 MeV neutrons and 100 MeV protons.

Table 2-5
Comparison between measured and calculated values of k_s.

Core	Source	Calculation	Experiment	C/E
Th-HEU-5PE	14 MeV neutrons	0.46007 ± 0.00001	0.47300 ± 0.00091	0.96 ± 0.01
	100 MeV protons	0.67014 ± 0.00001	0.67096 ± 0.00183	1.00 ± 0.01

2.5 Conclusion

The ADS experiments were carried out to reveal the impact of the neutron source on β_{eff}, at the KUCA. The subcriticality was interestingly measured with the variation of the subcriticality in the uranium-loaded ADS experiments. Further, the fundamental reactor physics parameters, including prompt neutron decay constants, subcriticality, reaction rate distributions and subcritical multiplication factor, were successfully obtained with the variation of external neutron source in the thorium-loaded ADS experiments.

In the kinetic ADS experiments with the thorium-loaded core, notable remark was placed on the dependence of external neutron source through the experimental analyses of prompt neutron decay constants. The prompt neutron decay constants showed large values in the experiments with the use of 100 MeV protons compared with 14 MeV neutrons.

In the subcritical measurements with the uranium-loaded core, as another approach of kinetic parameters, the measured subcriticality was compared with the calculated one after the conversion of subcriticality from dollar unit into pcm with β_{eff} by eigenvalue calculation with MCNP6.1. As for the uranium-loaded core, the critical state could be attained by the partial insertion of the control rod; consequently the impact of the β_{eff} on subcriticality and the external neutron source was able to be investigated by the comparison of subcriticality deduced in the subcritical states with one deduced from the combination of excess reactivity and control rod worth in the critical experiments, at shallow subcriticality. The results of subcriticality measurements by the area ratio method showed relative difference of 10% compared with that in the critical experiments even at the shallow subcriticality. Further, the accuracy index of the conventional analysis of the experiments were confirmed as around 10% through the comparison between measured and calculated subcriticality until about 7500 pcm. Also, the subcriticality was deduced differently with the variation of

external neutron source, on the basis of β_{eff} calculated by the eigenvalue calculations, with the thorium-loaded core.

In the static ADS experiments, reaction rate distributions revealed good agreement between the experiments and the calculations with the variation of external neutron source. On the basis of reaction rate distributions, the significant impact of external neutron source was found in the experimental analyses of k_s.

On the basis of the results in the ADS experiments in the variation of the subcriticality and the external neutron source, the subject on the experimental analyses with β_{eff} was able to be extracted: confirmation of the β_{eff} increase as the subcriticality through the through the measurements of β_{eff}, investigation of the difference between measured subcriticality obtained with the use of different external neutron source and accuracy improvement in the subcriticality measurements by the proposal of β_{eff} calculation considering the external neutron source.

CHAPTER 3

MEASUREMENTS OF EFFECTIVE DELAYED NEUTRON FRACTION

3.1 Introduction

The calculation methodology of the effective delayed neutron fraction (β_{eff}) was proposed with the use of the neutron yield and fission spectrum of delayed neutrons, for estimating the kinetic characteristics in a critical reactor operation[1]. The accuracy of β_{eff} is then considered dependent directly on that of delayed neutrons in nuclear data evaluated by differential experiments. In the process of the development of neutron noise analyses, measurements of β_{eff} were made to verify the accuracy of the nuclear data and to reflect the results to the evaluation of the nuclear data evaluated through integral experiments. Also, for the measurement of β_{eff} by the power spectrum method[2] and the neutron noise analyses, the external neutron source was set at the center of the core in the subcritical state, to minimize the excitation of higher-mode components of neutron flux. The validity of these measurement methodologies has been verified by experimental benchmark analyses conducted in the Fast Critical Assembly[3-9] and the Westinghouse Idaho Nuclear Company slab tank assembly[10].

In the accelerator-driven system (ADS), reactor physics tests are considered useful for measuring the subcriticality in dollar units with the use of a pulsed neutron source and comparing it with the calculated subcriticality in pcm units through the use of β_{eff}, before the actual operation of the ADS. Here, in ADS experiments, the measurement of β_{eff} is expected to provide complementary verification of the calculation and of the reliability of

nuclear data. Furthermore, with focus on the measurement of β_{eff}, explorative experiments are conducted in an appropriate environment for conceivable measurement. In the actual ADS, however, the estimation methodology with few parameters is considered necessary for burden reduction in a severe environment, because the high-level background noise is predicted to result in decreasing the accuracy of measurement.

To reduce the parameters required for measuring β_{eff}, the Nelson number method[11] based on the Rossi-α method[12] is used because β_{eff} is then obtained directly with the combined use of source intensity, measured subcriticality in dollar units and two parameters (calculations) to correct the location of the external neutron source. To apply the Nelson number method to the measurement of β_{eff}, a stable neutron source having a neutron spectrum closed to the fission spectrum, such as ^{252}Cf, was assumed to set at the center of the core in a near critical state.

For the subcritical system which cannot be attained critical states, including the ADS, the prediction of the calculation is verified through the measurement in subcritical states. Further, the selection freedom of the neutron source is considered limited because of the difficulty of the installation. In the case of ADS, the reactor physics test is prepared for the subcriticality calibration with the use of pulsed neutron source (spallation neutrons generated by the interaction of high-energy protons onto a heavy metal target) placed outside the core. In the test, β_{eff} is considered an important parameter to be measured with the use of pulsed neutrons that have a wide range of neutron spectrum. The formulation[13] of the Rossi-α method in the pulsed neutron source has been already available for application to the subcriticality measurement in the pulsed neutron source (PNS) experiments. Accordingly, in this study, the methodology was applied for the stable neutron source outside the core to examine the capability of the Nelson number method and the correction parameters obtained by the Monte Carlo calculations. Subsequently, the measurement

methodology was developed uniquely to deduce the β_{eff} value with the pulsed neutron source (spallation neutrons) in the ADS operation mode being around k_{eff} = 0.93, with the combined use of the results of experiments and calculations: subcriticality by the area ratio method[14] and neutron noise data by the Rossi-α method in PNS experiments.

The objective of this study was to examine the applicability of a proposed methodology to estimate β_{eff} in the ADS experiments with spallation neutrons.

3.2 Measurement Methodology

3.2.1 Stable Neutron Source

Among β_{eff} measurement methodologies, the Nelson number method based on the Rossi-α method can be applied to the measurements without the detector efficiency and the neutron life time. In the Rossi-α method, the joint probability $P(t_1,t_2)$ between two neutron signals detected at times t_1 and t_2, is expressed as follows:

$$P(dt_1, dt_2)\, dt_1 dt_2 = C\, dt_1 dt_2 + A e^{-\alpha(t_2 - t_1)}\, dt_1 dt_2 \quad , \tag{3-1}$$

where α is the prompt decay constant, C average count rate of the detector, and A correlation amplitude. C and A are expressed as follows:

$$A = g\left(\frac{\lambda_{\text{d}}\, \lambda_{\text{f}} \left\langle \nu_{\text{p}} \left(\nu_{\text{p}} - 1 \right) \right\rangle}{2\alpha} \right) \quad , \tag{3-2}$$

$$C = \frac{\lambda_{\text{d}}\ g^{*} S}{1 - k_{\text{eff}}} \quad , \tag{3-3}$$

where $\left\langle \nu_{\text{p}} \left(\nu_{\text{p}} - 1 \right) \right\rangle$ is the second moment of the prompt neutron multiplicity distribution for induced prompt fission neutrons, λ_{d} the detection efficiency for neutron and λ_{f} the detection efficiency of a fission reaction and g the correction factor taking into account the variation in the probability of detecting correlated counts originating from neutrons of different worth[11], also, S is the intensity of source neutrons, and g* the correction factor for spatial and energy distribution of the source neutrons[11]. For the estimation of β_{eff}, the

parameters of *A* and *C* obtained by the fitting with Eq. (3-1), are used with the value of α, which is defined with the use of neutron lifetime *l*, as follows:

$$\alpha = \frac{\beta_{\text{eff}} - \rho}{\Lambda} = \frac{1-k_{\text{p}}}{l} = \frac{1-(1-\beta_{\text{eff}})k_{\text{eff}}}{l} = \frac{\beta_{\text{eff}}}{l}\,\frac{1-\rho_{\$}}{1-\rho_{\$}\beta_{\text{eff}}} \quad , \tag{3-4}$$

where ρ and $\rho_{\$}$ are the subcriticality in $\Delta k/k$ and dollar units, Λ the generation time. Further, λ_{f} can be rewritten with the use of β_{eff} and effective multiplication factor by prompt neutron only k_{p} and k_{eff} as follows:

$$\lambda_{\text{f}} = \frac{1}{l_{\text{f}}} = \frac{k_{\text{p}}}{l\langle \nu_{\text{p}} \rangle} = \frac{(1-\beta_{\text{eff}})k_{\text{eff}}}{l\langle \nu_{\text{p}} \rangle} \quad , \tag{3-5}$$

where l_{f} is the mean time between fission iterations, $\langle \nu_{\text{p}} \rangle$ the average number of prompt neutrons released per fission.

The relationship between three parameters to β_{eff} and $\rho_{\$}$ can be expressed by defining the Nelson number *N*, with the combined use of Eqs. (3-2), (3-3), (3-4) and (3-5), as follows:

$$N = \left(\frac{2g^{*}S}{g\langle \nu_{\text{p}} \rangle \Gamma}\right)\left(\frac{A}{\alpha C}\right) = \left(\frac{1-\beta_{eff}}{\beta_{eff}}\right)\left[\frac{\rho_{\$}}{(1-\rho_{\$})^{2}}\right] \quad , \tag{3-6}$$

where Γ is neutron dispersion factor defined by $\langle \nu_{\text{p}}(\nu_{\text{p}}-1)\rangle / \langle \nu_{\text{p}} \rangle^{2}$, Solving Eq. (3-6) for β_{eff}, β_{eff} can be obtained from the Nelson number and $\rho_{\$}$ as follows:

$$\beta_{eff} = \frac{\rho_\$}{N(1-\rho_\$)^2 - \rho_\$} \quad . \tag{3-7}$$

Here, correction factors g and g* were obtained with following calculations [11]:

$$g = \frac{\int \mathbf{P}(\mathbf{r})\, d\mathbf{r} \int \mathbf{P}(\mathbf{r})\, \mathbf{I}^2(\mathbf{r}) d\mathbf{r}}{\left(\int \mathbf{P}(\mathbf{r})\, \mathbf{I}(\mathbf{r}) d\mathbf{r} \right)^2} \quad , \tag{3-8}$$

$$g^* = \frac{\int S(\mathbf{r})\, \mathbf{I}_\mathbf{q}(\mathbf{r})\, d\mathbf{r} \int \mathbf{P}(\mathbf{r})\, d\mathbf{r}}{\int \mathbf{P}(\mathbf{r})\, \mathbf{I}(\mathbf{r})\, d\mathbf{r} \int \mathbf{s}(\mathbf{r})\, d\mathbf{r}} \quad , \tag{3-9}$$

$$\mathbf{P}(\mathbf{r}) = \int \Sigma_\mathrm{f}(\mathbf{r}, E)\, \phi(\mathbf{r}, E)\, dE \quad , \tag{3-10}$$

$$\mathbf{I}(\mathbf{r}) = \int \chi(\mathbf{r}, E)\, \phi^+(\mathbf{r}, E)\, dE \quad , \tag{3-11}$$

$$\mathbf{I}_\mathbf{q}(\mathbf{r}) = \int \chi_\mathrm{q}(\mathbf{r}, E)\, \phi^+(\mathbf{r}, E)\, dE \quad , \tag{3-12}$$

where ϕ and ϕ^+ are the forward and adjoint fluxes, respectively, Σ_f the macroscopic fission cross section, and χ and χ_q the fission spectrum and the spectrum of the external neutron source, respectively.

3.2.2 Pulsed Neutron Source

In the Rossi-α method for the pulsed neutron source, the joint probability $P(t_1,t_2)$ can be evaluated, alike in the case of the stable neutron source, by categorizing the same fission

chain reactions into correlated probability P_C and the different fission chain reactions and the neutron sources into uncorrelated probability P_U, as follows:

$$P(t_1,t_2)\,dt_1\,dt_2 = P_C(t_1,t_2)\,dt_1\,dt_2 + P_U(t_1,t_2)\,dt_1\,dt_2 \ . \tag{3-13}$$

P_C in the existence of the pulsed neutron source can be expressed with same probability in case of the stable neutron source used by Eq. (3-2), as follows:

$$P_C(t_1,t_2) = g\left(\frac{\lambda_d\,\lambda_f\left\langle \nu_p\left(\nu_p-1\right)\right\rangle}{2\alpha}\right)e^{-\alpha(t_2-t_1)}\,dt_1\,dt_2 \ . \tag{3-14}$$

For uncorrelated probability P_U, the formulation originated by its signals is sensitive to the pulsed shape of the external neutron source[13]. In the present study, the shape was regarded as the Gaussian function, and the uncorrelated probability is represented by constant term $P_{U,\,const}$ and trigonometric term $P_{U,\,trig}$ follows:

$$\begin{aligned} &P_U(t_1,t_2)\,dt_1\,dt_2 \\ &= P_{U,const}(t_1,t_2)\,dt_1\,dt_2 + P_{U,trig}(t_1,t_2)\,dt_1\,dt_2 \\ &= \frac{\lambda_d\,g^*\,S\,\Lambda\sqrt{2\pi}\,\sigma}{(-\rho)T_0}\,dt_1\,dt_2 \\ &\quad + \frac{\lambda_d\,g^*\,S(-\rho)T_0}{2\Lambda\sqrt{2\pi}\,\sigma}\sum_{n=1}^{\infty}\frac{1}{\alpha^2+\left(2n\pi/T_0\right)^2}e^{-\left(2n\pi/T_0\right)^2\sigma^2}\cos\left\{\left(2n\pi/T_0\right)\left(t_2-t_1\right)\right\}dt_1\,dt_2 \end{aligned} \tag{3-15}$$

where T_0 is the pulsed period, and σ the pulsed width. Note that the formula of the $P_{U,\,trig}$ is

highly depended on the shape of the neutron source, and represents uncorrelated probability with the neutron source having Gaussian distribution as time from the property of the neutron source with the use of FFAG proton accelerator. With the result of the Rossi-α method in the PNS experiments, the intensity of P_C and P_U are obtained from the fitting by Eq. (3-13). Since P_C is predicted to decay rapidly, however, the fitting is considered difficult for obtaining the both intensities together. Accordingly, the uncorrelated terms were deduced by first fitting in the region, where P_C is sufficiently decayed in Eq. (3-15), with fitting parameters B, D and σ as follows:

$$P_U(t_1,t_2)\,dt_1\,dt_2 = B\,dt_1\,dt_2 + D\sum_{n=1}^{1000}\frac{1}{\alpha^2+(2n\pi/T_0)^2}e^{-(2n\pi/T_0)^2\sigma^2}\cos\{(2n\pi/T_0)(t_2-t_1)\}\,dt_1\,dt_2 \quad , \tag{3-16}$$

where B is the fitting parameter for the constant value shown in Eq. (3-16) as follows:

$$B = \frac{\lambda_d\, g^* S \Lambda \sqrt{2\pi}\,\sigma}{(-\rho)T_0} \quad , \tag{3-17}$$

and the upper value of summation was set as 1000 leaving a margin from the saturation of the fitting results by setting about 300 in the upper value. With the fitting results of B, D and σ, P_C is deduced by subtracting uncorrelated terms from the result of the Rossi-α method in the PNS experiments shown in Eq. (3-13), as follows:

$$P_C(t_1,t_2)\,dt_1\,dt_2 = P(t_1,t_2)\,dt_1\,dt_2$$

$$-\left[B\,dt_1\,dt_2 + D\sum_{n=1}^{1000}\frac{1}{\alpha^2+\left(2n\pi/T_0\right)^2}e^{-\left(2n\pi/T_0\right)^2\sigma^2}\cos\left\{\left(2n\pi/T_0\right)\left(t_2-t_1\right)\right\}dt_1\,dt_2 \right] . \quad (3\text{-}18)$$

Here, the intensity of correlated probability A is obtained by fitting Eq. (3-18) as follows:

$$P_{\mathrm{C}}\left(t_1,t_2\right)dt_1\,dt_2 = Ae^{-\alpha\left(t_2-t_1\right)}\,dt_1\,dt_2 \ . \quad (3\text{-}19)$$

where A is expressed as follows:

$$A = g\left(\frac{\lambda_{\mathrm{d}}\,\lambda_{\mathrm{f}}\left\langle\nu_{\mathrm{p}}\left(\nu_{\mathrm{p}}-1\right)\right\rangle}{2\alpha}\right) \ . \quad (3\text{-}20)$$

For the estimation of β_{eff}, Λ is rewritten with the use of k_{eff} as follows:

$$\Lambda = \frac{l}{k_{\mathrm{eff}}} \ . \quad (3\text{-}21)$$

With the use of Eqs. (3-4), (3-5) and (3-21), the intensity of correlated probability A in Eq. (3-19) can be expressed as follows:

$$
\begin{aligned}
A &= \frac{g\lambda_d \left\langle \nu_p \left(\nu_p - 1\right)\right\rangle k_p}{2\alpha l \left\langle \nu_p \right\rangle} \\
&= \frac{g\lambda_d \left\langle \nu_p \left(\nu_p - 1\right)\right\rangle k_p}{2\alpha \Lambda \left\langle \nu_p \right\rangle k_{eff}} \\
&= \frac{g\lambda_d \left\langle \nu_p \left(\nu_p - 1\right)\right\rangle (1-\beta_{eff})\, k_{eff}}{2(1-\rho_\$)\beta_{eff} \left\langle \nu_p \right\rangle k_{eff}} \\
&= \frac{g\lambda_d \left\langle \nu_p \left(\nu_p - 1\right)\right\rangle (1-\beta_{eff})}{2(1-\rho_\$)\beta_{eff} \left\langle \nu_p \right\rangle} \quad .
\end{aligned}
\tag{3-22}
$$

Also, *B* shown in Eq. (3-17) can be rewritten with the use of and α by Eq. (3-4), as follows:

$$
\begin{aligned}
B &= \frac{\lambda_d\, g^* S \Lambda \sqrt{2\pi}\,\sigma}{(-\rho) T_0} \\
&= \frac{\lambda_d\, g^* S (1-\rho_\$) \sqrt{2\pi}\,\sigma}{(-\rho_\$) T_0\, \alpha} \quad .
\end{aligned}
\tag{3-23}
$$

Here, the Nelson number for pulsed neutron source N_{PNS} is defined with the combination of α, B in Eq. (3-23), *A* in Eq. (3-22) as follows:

$$
N_{PNS} = \left(\frac{2\sqrt{2\pi}\,\sigma g^* S \left\langle \nu_p \right\rangle}{g \left\langle \nu_p \left(\nu_p - 1\right)\right\rangle T_0} \right) \left(\frac{A}{\alpha B} \right) = \frac{(1-\beta_{eff})(-\rho_\$)}{\beta_{eff} (1-\rho_\$)^2} \quad , \tag{3-24}
$$

The correction factors *g* and *g** were obtained through the calculations by Eqs. (3-8), (3-9), (3-10) and (3-11). From the relation between N_{PNS} and β_{eff} shown in Eq. (3-14), β_{eff} is obtained experimentally as follows:

$$\beta_{\text{eff}} = \frac{-\rho_{\$}}{N\left(1-\rho_{\$}\right)^2 - \rho_{\$}} \quad . \tag{3-23}$$

The procedure for the deduction of β_{eff} in the PNS experiments is shown in Fig. 3-1.

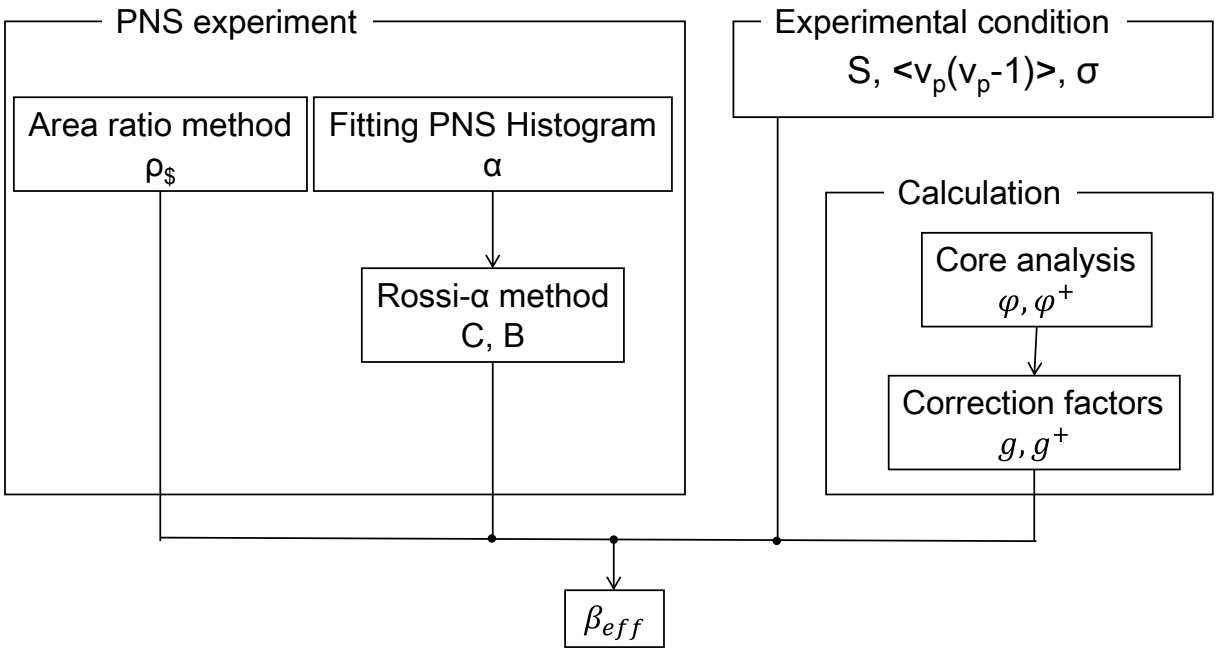

Fig. 3-1. Procedure for deduction of β_{eff} in PNS experiments.

3.3 Experimental Settings

3.3.1 Stable Neutron Source

Experiments on the measurement of β_{eff} were carried out at the KUCA A-core which is solid-moderated and -reflected one as shown in Fig. 3-2(a). The core was composed of the assemblies of normal fuel rod "F" shown in Fig. 3-2(b), partial fuel rod "4," and polyethylene reflector rod shown in Fig. 3-2(c). Both fuel rods "F" and "4" were composed of 93% highly-enriched uranium and polyethylene moderator, and had a H/U value of 51.6. An americium-beryllium (Am-Be: Fig. 3-2(a)) neutron source was installed outside the core as a stable external source with a neutron emission rate of 4.13×10^{6} n/s.

At a critical state, both excess reactivity and control rod worth (C1, C2 and C3) were measured by the positive period method and the rod drop method, respectively. Further, measured subcriticality in dollar unit was used in the measurements of β_{eff}, by the Nelson number method with the use of a ^{3}He detector installed outside the core. To examine the applicability of the measurement methodology with the variation of the subcriticality, subcriticality was ranging between 0.7 and 2.8 $ by the insertion of the control and the safety rods as shown in Table 3-1.

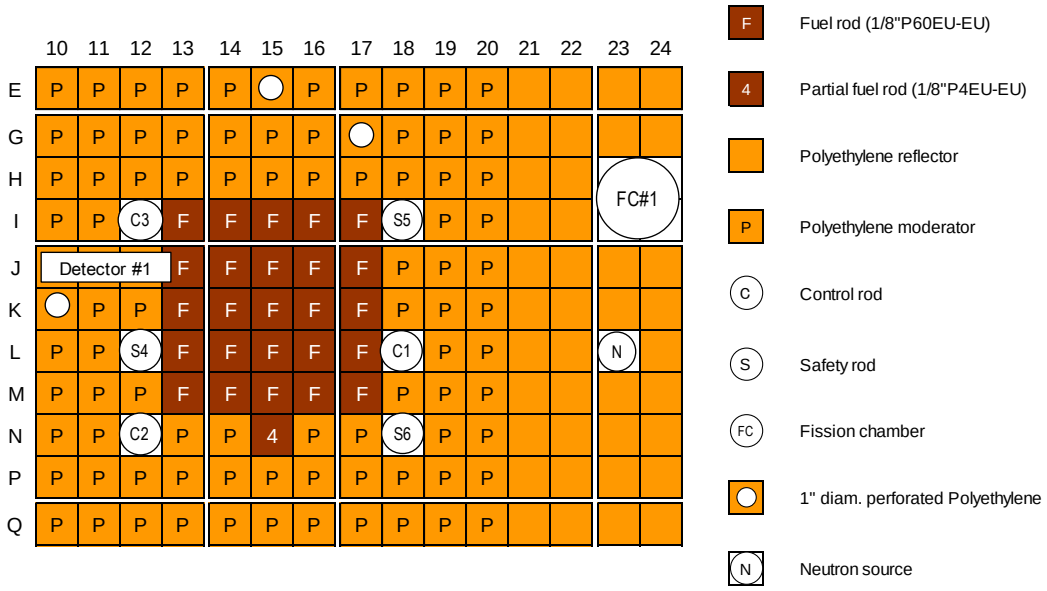

Fig. 3-2(a) Top view of the core for the measurement of β_{eff} with stable neutron source.

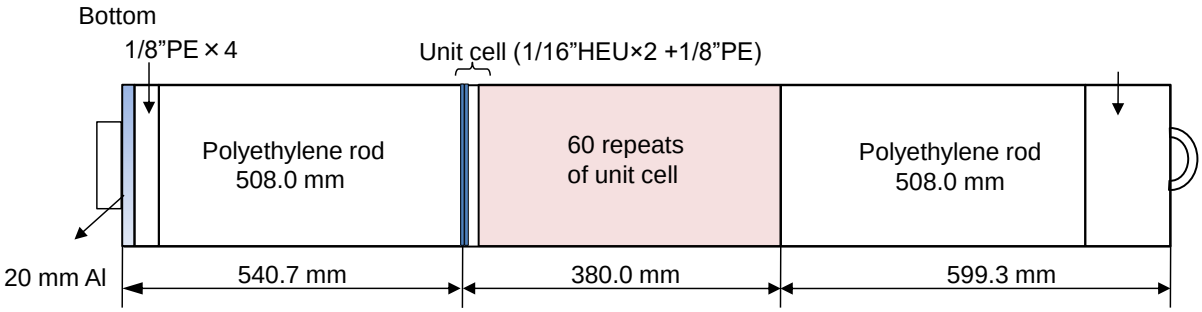

Fig. 3-2(b) Schematic diagram of fuel rod "F" shown in Fig. 3-2(a).

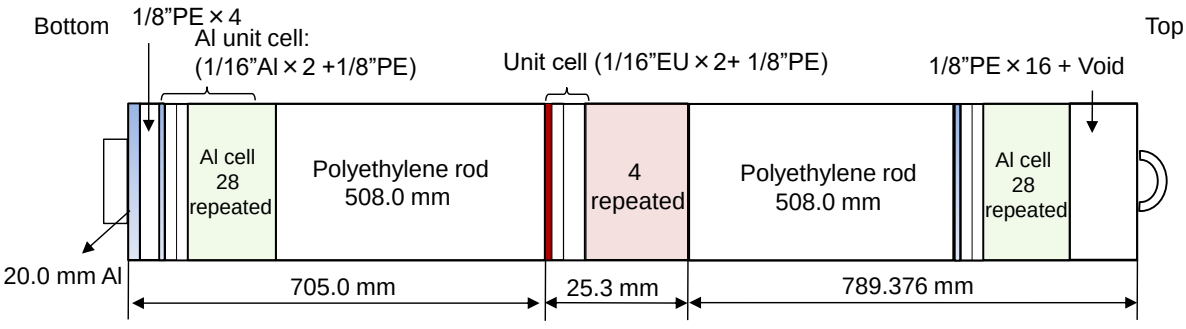

Fig. 3-2(c) Schematic diagram of fuel rod "4" shown in Fig. 3-2(a).

Table 3-1
Measured subcriticality by the positive period method and the rod drop method.

Case	Rod insertion	Subcriticality ($)
A-I	C1	0.777 ± 0.026
A-II	C1, C2, C3	1.269 ± 0.030
A-III	C1, C2, C3, S4	2.286 ± 0.039
A-IV	C1, C2, C3, S4, S5, S6	2.777 ± 0.043

3.3.2 Pulsed Neutron Source

1/8"P60EU-EU(3) core was used for the measurement of β_{eff} in the ADS experiments with 100 MeV protons as shown in Fig. 3-3(a). Each fuel rod (1/8"P60EU-EU) was made up by a highly-enriched uranium (HEU; 2" × 2" and 1/16" thick) and a polyethylene moderator (PE; 2" × 2" and 1/4" thick) in an aluminum sheath 54×54×1520 mm^3 as shown in Figure 2-1(b).

A proton accelerator (FFAG accelerator)[16-17] was operated to inject 100 MeV protons (beam spot 50 mm, intensity 50 pA (Cases B-I through B-III in Fig. 3-3(a)) and 75 pA (Cases B-IV through B-VII in Figs. 3-3(b) and 3-3(c)) and pulsed frequency 20 Hz) onto a tungsten target (W) (50 mm diam. and 12 mm thick) located at position (15, H; Fig. 3-3(a)) to generate spallation neutrons.

Time evolution according to the injection of spallation neutrons was obtained from

the signals of a BF_3 detector installed diagonally to the target at position (10, U; Fig. 3-3(a)) and an optical fiber detector[18] (coated with a powdered mixture of ^{6}LiF (95% enrichment) for detection based on ^{6}Li(n, t)^{4}He reactions and ZnS(Ag) for scintillation in the core) installed at position (15-16, M-N; Fig 3-3(a)). The PNS experiments were conducted for 10 minutes in each case to acquire neutron signals for data analyses by the area ratio method and the Rossi-α method. The pulsed width of the neutron source was deduced by the fitting for each detector with Eq. (3-16), as shown in Table 3-2.

Subcriticality was obtained by full insertion of control and safety rods, and by the substitution of the fuel assembly for polyethylene rods, as shown in Table 3-2. The excess reactivity and control rod worth (C1, C2 and C3) were measured by the positive period method and the rod drop method, respectively. In Cases B-I to B-III, the subcriticality was experimentally deduced with the combined use of control rod worth and its calibration curve obtained by the positive period method. Moreover, in Cases B-IV through B-VII, some of the fuel rods "F" (Fig. 3-3(a)) were replaced by polyethylene reflectors and configured as shown in Figs. 3-3(b) and 3-3(c). The subcriticality in dollar units was acquired experimentally by the extrapolate area ratio method[14]. The subcriticality level then ranged between 1300 and 7500 pcm.

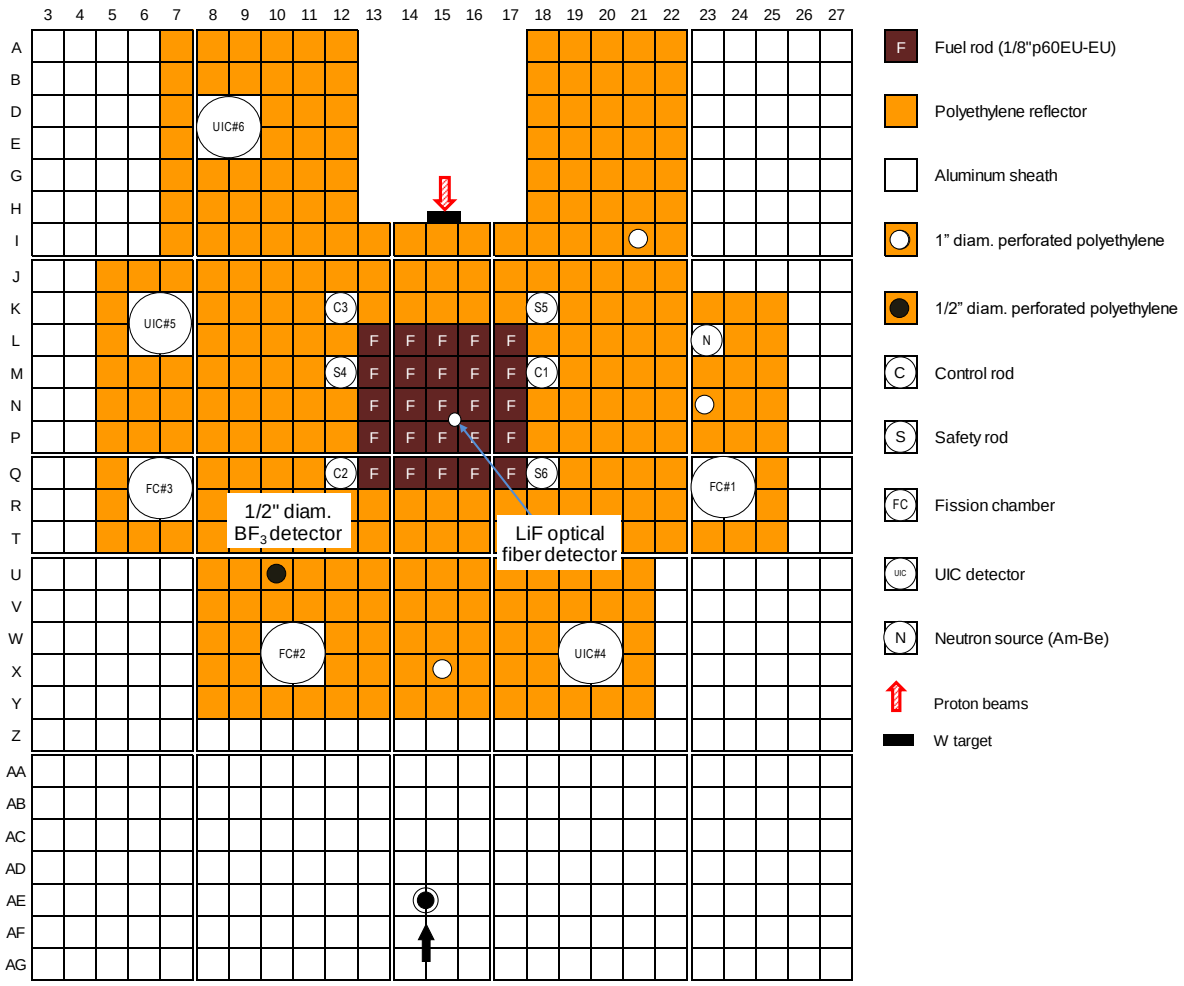

Fig. 3-3(a) Top view of 1/8"P60EU-EU(3) core for the measurement of β_{eff} with spallation neutrons in Cases B-I to B-III.

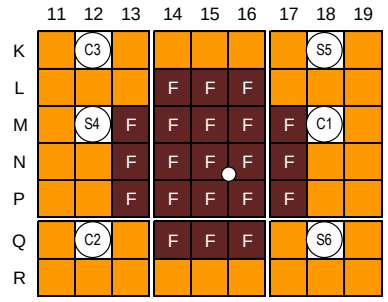

Fig. 3-3(b)
Fuel substitution pattern I in 1/8”P60EU-EU(3) core for Cases B-IV to B-V.

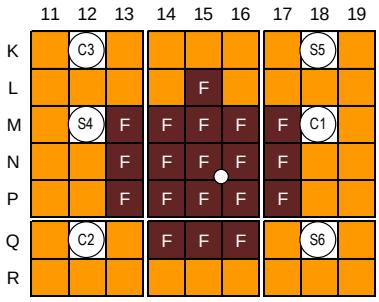

Fig. 3-3(c)
Fuel substitution pattern II in 1/8”P60EU-EU(3) core for Cases B-VI to B-VII.

Table 3-2
Deduced pulsed width and measured subcriticality in dollar units by fuel rod substitution and control rod insertion.

Case	Number of fuel rods	Rod insertion pattern	Pulsed width in optical fiber and (BF_3) detectors (s)	Subcriticality ($) (methodology)
B-I	25	C1, C2, C3	(2.10 ± 0.05)E-04	1.20 ± 0.03
			((4.30 ± 0.20)E-04)	(control rod worth)
B-II	25	C1, C2, C3,	1.25 ± 0.05)E-04	2.01 ± 0.06
		S4	((3.10 ± 0.20)E-04)	(control rod worth)
B-III	25	C1, C2, C3,	(1.00 ± 0.05)E-04	2.66 ± 0.07
		S4, S5, S6	((2.90 ± 0.20)E-04)	(control rod worth)
B-IV	21	–	(1.00 ± 0.05)E-04	3.32 ± 0.02
			((2.70 ± 0.10)E-04)	(area ratio method)
B-V	21	C1, C2,	(5.12 ± 0.25)E-05	6.13 ± 0.05
		S4, S6	((2.20 ± 0.05)E-04)	(area ratio method)
B-VI	19	–	(5.00 ± 0.42)E-05	6.80 ± 0.05
			((2.75 ± 0.02)E-04)	(area ratio method)
B-VII	19	C1, C2,	(5.00 ± 0.42)E-05	10.16 ± 0.09
		S4, S6	((2.60 ± 0.02)E-04)	(area ratio method)

3.4 Experimental Analysis

3.4.1 Stable Neutron Source

For the preparation of an evaluation of β_{eff} by the Nelson number method with 100 MeV protons, correction factors g and g^* are requisite to be calculated with the nuclear data having over 20 MeV neutron energy because the spallation neutrons has the energy spectrum over 20 MeV. For the calculation considering neutron energy over 20 MeV by the deterministic method, a preparation of the special cross section is required by the nuclear data processing code with the neutron spectrum of the target core. However, the nuclear data library for high-energy neutron is already provided for the Monte Carlo calculation such as JENDL/HE-2007[19]. Thus, the calculations of the correction factors by MCNP6.1[20] were examined through the comparison with those by conventional method of the diffusion calculations (SRAC[21]) with 107 energy groups in two dimensional (x-y). In the comparison of the calculations, JENDL-4.0[22] was used for the nuclear data library. The calculations of adjoint flux by MCNP6.1 were manually obtained for three-dimensional calculations as follows: an external neutron source in the Watt spectrum of ^{235}U was set inside an HEU plate; the reaction rates for the response of $\nu\Sigma_f$, which is discussed as more appropriate than Σ_f to estimate the adjoint flux[24], were tallied over the core with NONU option to avoid the neutron multiplication; these reaction rates approximately corresponded to the adjoint flux at the position of the HEU plate; this fixed-source problem was repeated by changing the position of the external neutron source in HEU plate. The correction factor g was observed to be constant, as shown in Table 3-3, conversely, a large correction was needed for neutron source by g^* indicating much small values with a variation by control rod insertion because the external neutron source was located outside the core and source efficiency was differed by the insertion of the control rods. In the comparison between the correction factors by

SRAC and MCNP6.1, the values of g agreed well, however, a discrepancy about 20% was found in the values of g^*. In general, the diffusion calculation is considered to overestimate the neutron leakage compared with the transport calculation, evaluating the correction factor g^* large. The β_{eff} measurement is considered requisite to examine the validation of these correction factors.

Table 3-3
Variation of correction factors g and g* by diffusion and transport calculations

Case	g		g^*	
	SRAC	MCNP6.1	SRAC	MCNP6.1
A-I	1.05	1.03 ± 0.01	1.02×10^{-2}	$(8.05 \pm 0.01)\times10^{-3}$
A-II	1.05	1.03 ± 0.01	1.03×10^{-2}	$(8.12 \pm 0.03)\times10^{-3}$
A-III	1.05	1.03 ± 0.01	1.06×10^{-2}	$(8.19 \pm 0.04)\times10^{-3}$
A-IV	1.05	1.04 ± 0.01	8.63×10^{-3}	$(6.73 \pm 0.04)\times10^{-3}$

β_{eff} was obtained by Eq. (3-7) with the use of two correction factors in the variation of the subcriticality, and measured β_{eff} compared with ones obtained by the eigenvalue calculations with the use of MCNP6.1 together with JENDL-4.0, as shown in Table 3-4. Measured β_{eff}, involving the error of measured subcriticality and fitted curve for the estimation of the parameters A, C and α, showed good agreement with calculated ones around the relative difference of 7%, indicating that the correction factors were accurately estimated by Monte Carlo calculations even if the external neutron source located outside

the core. These results revealed a possibility to apply to a measurement in case of an installation of external neutron source outside the core. Further, the calculation of the correction factors by MCNP6.1 with manual processing for the adjoint flux were validated through the comparison between measured and calculated β_{eff}.

Table 3-4
Effective delayed neutron fraction β_{eff} (pcm) by MCNP6.1 and measurement with correction factors by SRAC and MCNP6.1.

Case	MCNP6.1	Nelson number method	
		SRAC	MCNP6.1
A-I	785 ± 21	810 ± 18 (3.18%)	785 ± 21 (5.95%)
A-II	791 ± 21	781 ± 15 (1.26%)	791 ± 21 (2.03)
A-III	836 ± 22	780 ± 18 (6.70%)	836 ± 22 (-2.36)
A-IV	781 ± 21	801 ± 18 (2.56%)	781 ± 21 (6.90%)

Quantities of parentheses indicate the relative difference to MCNP6.1

3.4.2 Pulsed Neutron Source

The PNS experiments were carried out for the neutron noise analyses by the Rossi-α method. Moreover, the PNS histogram was obtained to acquire α values to supplement neutron noise analyses, as shown in Fig. 3-4. To obtain the intensity of the second term in

Eq. (3-15), the fitting based on Eq. (3-16) is required in the region where the correlation probability is negligible. From the PNS histogram shown in Figure 3-4, the decay of the correlation probability was confirmed at 0.025 s, and intensity *B* was obtained by the fitting for the joint probability by the Rossi-α method in the PNS experiments, on the basis of Eq. (3-17) in the region between 0.025 and 0.125 s. The intensity of the correlation term in Eq. (3-14) was then obtained by subtracting of the uncorrelated term from the joint probability in Eq. (3-18) and fitting by Eq. (3-19). The correlated probability decreased rapidly, compared with the uncorrelated probability as shown in Fig. 3-5. Instead of decreasing exponentially, the correlated probability increased in the vicinity of zero, the reason being the overestimation of the uncorrelated probability in the region arising by varying the shape of the external neutron source from the Gaussian to the pulsed, because the formulation of uncorrelated probability has the sensitivity to the shape of the external neutron source.

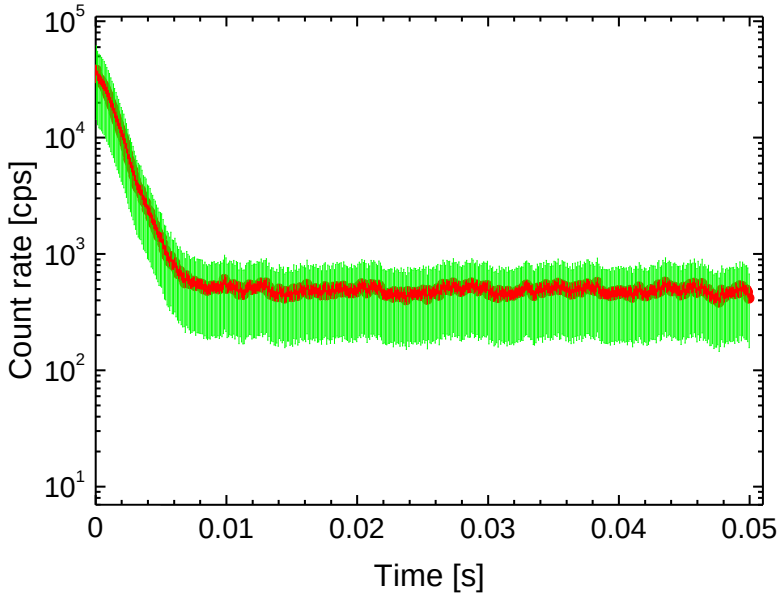

Fig. 3-4 PNS histogram of optical fiber detector in Case B-I.

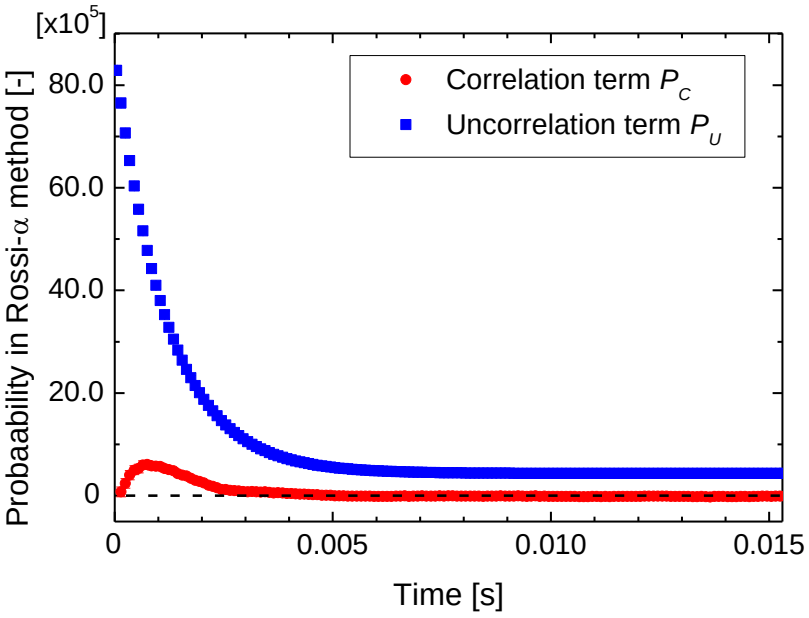

Fig. 3-5 Correlated and uncorrelated probabilities of fiber detector in Case B-I by Rossi-α method in PNS experiments.

In the fitted parameters, α and *B* values differed from each other when the subcriticality was varied, as shown in Fig. 3-6(a) and 3-6(b), respectively, because of the increase of the subcriticality in the α value and the decrease of neutrons in *B*. For the intensity of correlated probability *A*, the optical fiber indicated an asymptotic tendency of monotonic decrease, by the change in the subcriticality attributed to control rod insertion and fuel rod replacement in Cases B-I through B-VII, as shown in Fig. 3-6(c); the intensity of fission reactions decreased by the subcriticality. The BF_3 detector, however, showed the increasing tendency in Cases B-IV, B-V and B-VI. Since low correlated probability of the fission neutrons could be predicted in BF_3 installed outside the core, the accuracy of the reconstruction of correlated probability is considered low.

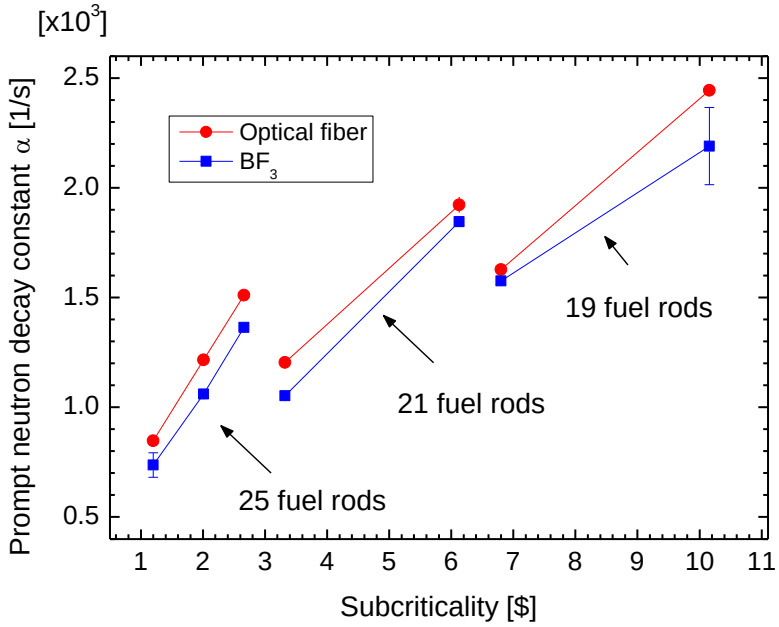

Fig. 3-6(a) Prompt neutron decay constant α obtained by the Rossi-α method in PNS experiments by varying subcriticality.

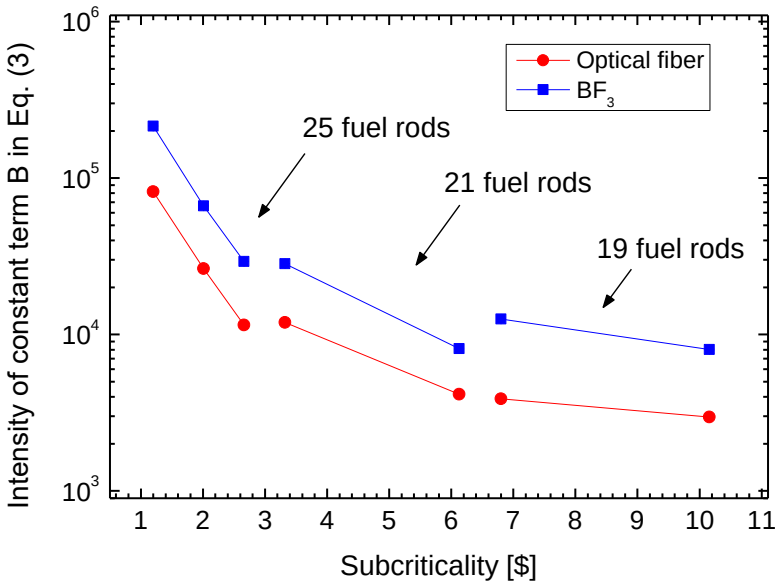

Fig. 3-6(b) Intensity of uncorrelated probability *B* obtained by the Rossi-α method in PNS experiments by varying subcriticality.

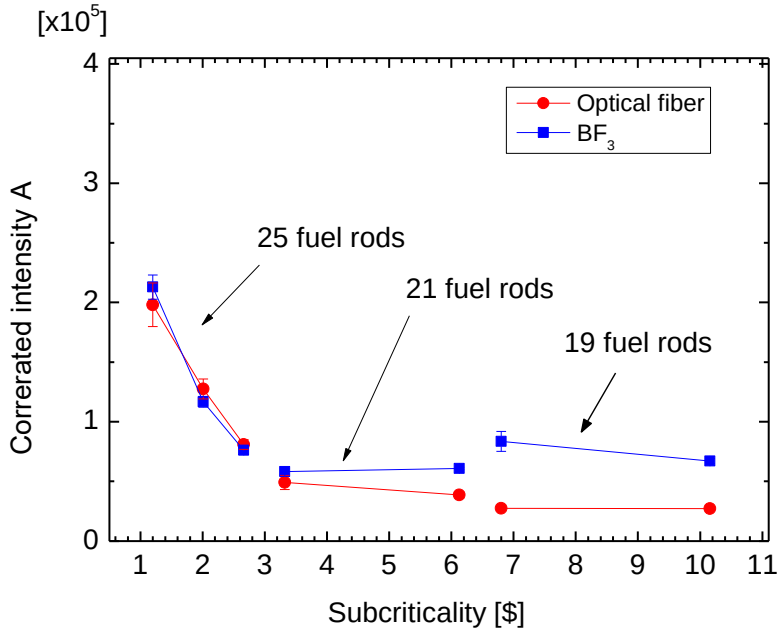

Fig. 3-6(c) Intensity of correlated probability *A* obtained by the Rossi-α method in PNS experiments by varying subcriticality.

To obtain correction factors *g* and *g** by Eqs. (3-8) and (3-9), respectively, the calculations of reaction rates and adjoint flux were performed by MCNP6.1 together with JENDL-4.0 (uranium and boron) and JENDL/HE-2007 (all nuclides except uranium and boron); total histories for adjoint flux and reaction rates were 1×10^7 and 1×10^6, respectively; the statistical error of the calculations was less than 1%. The adjoint flux was manually obtained in the same method with the case of stable neutron source mentioned Sec. 3.4.1. The correction factor *g* remained constant on subcriticality, and conversely the decreasing tendency was indicated on g* values by varying the subcriticality, as shown in Table 3-5.

Table 3-5
Calculated correction factors g and g^* by Eqs. (3-8) and (3-9) with JENDL-4.0 and JENDL/HE-2007.

Case	g	g*
B-I	1.03 ± 0.01	$(4.29 \pm 0.01)\times10^{-3}$
B-II	1.03 ± 0.01	$(4.28 \pm 0.01)\times10^{-3}$
B-III	1.04 ± 0.01	$(4.18 \pm 0.01)\times10^{-3}$
B-IV	1.03 ± 0.01	$(3.84 \pm 0.01)\times10^{-3}$
B-V	1.03 ± 0.01	$(3.74 \pm 0.01)\times10^{-3}$
B-VI	1.03 ± 0.01	$(2.84 \pm 0.02)\times10^{-3}$
B-VII	1.03 ± 0.01	$(2.75 \pm 0.01)\times10^{-3}$

With the results shown in Table 3-4 and fitted parameters α, A and B, β_{eff} values were deduced by Eq. (3-23) in the ADS experiments. The result of measured β_{eff} compared with that of calculated β_{eff} by MCNP6.1 as shown in Table 3-6, revealing that the result of the optical fiber at the core center indicates acceptable accuracy of the results by MCNP6.1 within a relative difference of about 13% in the subcritical range of the ADS operation (Cases B-I through B-VII) around $k_{eff} = 0.93$. With the BF_3 detector, the difference between the measured and calculated β_{eff} was very large. The resulting low accuracy is attributable

to the variation in the shape of the pulsed neutron source and the extraction of correlated probability with pulsed width of neutron source based on Eq. (3-16). Thus, the emphasis placed where the optical fiber detector located at the core center showed good accuracy because the effect of the neutron flux distribution in high-mode components is not effective and the correlated neutrons to the same family in fission chain is largely detected. Inversely, when the detector located outside of the core, the measurement accuracy is considered deteriorated by the difficulty in the extraction of the correlated term related to correlated neutron detections with Eq. (3-18). From these results, the applicability of the measurement methodology for β_{eff} was demonstrated in the subcritical range of the ADS operation around k_{eff} = 0.93. Furthermore, to obtain good accuracy of β_{eff} values with the proposed methodology, improvement of correlated probability is attainable with the use of a specific shape (Gaussian distribution) of the external neutron source.

Table 3-6
Comparison between measured and calculated β_{eff} values.

Case	k_{eff}	Effective delayed neutron fraction β_{eff} (pcm)		
	MCNP6.1	MCNP6.1	Optical fiber	BF_3
B-I	0.99093	817 ± 11	870 ± 81 (-6.5 ± 0.6)	911 ± 29 (-11.5 ± 0.4)
B-II	0.98274	794 ± 11	876 ± 58 (-10.3 ± 0.7)	845 ± 33 (-6.5 ± 0.3)
B-III	0.97627	814 ± 11	855 ± 45 (-5.0 ± 0.3)	725 ± 36 (11.0 ± 0.6)
B-IV	0.97662	801 ± 11	903 ± 109 (-12.7 ± 1.5)	704 ± 28 (12.1 ± 0.5)
B-V	0.95680	826 ± 12	915 ± 75 (-10.8 ± 0.9)	303 ± 7 (63.3 ± 1.7)
B-VI	0.95278	817 ± 11	921 ± 84 (-12.7 ± 1.2)	189 ± 19 (76.9 ± 7.8)
B-VII	0.93358	815 ± 11	811 ± 72 (-0.4 ± 0.1)	162 ± 14 (90.1 ± 7.1)

Quantities in parentheses indicate relative difference (%)
Standard deviations are 9 pcm for k_{eff} estimations.

3.5 Conclusion

For the preparation of the reactor physics test of ADS operation, the possibility to obtain β_{eff} was investigated in the ADS experiments. In the methodology for estimating the value of β_{eff}, the Rossi-α method was applied to the neutron noise analyses at the subcritical core with stable neutrons and the PNS experiments with pulsed spallation neutrons. In the experiments with stable neutron source, the applicability of the Nelson number method was investigated to extend the capability for the neutron source placed outside the core. In the PNS experiments, with the fitting curve obtained by neutron noise analyses, the signals from two detectors installed at center of the core (optical fiber detector) and outside the core (BF_3 detector), and the correction factors, β_{eff} was measured and compared with the value calculated by MCNP6.1.

In the case of stable neutron source, the measurements of β_{eff} by the Nelson number method were conducted to examine its applicability with the use of external neutron source and the correction factors which are calculated manually with MCNP6.1 for the extension of the Nelson number method to subsequent PNS experiment. Results of the measured β_{eff} showed good agreement with those of calculated ones, indicating validity of the calculation method of the correction factors and the applicability of the measurements to the existence of external neutron source outside the core.

In the case of pulsed neutron source, the optical fiber detector showed that the accuracy of the measured value, compared with the calculated one, was within a relative difference of about 10% in the subcritical range of the ADS operation around k_{eff} = 0.93. The result with BF_3 detector installed outside the core did not compare with the calculated one because of the low accuracy attributed to the uncorrelated probability. The applicability of the measurement methodology based on the Rossi-α method was demonstrated by the

comparison between calculated and measured β_{eff} values in ADS experiments with spallation neutrons. For further improvement of the measured β_{eff}, the results could be considered that the shape of the external neutron source should be the Gaussian distribution strictly.

CHAPTER 4

CALCULSTIONS OF EFFECTIVE DELAYED NEUTRON FRACTION

4.1 Introduction

In a core operation at a subcritical state by the accelerator-driven system (ADS), the effective delayed neutron fraction is required to convert the reactivity in dollar units into pcm units with the use of nuclear design calculation methodologies. Among these calculation methodologies, the Monte Carlo method (stochastic methodology) has the main advantage, compared with the deterministic methodology, of allowing for calculations in accurate reactor modeling with fewer approximations; the value of β_{eff} is then easily obtained by the Monte Carlo method with the use of the iterated fission probability (IFP)[1] and the next fission probability[2].

The calculation methodology of IFP[3-5] and the next fission probability for β_{eff} evaluation by the stochastic methodology had been validated on the basis of benchmarks for various spectra and loading materials, and by comparison with the deterministic methodology. When forward calculations by the stochastic methodology are applied to nuclear design calculations, β_{eff} has been obtained approximately by the k-ratio method[6] as the ratio of two effective multiplication factors involving total (prompt and delayed) and prompt neutrons. The validity of the approximation employed in the k-ratio method was confirmed through benchmarks in various critical reactors[7-8]. In these methods, the values of β_{eff} are obtained by the eigenvalue calculations under the assumption that the neutron flux distributions in fundamental-mode are dominant over the reactors. These methodologies are, however, considered to be difficult to apply for an accurate estimation

of measured subcriticality in pcm units with the use of β_{eff} by the eigenvalue calculations, because, in fact, the neutron flux distributions in higher-mode components are considered easily induced, under the existence of an external neutron source, during the injection of high-energy neutrons.

A subsequent issue that remains to be resolved concerning the calculation of β_{eff} by the eigenvalue methods is the accurate estimation of subcriticality during the operation of an ADS under the existence of external neutron source. During the actual ADS operation, subcriticality monitoring is required to estimate its subcriticality in the variation by the beam trip, the beam restart, the change of source efficiency and the fuel composition. In the preparation of the development of subcriticality estimation methodology, the area ratio method had been applied for its capability in the YALINA-Booster[9] and in the TRADE program[10]. In those studies, the issue of β_{eff} in the subcritical state has not been discussed, especially when the measured subcriticality is varied by the condition of the beam or the spectrum of the external neutron source. In kinetic analyses on ADS[11-13], although adjoint flux distribution was defined under the existence of external neutron source, an issue of the proper determination of the weighting function still remains in the definition to obtain the kinetic parameters in the fixed-source calculations.

Here, an alternative methodology is proposed with the combined use of the k-ratio method and the reaction rates obtained by the fixed-source calculations, to estimate an appropriate value of β_{eff} without weighting functions, when the subcriticality level or the spectrum of the external neutron source is varied. The objective of this study is to investigate the applicability of the proposed methodology to the estimation of subcriticality in pcm units considering the variation of the subcriticality level and the spectrum of the external neutron source.

4.2 Theoretical Background

4.2.1 Eigenvalue Calculation

The delayed neutron fraction is defined as the ratio of the delayed neutron generation to the total neutron generation as follows:

$$\beta = \frac{\langle F^{\mathrm{d}} \phi \rangle}{\langle F \phi \rangle} \quad , \tag{4-1}$$

where ϕ and is forward angular flux, respectively, and < > the integration over angle, space and energy. F, F^d and F^p are production operators of total, delayed and prompt neutron generations by fission reactions, respectively, as follows:

$$F = \int dE' \chi(E' \to E) \nu(E') \Sigma_{\mathrm{f}}(E') \quad , \tag{4-2}$$

$$F^{\mathrm{d}} = \int dE' \chi^{\mathrm{d}}(E' \to E) \nu^{\mathrm{d}}(E') \Sigma_{\mathrm{f}}(E') \quad , \tag{4-3}$$

$$F^{\mathrm{p}} = F - F^{\mathrm{d}} \quad , \tag{4-4}$$

where χ and χ^{d} are the energy spectra of total and delayed neutrons, respectively; ν and ν^{d} the neutron yields for total and delayed neutrons, respectively, E the energy of scattered neutrons, E' induced neutron energy and Σ_{f} the macroscopic fission cross sections. And, β_{eff} is defined as the ratio of the contribution of delayed neutrons to total neutrons for reactivity with the use of adjoint angular flux ϕ^{+} for weighting function, as follows:

$$\beta_{eff} = \frac{\langle \phi^{+}, F^{\mathrm{d}} \phi \rangle}{\langle \phi^{+}, F \phi \rangle} \quad , \tag{4-5}$$

The effective multiplication factor k_{eff} and prompt multiplication factor k_{p} are then expressed by the neutron fluxes, as follows:

$$k_{eff} = \frac{\left\langle \phi^{+}, F\,\phi \right\rangle}{\left\langle \phi^{+}, L\,\phi \right\rangle} \quad , \tag{4-6}$$

$$k_{p} = \frac{\left\langle \phi_{\mathrm{p}}^{+}, F^{\mathrm{p}}\,\phi_{\mathrm{p}} \right\rangle}{\left\langle \phi_{\mathrm{p}}^{+}, L\,\phi_{\mathrm{p}} \right\rangle} \quad , \tag{4-7}$$

where L is loss operator account for leakage, absorption and scattering, and ϕ_{p} and ϕ_{p}^{+} are the forward and adjoint fluxes taking into account prompt neutrons, respectively. In the k-ratio method, the multiplication factors k_{eff} and k_{p} are used to obtain an approximate value of β_{eff} as follows:

$$\beta_{eff\,,\,eigen} = \frac{\left\langle \phi^{+}, \left(F - F^{\mathrm{p}}\right)\phi \right\rangle}{\left\langle \phi^{+}, F\,\phi \right\rangle} = 1 - \frac{\left\langle \phi^{+}, F^{\mathrm{p}}\,\phi \right\rangle}{\left\langle \phi^{+}, F\,\phi \right\rangle} \approx 1 - \frac{k_{\mathrm{p}}}{k_{\mathrm{eff}}} \quad . \tag{4-8}$$

Here, two multiplication factors k_{RR} and $k_{\mathrm{RR,\,p}}$ by total and prompt neutrons are newly defined with the use of reaction rates, respectively, as follows:

$$k_{RR} = \frac{\left\langle F\,\phi \right\rangle}{\left\langle L'\phi \right\rangle} \quad , \tag{4-9}$$

$$k_{\mathrm{RR,p}} = \frac{\left\langle F^{\mathrm{p}}\,\phi_{\mathrm{p}} \right\rangle}{\left\langle L'\phi_{\mathrm{p}} \right\rangle} \quad . \tag{4-10}$$

Since scattered neutrons are eventually absorbed in the core and the reflector or leaked out from the core, denominator in Eqs. (4-9) and (4-10) can be expressed in terms of leak out and the absorption reactions only. When numerator and denominator are interpreted as integrated reaction rates of the destruction and fission operators, respectively, the loss operator of *L*' is defined, taking into account leakage and absorption as follows:

$$L' = \vec{\Omega} \cdot \nabla + \Sigma_{\mathrm{a}}(E) \quad , \tag{4-11}$$

where $\vec{\Omega}$ is the direction of the neutron flight, and Σ_{a} the macroscopic absorption cross sections. Then, $\beta_{\mathrm{eigen}}^{\mathrm{RR}}$ deduced by the reaction rates was expressed approximately by a substitution of the multiplication factors by Eqs. (4-9) and (4-10) in Eq. (4-8), as follows:

$$\beta_{\mathrm{eigen}}^{\mathrm{RR}} \approx 1 - \frac{k_{\mathrm{RR,p}}}{k_{\mathrm{RR}}} \quad . \tag{4-12}$$

4.2.2 Fixed-Source Calculation

From the definition of $\beta_{\mathrm{eigen}}^{\mathrm{RR}}$ shown in Eq. (4-12), the methodology using eigenvalue calculations is extended into a methodology using the fixed-source calculations. In the fixed-source problem, the transport equation is expressed by introducing source term *s* to acquire neutron flux formed in the subciritical core ϕ_{sub} as follows:

$$L\phi_{\mathrm{sub}} = F\phi_{\mathrm{sub}} + s \quad , \tag{4-13}$$

where *L* and *F* indicate the loss and fission operators, respectively. To distinguish source

and fission neutrons, ϕ_{sub} was assumed to be expressed in terms of ϕ_{source} and ϕ_{core} as follows:

$$\phi_{\text{sub}} = \phi_{\text{source}} + \phi_{\text{core}} \quad , \tag{4-14}$$

where ϕ_{source} means the neutron flux corresponding to due to the source neutrons, and ϕ_{core} the neutron flux corresponding to due to the fission chain reactions. When the source problem is solved by applying $\nu=0$ to Eq. (4-13), the multiplied angular flux is not formed, and source term is expressed as follows:

$$s = L\phi_{\text{source}} \quad . \tag{4-15}$$

Substituting Eq. (4-15) in Eq. (4-13), the source term is replaced by the product of L and ϕ_{source}, and the neutron balance equation is expressed as follows:

$$L\phi_{\text{sub}} = F\phi_{\text{sub}} + L\phi_{\text{source}} \quad . \tag{4-16}$$

Here, on the basis of the manner in which effective eigenvalues are calculated with the neutron flux corresponding to due to fission neutrons, a pseudo multiplication factor k^{pseudo} is defined in the pseudo eigenvalue calculations with the use of neutron flux under the existence of external neutron source as follows:

$$L\phi_{\text{core}} = \frac{1}{k^{\text{pseudo}}} F\phi_{\text{core}} \quad . \tag{4-17}$$

Then, pseudo multiplication factors $k_{\mathrm{RR}}^{\mathrm{pseudo}}$ and $k_{\mathrm{RR,p}}^{\mathrm{pseudo}}$ are obtained by substituting Eqs. (4-14) and (4-16) in Eq. (4-17), with the use of reaction rates by the fixed-source calculations, as the same manner in Eqs. (4-9) and (4-10), respectively, as follows:

$$k_{\mathrm{RR}}^{\mathrm{pseudo}} = \frac{\langle F\,\phi_{\mathrm{core}} \rangle}{\langle L\,\phi_{\mathrm{core}} \rangle} = \frac{\langle F\,\phi_{\mathrm{sub}} \rangle - \langle F\,\phi_{\mathrm{source}} \rangle}{\langle L'\phi_{\mathrm{sub}} \rangle - \langle L'\phi_{\mathrm{source}} \rangle}, \tag{4-18}$$

$$k_{\mathrm{RR,p}}^{\mathrm{pseudo}} = \frac{\langle F^{\mathrm{p}}\,\phi_{\mathrm{core,p}} \rangle}{\langle L\,\phi_{\mathrm{core,p}} \rangle} = \frac{\langle F^{\mathrm{p}}\,\phi_{\mathrm{sub,p}} \rangle - \langle F^{\mathrm{p}}\,\phi_{\mathrm{source,p}} \rangle}{\langle L'\phi_{\mathrm{sub,p}} \rangle - \langle L'\phi_{\mathrm{source,p}} \rangle}. \tag{4-19}$$

The $k_{\mathrm{RR}}^{\mathrm{pseudo}}$ ($k_{\mathrm{RR,p}}^{\mathrm{pseudo}}$) can be calculated with two runs considering total (prompt) neutrons: for the calculation of ϕ_{sub} ($\phi_{\mathrm{sub,\,p}}$) with standard fixed-source calculation and for that of ϕ_{source} ($\phi_{\mathrm{source,\,p}}$) with the fixed-source calculation under the option of ν=0. Finally, $\beta_{\mathrm{source}}^{\mathrm{RR}}$ can be obtained with the reaction rates by the fixed-source calculations by substituting Eqs. (4-18) and (4-19) in Eq. (4-8) as follows:

$$\beta_{\mathrm{source}}^{\mathrm{RR}} \approx 1 - \frac{k_{\mathrm{RR,p}}^{\mathrm{pseudo}}}{k_{\mathrm{RR}}^{\mathrm{pseudo}}}. \tag{4-20}$$

4.3 Analysis in Homogeneous Core

4.3.1 Eigenvalue Calculation for Critical Core

Before the evaluation of effective delayed neutron by proposed methodology in fixed-source calculations, the validity of the proposed methodology for k_{RR} and β_{RR} was examined in eigenvalue calculations with homogeneous cores.

β_{eigen}^{RR} in Eq. (4-12) is defined with the reaction rates as a parameter corresponding to the effective (adjoint flux weighted) delayed neutron fraction β_{eff}. To verify the agreement of β_{eigen}^{RR} with β_{eff}, bare spherical cores composed of the mixture of ^{1}H and ^{235}U were selected for the analysis by ANISN in the SRAC code system[14] based on the discrete ordinate method and by MCNP6.1[15] (10^9 total history; 1,000 active cycle) based on the continuous energy Monte Carlo method to calculate conventional β_{eff} with the adjoint flux and β_{eigen}^{RR} by the k-ratio method with reaction rates. As a series of the validation evaluation, the difference of k_{eff} is examined in ANISN and MCNP6.1 together with JENDL-4.0[16] with the variation of the H/U value and the radius of the homogeneous spherical bare core at critical state.

For the preparation of the discussion on β_{eigen}^{RR} calculated by MCNP6.1 and ANISN, the values of k_{eff} were compared in different H/U values and radius of the core. The comparison showed the value of k_{eff} by ANISN were calculated about 300 pcm lower with weak dependence on the core spectrum than that by MCNP6.1, as shown in Tables 4-1(a) and 4-1(b). This discrepancy is considered, besides the energy group effect, by affecting the difference of the scattering treatment for high anisotropic material such as hydrogen. Then, to evaluate these two effects separately, the infinite multiplication factors k_∞ were calculated by switching the boundary condition from vacuum to reflect. The discrepancy in the k_∞ increased to about 140 pcm in hard spectrum cores. In the comparison, the

discrepancy was confirmed to be about 280 pcm caused by the complexed effects of different scattering treatment and energy group between MCNP6.1 and ANISN.

Table 4-1(a)
Difference of effective multiplication factor k_{eff} and infinite multiplication factor k_{∞} in variation of spectrum for spherical cores with 2 m radius between MCNP6.1 and ANISN.

H/U	Number density (10^{24}/barn/cm)		k_{eff} and (k_{∞})		Difference in k_{eff} and (k_{∞}) [pcm]
	^{235}U	^{1}H	MCNP6.1*	ANISN	
400	1.80854E-05	7.23417E-03	1.00000 (1.71557)	0.99709 (1.71536)	291 (21)
300	2.25979E-05	6.77937E-03	1.00000 (1.78380)	0.99716 (1.78362)	284 (18)
200	3.16838E-05	6.33676E-03	1.00000 (1.85266)	0.99734 (1.85247)	266 (19)
100	5.88805E-05	5.88805E-03	1.00000 (1.90838)	0.99749 (1.90785)	251 (53)
50	1.12455E-04	5.62277E-03	1.00000 (1.90581)	0.99709 (1.90443)	291 (138)

*Standard deviation are 3 pcm and 1 pcm in vacuum and reflect boundary condition, respectively.

Table 4-1(b)
Difference of effective multiplication factor k_{eff} and infinite multiplication factor k_∞ in variation of spectrum for spherical cores with 1 m radius between MCNP6.1 and ANISN.

H/U	Number density		k_{eff} and (k_∞)		Difference in k_{eff} and (k_∞) (pcm)
	^{235}U	^{1}H	MCNP6.1*	ANISN	
400	3.61700E-05	1.44680E-02	1.00000 (1.71556)	0.99707 (1.71535)	291 (21)
300	4.51969E-05	1.35591E-02	1.00000 (1.78378)	0.99718 (1.78362)	284 (16)
200	6.33675E-05	1.26735E-02	1.00000 (1.85266)	0.99734 (1.85247)	266 (19)
100	1.17762E-04	1.17762E-02	1.00000 (1.90839)	0.99749 (1.90786)	251 (53)
50	2.24927E-04	1.12463E-02	1.00000 (1.90581)	0.99749 (1.90443)	291 (138)

*Standard deviation are 3 pcm and 1 pcm in vacuum and reflect boundary condition, respectively.

The reproduction of k_{eff} by reaction rates is examined with β_{eigen}^{RR} by Eq. (4-9) with MCNP6.1 before verifying the agreement of β_{eigen}^{RR} calculated by k-ratio method with reaction rates to β_{eff} calculated with adjoint flux in critical cores. In the evaluation with Eq. (4-9), the absorption reaction and leakage from the core were considered in the denominator because neutrons eventually vanish from the core by the absorption reactions and the leakage. And, the neutrons produced by fission reactions and (n, 2n) reactions were considered in the numerator of the production operator in Eq. (4-9). As shown in Table 4-2, the values of k_{RR}

fairly reproduced k_{eff} within their standard deviations, indicating further applicability to the estimation of β_{eff} by the k-ratio method with reaction rates.

Table 4-2
Validation of multiplication factor k_{RR} by reaction rate calculation for effective multiplication factor k_{eff} in variation of core spectrum and core radius.

H/U	Radius (m)	k_{eff}	k_{RR}
400	1	1.00000 ± 0.00003	0.99998 ± 0.00001
	2	1.00000 ± 0.00003	1.00001 ± 0.00001
300	1	1.00000 ± 0.00003	1.00000 ± 0.00001
	2	1.00000 ± 0.00003	0.99999 ± 0.00001
200	1	1.00000 ± 0.00003	0.99998 ± 0.00001
	2	1.00000 ± 0.00003	0.99999 ± 0.00001
100	1	1.00000 ± 0.00003	0.99999 ± 0.00001
	2	1.00000 ± 0.00003	1.00002 ± 0.00001
50	1	1.00000 ± 0.00003	1.00002± 0.00001
	2	1.00000 ± 0.00003	1.00000 ± 0.00001

In the comparison of β_{eigen}^{RR} between ANISN and MCNP6.1, as shown in Table 4-3, their agreements were confirmed within the standard deviation. However, small differences were found between β_{eff} and β_{eigen}^{RR} obtained by weighting with the next fission probability in MCNP6.1 and by the k-ratio method. This discrepancy is considered to be induced by the approximation imposed in the k-ratio method in Eq. (4-8). A dependence of the β_{eff} value is found on the H/U value regardless of the radius of the core. Here, a possibility can be considered that β_{eff} depends on the values of delayed neutron fraction β varied by the core spectrum. Then, β was calculated along to the position in different H/U core, as follows:

$$\beta(\mathbf{r}) = \frac{\int \upsilon_d(E)\Sigma_f(\mathbf{r},E)\varphi(\mathbf{r},E)dE}{\int \upsilon(E)\Sigma_f(\mathbf{r},E)\varphi(\mathbf{r},E)dE} \quad . \tag{4-21}$$

Since β showed a weak dependence on the core spectrum and the tendency distributed oppositely to that in β_{eff} along the core spectrum, as shown in Fig. 4-1, the increase of the β_{eff} is considered to be affected by the increase of the leakage of prompt neutrons from the core as the core spectrum becomes a hard one. The values of β_{eigen}^{RR} agreed with β_{eff} by the k-ratio method, verifying the equivalence of β_{eigen}^{RR} by the k-ratio method with reaction rates and β_{eff} in the simple homogeneous cores. And, the applicability and the precision by the proposed methodology were also verified through the comparison in the critical core.

Table 4-3
Comparison of effective delayed neutron fraction β_{eff} calculated by ANISN, MCNP6.1, $1-k_p/k_{eff}$ by k-ratio method with MCNP6.1, and $1 - k_{RR,\,p}/k_{RR}$ by k-ratio method with MCNP6.1 reaction rate calculation.

H/U	Radius [m]	Effective delayed neutron fraction [pcm]			
		ANISN	MCNP6.1	$1 - k_p/k_{eff}$	$1 - k_{RR,\,p}/k_{RR}$
400	1	834	832 ± 5	833 ± 4	830 ± 1
	2	834	832 ± 5	829 ± 4	830 ± 1
300	1	850	841 ± 5	847 ± 4	846 ± 1
	2	850	846 ± 5	856 ± 4	856 ± 1
200	1	866	866 ± 5	859 ± 4	858 ± 1
	2	866	858 ± 5	861 ± 4	860 ± 1
100	1	880	875 ± 5	877 ± 4	878 ± 1
	2	880	861 ± 5	880 ± 4	885 ± 1
50	1	880	875 ± 5	875 ± 4	874 ± 1
	2	884	869 ± 5	874 ± 4	±

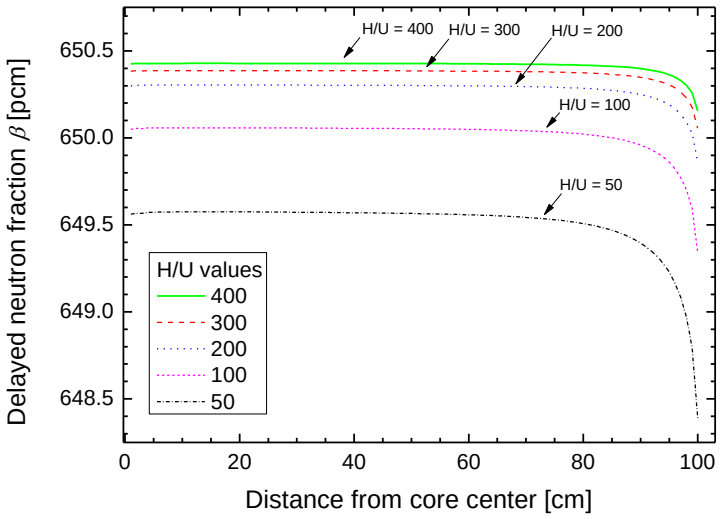

Fig. 4-1 Distribution of delayed neutron fraction β along to the distance from the core center in critical cores.

4.3.2 Eigenvalue calculation for Subcritical Core

To examine the applicability of the methodology by the k-ratio method with reaction rates for the estimation of β_{RR} in subcritical cores, which have the spherical core of middle range in the core spectrum (H/U = 100) and of 1 m in radius, were selected for its calculation by MCNP6.1 and ANISN. The subcriticality was ranged between 0.9999 and 0.9000 in k_{eff} by varying the number density of homogeneous mixture of ^{1}H and ^{235}U. To compare β_{RR} with β_{eff}, the calculations were performed under the condition of 10^6 history and 1000 cycles for the standard deviation of the β_{eigen}^{RR} and the reaction rates within 3 pcm and 0.02%, respectively.

In the subcritical core, the β_{eff} between by ANISN and MCNP6.1 showed good agreement regardless of the variation of the subcriticality as shown in Table 4-4. And, although the values of the β_{eigen}^{RR} by the k-ratio method with reaction rates showed a slight

difference from that by MCNP6.1 at deeper subcritical states, the agreement of β_{eigen}^{RR} to β_{eff} by the k-ratio method indicates the applicability of the proposed methodology to the estimation for subcritical cores. Here, the value of β_{eff} showed a dependency on the subcriticality, and increased as the subcriticality increased. A possibility could be considered the increased β values, however, the values showed almost same from the calculation in Eq. (4-21) by ANISN as shown in Fig.4-2. Then, from the variation of the spectrum at the core boundary as shown in Fig. 4-3, due to the increasing the leakage of the prompt neutrons along to the subcriticality, the value of β_{eff} is considered to increase along the subcriticality. Also, in the estimation of β_{eigen}^{RR} for the subcritical cores by varying the subcriticality, the equivalence of β_{eigen}^{RR} obtained with reaction rates was verified to β_{eff} obtained by the k-ratio method with adjoint flux for weighting function.

Table 4-4
Comparison of effective delayed neutron fraction calculated by ANISN, MCNP6.1, $1-k_p/k_{eff}$ by k-ratio method with MCNP6.1, and $1 - k_{RR,p}/k_{RR}$ by k-ratio method with MCNP6.1 reaction rate calculation in the subcritical cores (H/U = 100).

k_{eff}	Effective delayed neutron fraction (pcm)			
	ANISN	MCNP6.1	$1 - k_p/k_{eff}$	$1 - k_{RR,p}/k_{RR}$
1.000	880	875 ± 5	877 ± 4	877 ± 1
0.999	880	876 ± 5	877 ± 4	875 ± 1
0.980	886	889 ± 5	885 ± 4	879 ± 1
0.950	896	898 ± 5	889 ± 4	889 ± 1
0.900	913	915 ± 5	904 ± 5	904 ± 1

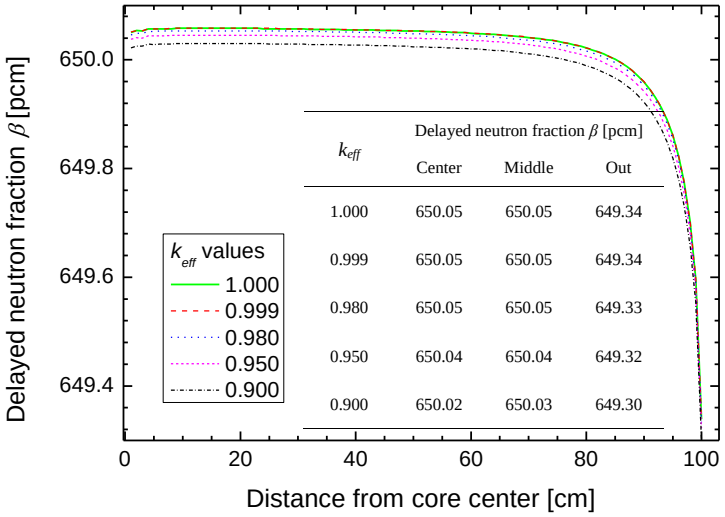

k_{eff}	Delayed neutron fraction β [pcm]		
	Center	Middle	Out
1.000	650.05	650.05	649.34
0.999	650.05	650.05	649.34
0.980	650.05	650.05	649.33
0.950	650.04	650.04	649.32
0.900	650.02	650.03	649.30

Fig. 4-2 Distribution of delayed neutron fraction β along to the distance from the core center in the subcritical cores.

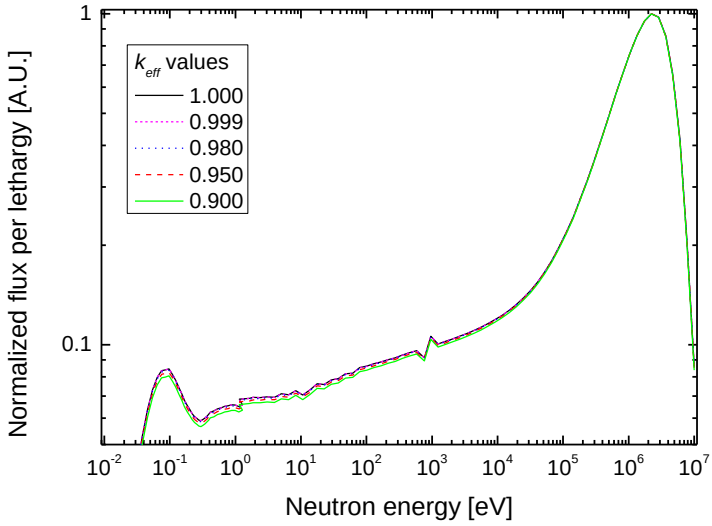

Fig. 4-3 Neutron spectra at the outer part of the subcritical cores in eigenvalue calculation.

4.3.3 Energy of External Neutron Source

On the basis of the calculation methodology by the k-ratio method with reaction rates in Eq. (4-20), β_{RR}^{source} is estimated in the existence of the neutron source for the subcritical cores, by varying the neutron energy of the isotopic neutron source, and its position. The calculation was performed for the subcritical core shown in Table 4-5 with the total history of 10^9 by MCNP6.1 together with JENDL-4.0.

Table 4-5
Comparison of effective delayed neutron fraction calculated by ANISN, MCNP6.1, $1-k_p/k_{eff}$ by k-ratio method with MCNP6.1, and $1 - k_{RR,p}/k_{RR}$ by k-ratio method with MCNP6.1 reaction rate calculation in the subcritical cores (H/U = 100).

k_{eff}	Effective delayed neutron fraction [pcm]			
	ANISN	MCNP6.1	$1 - k_p/k_{eff}$	$1 - k_{RR,\,p}/k_{RR}$
1.000	880	875 ± 5	877 ± 4	877 ± 1
0.999	880	876 ± 5	877 ± 4	875 ± 1
0.980	886	889 ± 5	885 ± 4	879 ± 1
0.950	896	898 ± 5	889 ± 4	889 ± 1
0.900	913	915 ± 5	904 ± 5	904 ± 1

The value of β_{RR}^{source} remarkably increased by the increase of the energy of neutron source and of the subcriticality regardless of its position, as shown in Figs. 4-4 and 4-5. By inducing the higher energy neutrons from outside of the core, the neutron flux is considered to be formed at the outer position, resulting in the increase of the leakage of the prompt neutrons compared with that of the delayed neutrons. From the difference of the neutron flux distributions between by the fixed-source and the eigenvalue calculations, the leakage of the neutrons decreases by the neutron source placed at the core center compared with the case without the neutron source, and the value of β_{RR}^{source} distributes under that of β_{eff}. Oppositely, in the case of the neutron source placed outside of the core, the leakage of the neutrons increases compared with that in the eigenvalue calculation, and the value of β_{RR}^{source} remarkably distributes over that of β_{eff}. Also, the dependence on the energy of the neutron source differed in its position between at the center and at the vicinity of the boundary.

Through the consideration of the β_{eff} value in the existence of the neutron source, the β_{RR}^{source} was obtained from the reaction rate calculations depending on its energy and its position.

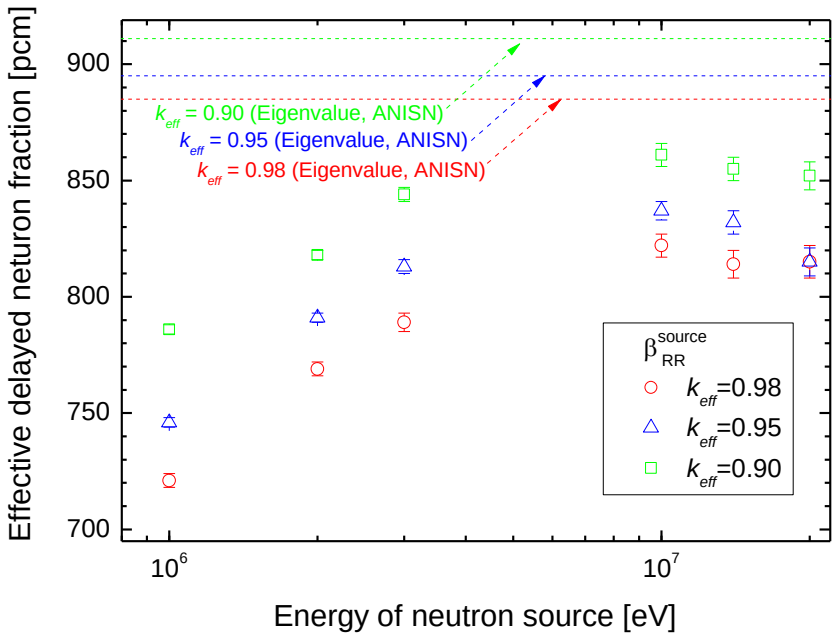

Fig. 4-4 Distribution of β_{RR}^{source} along to the energy of the neuron source at the core center as a point source.

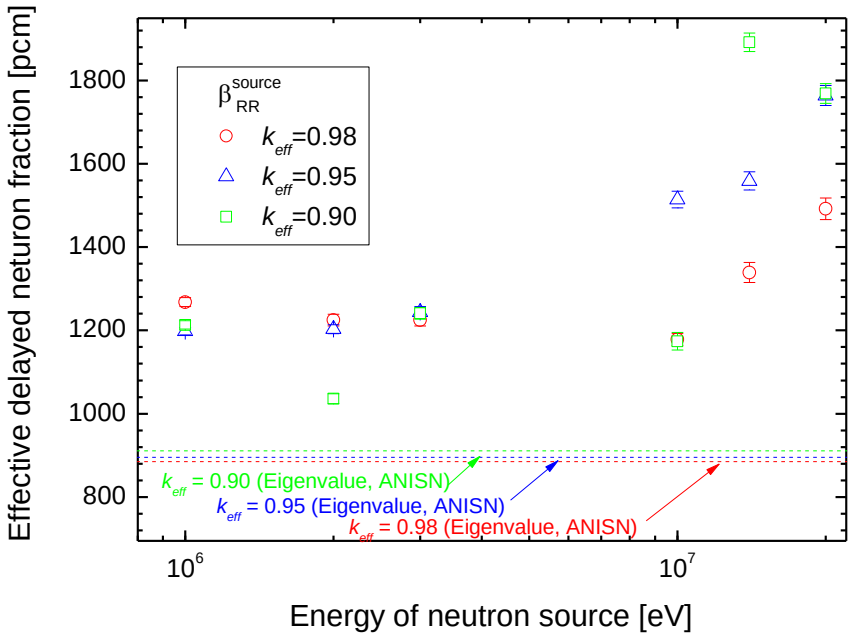

Fig. 4-5 Distribution of β_{RR}^{source} along to the energy of the neuron source at the core boundary as a spherical shell source.

4.4 Application to Experimental Analysis

4.4.1 Experimental settings

The critical core (1/8”P60EU-EU(3)) reference core; Fig. 2-1(a)) was assembled at the Kyoto University Critical Assembly (KUCA) A-core with 1/8”P60EU-EU fuel rods shown in Fig. 2-1(b) This core was selected for considering the variation of β_{eff} along the subcritilicality level. For the measurement of subcriticality, protons accelerated to 100 MeV were injected onto a disk-type tungsten (W) target in order to generate spallation neutrons. The accelerator was operated in pulsed mode and the repetition rate of the pulse was 20 Hz. The time width of the pulsed proton beam was 100 ns. The averaged proton current was 50 pA. The target was located at (15, H) grid in Fig. 2-1(a). The diameter and the thickness of the target were 50 mm and 12 mm, respectively. The subcriticality was measured by the extrapolated area ratio method[17] without considering the spatial effects. The neutron signals were obtained with the use of a BF_3 detector inserted diagonally at (10, U; Fig. 2-1(a)) to the core for the measurements of the subcriticality. For the reference core in the critical experiment, excess reactivity and control rod worth (C1, C2 and C3) were measured by the positive period method and the rod drop method, respectively. Experimental analyses were available to examine the precision of eigenvalue calculations by the Monte Carlo method and the accuracy of measured subcriticality by the extrapolated area ratio method. To achieve deep subcriticality, some of the fuel rods “F” (Fig. 2-1(a)) were substituted for polyethylene reflectors and configured as shown in Figs. 2-1(c) and 2-1(d), and the subcriticality level then ranged between about 1300 and 7500 pcm.

In this experiment, different external neutron sources (spallation neutrons by the injection of 100 MeV protons onto the W target, and 14 MeV neutrons by the injection of deuteron beams onto the tritium target) were used for considering the variation of β_{eff}

caused by the spectrum of external neutron source in the subcritical estimation.

The subcritical core at $k_{eff} \simeq 0.85$ (Th-HEU-5PE core shown in Figs. 2-2(a) and 2-22(b)), was composed of the polyethylene reflectors, fuel rods of thorium (Th; 2" × 2" and 1/8" thick), HEU and PE moderators, as shown in Fig. 2-2(c). 14 MeV neutrons were produced by 0.4 mA deuteron beam, 10 Hz pulsed frequency and 10 μs pulsed width. 100 MeV proton beams were injected onto the W target at 50 mm spot size, 10 pA intensity, 20 Hz pulsed frequency and 100 ns pulsed width.

The subcriticality was measured by same method with that in uranium-loaded ADS core. Here, the measured subcriticality could be affected by spatial effects especially in such deep subcritical core. Then, the neutron signals were obtained with the use of an optical fiber detector[18] at the core center (Figs. 2-2(a) and 2-2(b)) in Th-HEU-5PE core. The optical fiber (1 mm diam. and 200 mm long) was coated with a powdered mixture of ^{6}LiF (95% enrichment) for detection of thermal neutrons based on ^{6}Li(n, t)^{4}He reactions and ZnS(Ag) for scintillation.

4.4.2 Results and Discussion

For the validation estimation of the proposed methodology with reaction rates, the multiplication factor k_{RR} thus deduced should be compared with the results in k_{eff} shown in Eq. (4-6) by the Monte Carlo calculations to examine the validity of k_{RR} obtained by Eq. (4-9). Reaction rate calculations were performed by MCNPX-2.5.0[19]. Comparing the results of k_{eff} and k_{RR} in Eqs. (4-6) and (4-9), respectively, the results by the reaction rates in Eq. (4-9) revealed fairly good agreement with a difference of 10 pcm with those in Eq. (4-6) by MCNPX, as shown in Table 4-6. The results revealed that the proposed methodology of k_{RR}

with the use of reaction rates in Eq. (4-9) is appropriate through the comparison with the effective multiplication factor by the eigenvalue calculations. Note that (n, 2n) and (n, 3n) reactions were not considered for the estimation of the neutron productions, because there was no relevant difference between considering them or not in the uranium- and the thorium-loaded cores, respectively, in the eigenvalue calculations shown in Eq. (4-12).

Table 4-6
Comparison between effective multiplication factors k_{eff} by MCNPX-2.5.0 and k_{RR} in Eq. (4-9) with reaction rate calculations.

Core	Case	k_{eff} (MCNPX-2.5.0)	k_{RR} (MCNPX-2.5.0)
1/8"P60EU-EU(3) core* (Spallation neutrons)	I-1	0.99093 ± 0.00009	0.99096 ± 0.00013
	I-2	0.98274 ± 0.00009	0.98269 ± 0.00013
	I-3	0.97627 ± 0.00009	0.97619 ± 0.00013
	I-4	0.97662 ± 0.00009	0.97655 ± 0.00012
	I-5	0.95680 ± 0.00009	0.95667 ± 0.00012
	I-6	0.95278 ± 0.00009	0.95281 ± 0.00012
	I-7	0.93358 ± 0.00009	0.93353 ± 0.00012
Th-HEU-5PE (Spallation neutrons)	II-1	0.86397 ± 0.00008	0.86387 ± 0.00012
Th-HEU-5PE (14 MeV neutrons)	II-2	0.84924 ± 0.00008	0.84923 ± 0.00012

*: k_{eff} = 1.00344 ± 0.00009 (at critical state by MCNP2.5.0 with ENDF/V-VII.0)

On the basis of the theoretical preparation by the comparison between k_{eff} and k_{RR}, $\beta_{\text{eff,eigen}}$ and $\beta_{\text{eigen}}^{\text{RR}}$, as defined in Eqs. (4-8) and (4-12), can be obtained from the eigenvalue calculations, compared with the reference one obtained by MCNP6.1. Through the comparison with β_{eff} by MCNP6.1 shown in Table 4-7, the estimation of $\beta_{\text{eff, eigen}}$ in Eq. (4-8) demonstrated that the methodology is valid in the subcriticality level of interest. Also, the value of $\beta_{\text{eigen}}^{\text{RR}}$ in Eq. (4-12) with the use of reaction rates showed good agreement with those by MCNP6.1, as shown in Table 4-7, indicating a high-precision of the reaction rates and an applicability of the k-ratio method with reaction rates. From the results in Table 4-7, the proposed methodology by the k-ratio method was confirmed valid on the basis of the reaction rates by the eigenvalue calculations.

Table 4-7

Comparison between β_{eff} by MCNP6.1, $\beta_{\text{eff,eigen}}$ by the k-ratio method in Eq. (8), $\beta_{\text{eigen}}^{\text{RR}}$ by the k-ratio method with reaction rate calculations (eigenvalue calculation) in Eq. (4-12), $\beta_{\text{source}}^{\text{RR}}$ by the k-ratio method with reaction rate calculations (fixed-source calculation) in Eq. (4-20), and β (eigenvalue and fixed-source calculations) in Eq. (4-1).

Case	Effective delayed neutron fraction (and delayed neutron fraction) (pcm)			
	β_{eff} (MCNP6.1)	$\beta_{\text{eff,eigen}}$ (MCNPX-2.5.0)	$\beta_{\text{eigen}}^{\text{RR}}$ (MCNPX-2.5.0)	$\beta_{\text{source}}^{\text{RR}}$ (MCNPX-2.5.0)
I-1	817 ± 11	797 ± 9	791 ± 13 (649 ± 22)	809 ± 43 (637 ± 32)
I-2	794 ± 11	801 ± 9	795 ± 13 (649 ± 22)	873 ± 45 (636 ± 33)
I-3	814 ± 11	811 ± 9	807 ± 13 (649 ± 22)	880 ± 46 (636 ± 33)
I-4	806 ± 11	810 ± 9	809 ± 13 (649 ± 22)	826 ± 55 (637 ± 36)
I-5	822 ± 11	825 ± 9	838 ± 13 (649 ± 22)	819 ± 57 (637 ± 37)
I-6	808 ± 11	824 ± 9	806 ± 13 (649 ± 22)	865 ± 81 (636 ± 44)
I-7	829 ± 11	801 ± 9	783 ± 13 (649 ± 22)	792 ± 86 (635 ± 45)
II-1	808 ± 11	795 ± 9	803 ± 9 (652 ± 24)	910 ± 11 (645 ± 14)
II-2	798 ± 11	802 ± 9	802 ± 9 (653 ± 24)	881 ± 7 (635 ± 9)

Fixed-source calculations were performed by MCNPX-2.5.0 with 10^9 total histories with nuclear data libraries of ENDF/B-VII.0[20] and JENDL/HE-2007[21] as shown in Table 4-8. For the case of the spallation neutrons, since neutrons over 20 MeV neutrons could be produced by the 100 MeV proton injections into the W target, JENDL/HE-2007 has full advantage in the accuracy of the particle transport for neutrons over the energy of 20 MeV. However, because the yields for total and prompt neutrons are not provided in JENDL/HE-2007, ENDF/B-VII.0 was used for fissile and fissionable nuclei. β values calculated with the fluxes by eigenvalue and fixed-source calculations showed independency of the subcriticality, as shown in Table 4-7. However, the β values were decreased by the flux in fixed-source calculation. Then, $\beta_{\text{source}}^{\text{RR}}$ in Eq. (4-20) deduced by the fixed-source calculations indicated different values from β (fixed-source calculation), and these values were varied larger than those of β_{eff} by the eigenvalue calculations (MCNP6.1). In the Cases I-1 to I-7, the increase of buckling in the core can be the reason to increase β_{eff} and $\beta_{\text{source}}^{\text{RR}}$ by the fuel rod replacement (Cases I-1, I-4, I-6) and by the control rod incertion (Cases I-3, I-5, I-7) because of especially increasing the leakage of prompt neutrons having higher energy compared to delayed neutrons. The neutron flux distribution was distorted by the injection of spallation neutrons having dominantly lower energy with the comparison of 14 MeV neutrons in Case II-1. This distorted flux distribution was considered to be induced by the leakage of prompt neutrons, resulting in the increase of $\beta_{\text{source}}^{\text{RR}}$.

Table 4-8
List of nuclear data libraries for calculation of $\beta_{\text{source}}^{\text{RR}}$ in particle transport simulations of the ADS experiments.

	Neutrons	Protons
Spallation neutrons	JENDL/HE-2007 ENDF/B-VII.0 (for U and Th only)	JENDL/HE-2007
14 MeV neutrons	ENDF/B-VII.0	-

The target results of the measured subcrtiticality (pcm units) in the uranium-loaded core were obtained from measured subcriticality in dollar unit multiplied by β_{eff} (MCNP6.1), $\beta_{\text{eigen}}^{\text{RR}}$ and $\beta_{\text{source}}^{\text{RR}}$ in Eqs. (4-11) and (4-19) (Table 4-7), respectively, as shown in Table 4-9. The measured subcriticality with the use of $\beta_{\text{source}}^{\text{RR}}$ in Eq. (4-20) for conversion from dollar units into pcm units by the fixed-source calculations showed good agreement with the reference subcriticality within a relative difference of 10% in the variation of the subcriticality level. Further, $\beta_{\text{source}}^{\text{RR}}$ worked well for the results of measured subcriticality, comparing those of reference subcriticality. In Cases I-4 to I-7 (Table 4-9), there was a slight difference between β_{eff} and $\beta_{\text{source}}^{\text{RR}}$.

Table 4-9
Results of subcriticality on the basis of effective delayed neutron fractions estimated by MCNP6.1, $\beta_{\text{eigen}}^{\text{RR}}$ and $\beta_{\text{source}}^{\text{RR}}$.

Case	Reference subcriticality (pcm)	Measured subcriticality (pcm)		
		β_{eff} (MCNP6.1)	$\beta_{\text{eigen}}^{\text{RR}}$ (MCNPX-2.5.0)	$\beta_{\text{source}}^{\text{RR}}$ (MCNPX-2.5.0)
I-1	1200 ± 36	1147 ± 17 (1.05 ± 0.02)	1111 ± 20 (1.08 ± 0.02)	1136 ± 61 (1.06 ± 0.06)
I-2	2012 ± 60	1847 ± 27 (1.09 ± 0.02)	1850 ± 30 (1.09 ± 0.02)	2032 ± 105 (0.99 ± 0.05)
I-3	2657 ± 80	2419 ± 35 (1.09 ± 0.02)	2400 ± 40 (1.11 ± 0.02)	2615 ± 136 (1.02 ± 0.05)
I-4	2722 ± 32	2679 ± 39 (1.02 ± 0.02)	2688 ± 44 (1.02 ± 0.02)	2745 ± 183 (1.00 ± 0.07)
I-5	4891 ± 50	5036 ± 84 (0.96 ± 0.02)	5134 ± 88 (0.95 ± 0.02)	5015 ± 354 (0.97 ± 0.07)
I-6	5291 ± 54	5489 ± 85 (0.97 ± 0.02)	5475 ± 95 (0.97 ± 0.02)	5877 ±554 (0.90 ± 0.09)
I-7	7474 ± 75	8421 ± 144 (0.89 ± 0.02)	7952 ± 149 (0.94 ± 0.02)	8050 ± 874 (0.93 ± 0.10)

Quantities of parentheses indicate the C/E values.

In deep subcritical cores, the measured subcriticality in the area ratio method is generally considered inaccurately obtained in pcm units to compare with reference one because an assumption is imposed on the measurements: all source neutrons induce the fission reactions and neuron signals originate from correlated neutrons to the fission multiplication. Moreover, in case of different external neutron source for the deep subcritical core, as shown in Table 4-10, subcriticalities were compared in terms of the k_{eff}. The difference of the reference k_{eff} between spallation and 14 MeV neutrons is considered to be caused by the slight difference in the core configuration of the air gap shown in Figs 2-2(a) and 2-2(b). Here, the subcriticality with $\beta_{\mathrm{source}}^{\mathrm{RR}}$ was observed to reveal a comparative tendency through the comparison of the subcriticality with β_{eff} within the C/E value of 2%. The applicability of proposed methodology was also confirmed in the variation of external neutron source.

Finally, these results demonstrated the fact that proper values for subcriticality determination with the area ratio technique were successfully obtained for the subcriticality estimation with the use of proposed methodology by the fixed-source calculations.

Table 4-10
Comparison of k_{eff} and their C/E values estimated by MCNP6.1, β_{eigen}^{RR} and β_{source}^{RR} in different external neutron sources.

Case	Reference k_{eff}	Measured k_{eff}		
		β_{eff} (MCNP6.1)	β_{eigen}^{RR} (MCNPX-2.5.0)	β_{source}^{RR} (MCNPX-2.5.0)
II-1	0.86397 ± 0.00008	0.89707 ± 0.00387 (0.96 ± 0.01)	0.89945 ± 0.00392 (0.96 ± 0.01)	0.88559 ± 0.00418 (0.98 ± 0.01)
II-2	0.84924 ± 0.00008	0.84775 ± 0.02543 (1.00 ± 0.03)	0.84516 ± 0.02581 (1.00 ± 0.03)	0.83243 ± 0.02743 (1.02 ± 0.03)

Quantities of parentheses indicate the C/E values.

4.5 Conclusion

To estimate the effective delayed neutron fraction in the existence of the neutron source, the calculation methodology was newly proposed by applying the k-ratio method with the reaction rates in the fixed-source calculation. The proposed methodology was validated with the conventional methodology with the adjoint flux in the eigenvalue calculations for the bare homogeneous spherical cores by varying the core spectrum and the core radius.

As a preparation to apply the proposed methodology to the subcriticality measurement, the validation calculation of $\beta_{\mathrm{eigen}}^{\mathrm{RR}}$ by k-ratio method with reaction rates was examined with the homogeneous core in the critical and subcritical states. In the comparison between β_{eff} (weighted by the adjoint flux) and $\beta_{\mathrm{eigen}}^{\mathrm{RR}}$, the values agreed regardless of the variation of the core spectrum for the critical core. Also, in the analysis for the subcritical cores, by comparing between β_{eff} and $\beta_{\mathrm{eigen}}^{\mathrm{RR}}$, its validation demonstrates the equivalence between the proposed methodology and the conventional methodology. In the analysis of $\beta_{\mathrm{RR}}^{\mathrm{source}}$ for the subcritical cores with the neutron source, the dependence of $\beta_{\mathrm{RR}}^{\mathrm{source}}$ on the energy of the neutron source was found and differently distributed by the position of the neutron source placed at the core center and at the vicinity of the boundary.

Subsequently, the calculation methodology of $\beta_{\mathrm{source}}^{\mathrm{RR}}$ by the k-ratio method with external neutron source has been applied subcriticality estimation. Subcriticality measurements were carried at the KUCA-A cores to examine its applicability of proposed calculation methodology by varying the subcriticality and the external neutron source.

To examine the validity of the proposed methodology also for heterogeneous cores, the eigenvalue calculations were performed with the reaction rates, and the multiplication factor k_{RR} with reaction rates and $\beta_{\mathrm{eigen}}^{\mathrm{RR}}$ by the k-ratio method with reaction rates compared

with the reference ones obtained by MCNPX and MCNP6.1, respectively. The results of k_{RR} and β_{eigen}^{RR} showed good agreement with the reference ones, demonstrating an appreciation of the calculation methodology. For the estimation of subcriticality by the fixed-source calculations, β_{source}^{RR} was observed to be dependent on the variation of subcriticality and external neutron source. Finally, the subcriticality with β_{source}^{RR} were acquired well ranging between about 0.99 and 0.97 in k_{eff}, and revealed the comparative tendency in the deep subcriticality through the estimation with the use of β_{source}^{RR} obtained by the proposed calculation methodology.

CHAPTER 5

CONCLUSIONS

In this dissertation, β_{eff} was studied in the subcritical states with the external neutron source through the deduction and the calculations in the ADS experiments. The present thesis is mainly composed of three topics as follows:

(A) the investigation of the dependence of the external neutron source and the subcriticality on β_{eff} through the ADS experiments,

(B) the verification of the dependence of the subcriticality on β_{eff}, suggested in topic (A), through the experimental approach of β_{eff} with the stable and pulsed neutron source outside of the core, comparing with that obtained by the eigenvalue calculation,

(C) the development of the β_{eff} calculation methodology in the fixed-source calculations for the analysis of the subcritical core with the external neutron source, and the comparison of measured subcriticality with the use of β_{eff} obtained by the proposed methodology and the calculated subcriticality, demonstrating the applicability of β_{eff} by proposed methodology to the subcritical measurement.

As for the topic (A), ADS experiments were carried out at the KUCA-A core by varying the external neutron source (spallation neutrons obtained by the injection of 100 MeV protons onto W target and 14 MeV neutrons obtained by the D-T reactions) and the subcriticality, in order to examine the neutronic characteristics by obtaining the reactor

physics parameters.

In the subcritical state, the subcriticality was obtained by the extrapolated area ratio method of the PNS method. The measured subcriticality in dollar units was converted into that in pcm units with the use of β_{eff} obtained by the eigenvalue calculations. At the shallow subcriticality, when the measured subcriticality in PNS method was compared with that by another measurement method considering accurate compared with other methods, the difference was found within the relative difference of 10%. Also, the value of β_{eff} increased along to deepening the subcriticality in the eigenvalue calculations. Further, in the PNS method by varying the external neutron source, the subcriticality in dollar units indicated different values, and also the values of the prompt neutron decay constant differed each other. These experimental results suggested the possibility that the kinetic parameter, especially β_{eff}, varies with the subcriticality and the external neutron source.

From measured results of the reaction rate distributions, measured reaction rate distribution varied with the energy of the external neutron source. The reason of this variation was attributable to the difference of neutron leakage, when the different external neutron source was used, affecting the variation of β_{eff}.

Through the ADS experiments by varying the subcriticality and the external neutron source, further study is concluded to be conducted to investigate the dependency of the subcriticality and the external neutron source on β_{eff}.

As for the topic (B), on the basis of the fact, which the value of β_{eff} was increased by deepening the subcriticality, mentioned in the ADS experiments in topic (A), the dependency of the subcriticality on β_{eff} was investigated by the β_{eff} measurements. In previous measurements, the subcriticality was closed to the critical state, and the stable neutron source was located at the core center, assuming that the neutron flux is

approximated to that in the fundamental mode. Here, the applicability of the Nelson number method was investigated in β_{eff} measurements when the subcriticality was ranged between about 1800 and 2800 pcm, and the stable neutron source of Am-Be was located outside the core. The measured results showed the good agreement with the calculated ones within the relative difference of 10%, demonstrating its applicability when the stable neutron source was located outside the core.

In next, β_{eff} measurement method, as well as same concept with Nelson number method, was attempted to evaluate β_{eff} with the use of pulsed neutron source. Here, the β_{eff} evaluation equations showed agreement with the case of the stable neutron sources used, when the source intensity was newly defined by considering the pulsed width and repetition time in the pulsed neutron source. To evaluate the applicability of proposed method for the pulsed neutron source, the PNS experiments were carried out, and the dependency of the subcriticality on the β_{eff} was investigated through these measurements. The measured results showed the agreement with the β_{eff} obtained by the eigenvalue calculations within the relative difference of 12% in the subcritical range between k_{eff} = 0.99 and 0.93, demonstrating the validity of the proposed method in the PNS experiments. Further, the tendency of β_{eff} to increasing along to deepening the subcriticality was also obtained as mentioned in the results of the ADS experiments. However, since the measured β_{eff} is equivalent to that obtained by the eigenvalue calculations with a correction factor of the neutron flux in fundamental mode. Finally, the β_{eff} calculations were concluded requisite to investigate the influence of the external neutron source on β_{eff} considering the energy and the position of the external neutron source.

As for the topic (C), on the basis of the results shown in the topics (A) and (B), the calculation methodology on β_{eff} was newly proposed, and was aimed to reveal its

applicability through the subcriticality measurement at KUCA and the experimental analysis. For the evaluation of the applicability of the proposed methodology, the experiments conducted in topic (A) was employed for the subcriticality measurement. This proposed methodology can approximately reproduce β_{eff} obtained by the deduction of k_{eff} with the use of reaction rates. Also, k_{eff} with reaction rates was examined in the comparison with k_{eff} in the eigenvalue calculations. The comparison showed good agreement within the relative difference of 0.01% regardless of the subcriticality, demonstrating its validity to deduce the multiplication factor by the proposed methodology with reaction rates.

Further, since the multiplication factor is not defined under the existence of the external neutron source, the proposed methodology was extended into the fixed-source calculations by defining the imaginary multiplication factor. The subcriticality measurement with the use of β_{eff} obtained by the eigenvalue calculations showed 10% difference with the subcriticality by measurement method considered to be accurate compared with other methods at shallow subcriticality. Conversely, with the use of β_{eff} obtained by the proposed methodology, the accuracy improvement was found to be the relative difference of 3%. The β_{eff} obtained by the proposed methodology was applied to the subcriticality measurement until 7500 pcm, and the comparison showed agreement within the relative difference of 10% between the measured and the calculated subcriticalities. Also, in the deep subcritical core having $k_{\mathrm{eff}} \simeq 0.85$, the difference of k_{eff} between the measurement and the calculation was within 2%, indicating the applicability of β_{eff} obtained by the proposed methodology to the subcritical measurement. Thus, the validation and the applicability were demonstrated through the subcriticality measurement by varying the subcriticality and the external neutron source.

Through the present studies, the measurement methodology of β_{eff} was developed for

the subcritical core with both the stable and the pulsed neutron sources located outside the core. Also, the calculation methodology of β_{eff} considering the energy and the position of the external neutron source was developed, and was validated through the experimental analyses of the subcritical measurement. From these results, the knowledge of the accurate estimation of β_{eff} in various subcritical cores with the source neutron provides the accurate improvement of subcriticality measurements, and is expected to be applied to the safety assessment such in the ADS operations.

REFERENFCE

CHAPTER 1

1. International Atomic Energy Agency (IAEA), “Nuclear Power Reactors in the World,” IAEA-RDS-2/36 (2016).
2. International Atomic Energy Agency (IAEA), “The Power Reactor Information System (PRIS) and its Extension to Non-electrical Applications, Decommisioning and Delayed Projects Information,” Technical Report Series No. 428 (2005).
3. T. Vieno and H. Nordman, “Safety Assessment of Spent Fuel Disposal in Hästholmen, Kivetty, Olkiluoto and Romuvaara. TILA-99, report POSIVA 99-07, Posiva Oy, Helsinki, Finland (1999).
4. H. Oigawa, K. Nishihara, M. Kazuo, K. Takaumi, Y. Arai, Y. Morita, S. Nakayama and J. Katakura, “Status and Future Plan of Research and Development on Partitioning and Transmutation Technology for Long-lived Nuclides in JAERI,” JAERI Review 2005-043, JAERI (2005).
5. S. Honma, “Handbook on Process and Chemistry of Nuclear Fuel Reprocessing 3rd Edition,” JAEA-Review 2015-002, JAEA (2015).
6. Organization for Economic Co-operation and Development Nuclear Energy Agency (OECD/NEA), *Accelerator-driven Systems (ADS) and Fast Reactors (FR) in Advanced Nuclear Fuel Cycles: A Comparative Study*, NEA3109 (2002).
7. T. Mukaiyama, T. Takizuka, M. Mizumoto, U. Ikeda, T. Ogawa, A. Hasegawa, A. Hasegawa, H. Takeda and H. Takeno, “Review of Research and Development of Accelerator-Driven system in Japan for Transmutation of Long-Lived Nuclides,” *Prog.*

Nucl. Energy, **38**, 107 (2001).

8. *A European Roadmap for Developing Accelerator Driven System (ADS) for Nuclear Waste Incineration*, ETWG, (2001).
9. *A Roadmap for Developing Accelerator Transmutation of Waste (ATW) Technology*, Report to Congress DOE/RW-0519, (1999).
10. K. Tsujimoto, T. Sasa, K. Nishihara, H. Oigawa,and H. Takano, "Neutronics Design for Lead-Bismuth Cooled Accelerator-Driven System for Transmutation of Minor Actinide," *J. Nucl. Sci. Technol.*, **41**, 21 (2004).

11 T. Sugawara, K. Nishihara, K. Tsujimoto, T. Sasa and H. Oigawa, "Analytical Validation of Uncertainty in Reactor Physics Parameters for Nuclear Transmutation Systems," *J. Nucl. Sci. Technol.*, **47**, 521 (2010).

12. M. Salvatores, M. Martini, I. Slessarev, R. Soule, J. C. Cabrillat, J. P. Chauvin, Ph. Finck, R. Jacqmin and A.Tchistiaakov, "MUSE-1: A First Experiment at MASURCA to Validate the Physics of Sub-Critical Multiplying Systems Relevant to ADS," 2nd ADTT conference, Kalmar (Sweden), June 1996.
13. R. Soule, W. Assal, P. Chaussonnet, C. Destouches, C. Domergue, C. Jammes, J. M. Laurens, J. F. Lebrat, F. Mellier, G. Perret, G. Rimpault and H. Servière, "Neutronic Studies in Support of Accelerator-Driven Systems: The MUSE Experiments in the MASURCA Facility," *Nucl. Sci. Eng.*, **148** 124 (2004).
14. A. Gandini and M. Salvatores, "The Physics of Subcritical Multiplying Systems," *J. Nucl. Sci. Technol.*, **39**, 673 (2002).
15. H. Rief and H. Takahashi, "The Transient Behavior of Accelerator-driven Sub-critical Systems," *Int. Mtg.* "8ème journées SATURNE," May 1994.
16. H. Iwamoto, K. Nishihara, T. Sugawara and K. Tsujimoto, "Sensitivity and Uncertainty Analysis for an Accelerator-Driven System with JENDL-4.0," *J. Nucl. Sci. Technol.*, **50**,

856 (2013).

17. J. B. Dragt, J. W. M. Dekker, H. Gruppelaar and A. J. Janssen, “Methods of Adjustment and Error Evaluation of Neutron Capture Cross Sections; Application to Fission Product Nuclides,” *Nucl. Sci. Eng.*, **62**, 117 (1977).
18. T. Takeda, A. Yoshimura, T. Kamei and K. Shirakata, “Prediction Uncertainty Evaluation Methods of Core Performance Parameters in Large Liquid-Metal Fast Breeder Reactors,” *Nucl. Sci. Eng.*, **103**, 157 (1989).
19. T. Sano and T. Takeda, “Generalized Bias Factor Method for Accurate Prediction of Neutronics Characteristics,” *J. Nucl. Sci. Technol.*, **43**, 1465 (2006).
20. T. Kugo, T. Mori and T. Takeda, “Theoretical Study on New Bias Factor Methods to Effectively Use Critical Experiments for Improvement of Prediction Accuracy of Neutronic Characteristics,” *J. Nucl. Sci. Technol.*, **44**, 1509 (2007).
21. T. Sano, T. Takeda and M. Yamasaki, “A New Uncertainty Reduction Method for Fuel Fabrication Process with Erbia-Bearing Fuel,” *J. Nucl. Sci. Technol.*, **46**, 226 (2009).
22. T. Kugo, M. Andoh, K. Kojima, M. Fukushima, T. Mori, Y. Nakano, S. Okajima, T. Kitada and T. Takeda, ”Prediction Accuracy Improvement of Neutronic Characteristics of a Breeding Light Water Reactor Core by Extended Bias Factor Methods with Use of FCA-XXII-1 Critical Experiments,” *J. Nucl. Sci. Technol.*, **45**, 288 (2008).
23. K. Yokoyama, M. Ishikawa and T. Kugo, ”Extended Cross-Section Adjustment Method to Improve the Prediction Accuracy of Core Parameters,” *J. Nucl. Sci. Technol.*, **49**, 1165 (2012).
24. N. G. Sjostrand, “Measurement on a Subcritical Reactor Using a Pulsed Neutron Source,” *Arkiv Fysik*, **11**, 233 (1956).
25. T. Gozaini, “A Modified Procedure for the Evaluation of Pulsed Source Experiments in Subcritical Reactors,” *Nukleonik*, **4**, 348 (1962).

26. G. R. Keepin, *Physics of Nuclear Kinetics*, Addison Wesley, Reading, Massachusetts (1965).

27. M. M. Bretsher, "Perturbation Independent Methods for Calculating Research Reactor Kinetic Parameters," ANL/RERTR/TM30, Argonne National Laboratory (1997).

28. H. Hurwitz, "Physical Interpretation of the Adjoint Flux: Iterated Fission Probability," *Naval Reactor Physics Handbook*, Vol. I, pp. 864-869, A. Radkowsky, Ed., U. S. Atomic Energy Commission (1964).

29. R. K. Meulekamp and S. C. van der Marck, "Calculating the Effective Delayed Neutron Fraction with Monte Carlo," *Nucl. Sci. Eng.*, **152**, 142 (2006).

30. Y. Nauchi and T. Kameyama, "Proposal of Direct Calculation of Kinetic Parameters β_{eff} and Λ Based on Continuous Energy Monte Carlo Method," *J. Nucl. Sci. Technol.*, **42**, 503 (2005).

31. G. Chiba, Y. Nagaya and T. Mori, "On Effective Delayed Neutron Fraction Calculations with Iterated Fission Probability," *J. Nucl. Sci. Technol.*, **48**. 1168 (2011).

32. R. Perez-Belles, J. D. Kington and G. de Saussure, "A Measurement of the Effective Delayed Neutron Fraction for the Bulk Shielding Reactor-I," *Nucl. Sci. Eng.*, **12**, 505 (1962).

33. S. G. Carpenter, J. M Gasidlo and J. M. Stevenson, "Measurements of the Effective Delayed-Neutron Fraction in Two Fast Critical Experiments," *Nucl. Sci. Eng.*, **49**, 236 (1972).

34. R. P. Feynman, F. de Hoffmann and R. Serber, "Dispersion of the Neutron Emission in U-235 Fission," *J. Nucl. Energy*, **3**, 64 (1956).

35. D. B. McCulloch, "An Absolute Measurement of the Effective Delayed Neutron Fraction in the Fast Reactor ZEPHYR," AERE-R/M-176, Atomic Energy Resarch Establishment (1958).

36. J. T. Mihalczo, "New Method for Measurement of the Effective Fraction of Delayed Neutron from Fission," *Nucl. Sci. Eng.*, **46**, 147 (1971).

37. J. T. Mihalczo, "The Effective Delayed Neutron Fraction from Fission in an Unreflected Uranium Sphere from Time Correlation Measurements with Clifornium-252," *Nucl. Sci. Eng.*, **60**, 262 (1976).

38. E. F. Bennett, "An Experimental Method for Reactor-Noise Measurements of Effective Beta," ANL-81-72, Argonne National Laboratory (1981).

39. Y. Yamane, Y. Takemoto and T. Imai, "Effective Delayed Neutron Fraction Measurements in FCA-XIX Cores by using Modified Bennett Method," *Prog. Nucl. Energy*, **35**, 183 (1999).

40. K. Hashimoto, H. Ohsaki, T. Horiguchi, Y. Yamane and S. Shiroya, "Variance-to-Mean Method Generalized by Linear Difference Filter Techniquie," *Ann. Nucl. Energy*, **25**, 639 (1998).

41. G. D. Spriggs, "Two Rossi-α Techniques for Measuring the Effective Delayed Neutron Fraction," *Nucl. Sci. Eng.*, **113**, 161 (1993).

CHAPTER 2

1. C. Rubbia, J. A. Rubio, S. Buono, F. Carminati, N. Fiétier, J. Galvez, C. Gelès, Y. Kadi, R. Klapisch, P. Mandrillon, J. P. Revol and Ch. Roche, "A Conceptual Design of a Fast Neutron Operated High Power Energy Amplifier," CERN/AT95-44 ET, Switzerland (1995).

2. F. Carminati, P. Kapish, J. Revol, Ch. Roche, J. A. Rubio and C. Rubbia, "An Energy Amplifier for Cleaner and Inexhaustible Nuclear Energy Production Driven by a Particle

Beam Accelerator," CERN-AT-93-47-ET, Switzerland (1993).

3. A. Gandini and M. Salvatores, "The Physics of Subcritical Multiplying System," *J. Nucl. Sci. Technol.*, **39**, 673 (2002).
4. R. Soule, W. Assal, P. Chaussonnet, C. Detouches, C. Domergue, C. Jammes, J. M. Laurens, J. F. Lebrat, F. Mellier, G. Perret, G. Rimpault, H. Servière, G. Imel, G. M. Thomas, D. Villamarin, E. Gonzalez-Romero, M. Plaschy, R. Chawla, J. L. Kloosterman, Y. Rugama, A. Billebaud, R. Brissot, D. Heuer, M. Kerveno,C. Le Brun, E. Liatard, J.M. Loiseaux, O. Méplan, E. Merle, F. Perdu, J. Vollaire, P. Baeten, "Neutronic Studies in Support of Accelerator-Driven Systems: The MUSE Experiments in the MASURCA Facility," *Nucl. Sci. Eng.*, **148**, 124 (2004).
5. M. Plaschyet, C. Destouches, G. Rimpault and R. Chawla, "Investigation of ADS-Type Heterogeneities in the MUSE4 Critical Configuration," *J. Nucl. Sci. Technol.*, **42**, 779 (2005).
6. K. Nishihara, K. Iwanaga, K. Tsujimoto, Y. Kurata, H. Oigawa and T. Iwasaki, "Neutronics Design of Accelerator-Driven System for Power Flattening and Beam Current Reduction," *J. Nucl. Sci. Technol.*, **45**, 812 (2008).
7. C. H. Pyeon, M. Hervalt, T. Misawa, H. Unesaki, T. Iwasaki and S. Shiroya., "Static and Kinetic Experiments on Accelerator-Driven System with 14 MeV Neutrons in Kyoto University Critical Assembly," *J. Nucl. Sci. Technol.*, **45**, 1171 (2008).
8. C. H. Pyeon, M. Hervault, T. Misawa, H. Unesaki, T. Iwasaki and S. Shiroya, "First Injection of Spallation Neutrons Generated by High-Energy Protons into the Kyoto University Critical Assembly," *J. Nucl. Sci. Technol.*, **46**, 1091 (2009).
9. C. H. Pyeon, J. Y. Lim, U. Takemoto, T. Yagi, T. Azuma, H. Kim, U. Takahashi, T. Misawa and S. Shiroya, "Preliminary Study on the Thorium-Loaded Accelerator-Driven System with 100 MeV Protons at the Kyoto University Critical Assembly," *Ann. Nucl.*

Energy, **38**, 2298 (2011).

10. J. Y. Lim, C. H. Pyeon, T. Yagi and T. Misawa, "Subcritical Multiplication Parameters of the Accelerator-Driven System with 100 MeV Protons at the Kyoto University Critical Assembly," *Sci. Technol. Nucl. Install.*, **2012**, 395878 (2012).
11. H. Shahbunder, C. H. Pyeon, T. Misawa and S. Shiroya, "Experimental Analysis for Neutron Multiplication by using Reaction Rate Distribution in Accelerator-Driven System," *Ann. Nucl. Energy*, **37**, 592 (2010).
12. C. H. Pyeon, K. Sukawa, Y. Yamaguchi and T. Misawa, "Mockup Experiments on the Thorium-Loaded Accelerator-Driven System at the Kyoto University Critical Assembly," *Nucl. Sci. Eng.*, **177**, 156 (2014).
13. C. H. Pyeon, H. Shiga, K. Abe, H. Yashima, T. Nishio, T. Misawa, T. Iwasaki and S. Shiroya, "Reaction Rate Analysis of Nuclear Spallation Reactions Generated by 150, 190 and 235 MeV protons," *J. Nucl. Sci. Technol.*, **47**, 1090 (2010).
14. T. Yagi, T. Misawa, C. H. Pyeon and S. Shiroya, "A Small High Sensitivity Neutron Detector using a Wavelength Shifting Fiber," *Appl. Radiat. Isot.*, **69**, 176 (2011).
15. T. Misawa, T. Shiroya and S. Kanda, "Measurement of Prompt Decay Constant and Subcriticality by the Feynman-α Method," *Nucl. Sci. Eng.*, **104**, 53 (1990).
16. T. Misawa, T. Yagi and C. H. Pyeon, "Measurement of Subcriticality Using Delayed Neutron Source Combined with Pulsed Neutron Accelerator," *Proc. Int. Topl. Mtg. Physics of Reactors (PHYSOR 2014)*, Kyoto, Japan, Sep. 28-Oct. 3, 2014.
17. J. S. Hendricks, G. W. McKinney, L. S. Waters, T. L. Roberts, H. W. Egdorf, J. P. Finch, H. R. Trellue, E. J. Pitcher, D. R. Mayo, M. T. Swinhoe, S. J. Tobin, J. W. Durkee, F. X. Gallmeier, J. C. David, W. B. Hamilton and J. Lebenhaft, "MCNPX User's Manual, version 2.5.0.," LA-UR-05-2675, Los Alamos National Laboratory (2005).
18. M. B. Chadwick, P. Obložinský, M. Herman, N. M. Greene, R. D. McKnight, D. L. Smith,

P. G. Young, R. E. MacFarlane, G. M. Hale, S. C. Frankle, A. C. Kahler, T. Kawano, R. C. Little, D. G. Madland, P. Moller, R. D. Mosteller, P. R. Page, P. Talou, H. Trellue, M. C. White, W. B. Wilson, R. Arcilla, C. L. Dunford, S. F. Mughabghab, B. Pritychenko, D. Rochman, A. A. Sonzogni, C. R. Lubitz, T. H. Trumbull, J. P. Weinman, D. A. Brown, D. E. Cullen, D. P. Heinrichs, D. P. McNabb, H. Derrien, M. E. Dunn, N. M. Larson, L. C. Leal, A. D. Carlson, R. C. Block, J. B. Briggs, E. T. Cheng, H. C. Huria, M. L. Zerkle, K. S. Kozier, A. Courcelle, V. Pronyaev and S.C. van der Marck, "ENDF/B-VII.0: Next Generation Evaluated Nuclear Data Library for Nuclear Science and Technology," *Nucl. Data Sheets*, **107**, 2931 (2006).

19. K. Kobayashi, T. Iguchi, S. Iwasaki, T. Aoyama, S. Shimakawa, Y. Ikeda, N. Odano, K. Sakurai, K. Shibata, T. Nakagawa and M. Nakazawa, "JENDL Dosimetry File 99 (JENDL/D-99)," JAERI 1344, Japan Atomic Energy Agency, Japan (2002).
20. H. Takada, K. Kosako and T. Fukahori, "Validation of JENDL High-Energy File through Analyses of Spallation Experiments at Incident Proton Energies from 0.5 to 2.83 GeV," *J. Nucl. Sci. Technol.*, **46**, 589 (2009).
21. T. Gozani, "A Modified Procedure for the Evaluation of Pulsed Source Experiments in Subcritical Reacotors," *Nukleonik*, **4**, 348 (1962)
22. M. M. Bretscher, "Perturbation independent methods for calculating research reactor kinetic parameters," ANL/RERTR/TM30, Argonne National Laboratory (1997).

CHAPTER 3

1. G. R. Keepin, *Physics of Nuclear Kinetics*, AddisonWesley, Reading, Massachusetts (1965).

2. J. T. Mihalczo and V. K. Pare, “Theory of Correlation Measurement in Time and Frequency domains with ^{252}Cf,” *Ann. Nucl. Energy*, **2**, 97 (1975).

3. T. Sakurai, S. Okajima, M. Andoh and T. Osugi, “Experimental cores of Benchmark Experiments on Effective Delayed Neutron Fraction β_{eff} at FCA,” *Prog. Nucl. Energy*, **35**, 131 (1999).

4. V. A. Doulin, G. M. Mikhailov, A. L. Kotchetkov, I. P. Matveenko and S. P. Belov, “The β_{eff} Measurement Results on FCA-XIX Cores,” *Prog. Nucl. Energy*, **35**, 163 (1999).

5. G. D. Spriggs, T. Sakurai and S. Okajima, “Rossi-α Measurements in a Fast Critical Assembly,” *Prog. Nucl. Energy*, **35**, 169 (1999).

6. Y. Yamane, Y. Takemoto, T. Imai, S. Okajima and T. Sakurai, “Effective Delayed Neutron Fraction Measurements in FCA-XIX Cores by Using Modified Bennet Method,” *Prog. Nucl. Energy*, **35**, 183 (1999).

7. T. Sakurai and S. Okajima, “Measurement of Effective Delayed Neutron Fraction β_{eff} by ^{252}Cf Source Method for Benchmark Experiment of β_{eff} at FCA,” *Prog. Nucl. Energy*, **35**, 195 (1999).

8. T. Sakurai, H. Sodeyama and S. Okajima, “Measurement of Effective Delayed Neutron Fraction β_{eff} by Covariance-to-Mean Method for Benchmark Experiment of β_{eff} at FCA,” *Prog. Nucl. Energy*, **35**, 195 (1999).

9. T. Sakurai and S. Okajima, “Analysis of Benchmark Experiment of Effective Delayed Neutron Fraction β_{eff} at FCA,” *Prog. Nucl. Energy*, **35**, 209 (1999).

10 G. D. Spriggs, “A Measurement of the Effective Delayed Neutron Fraction of the Westinghouse Idaho Nuclear Company Slab Tank Assembly Using Rossi-α Techniques,” *Nucl. Sci. Eng.*, **115**, 76 (1993).

11 G. D. Spriggs, “Two Rossi-α Techniques for Measuring the Effective Delayed Neutron Fraction,” *Nucl. Sci. Eng.*, **113**, 161 (1993).

12 J. D. Orndoff, “Prompt Neutron Periods of Metal Critical Assemblies,” *Nucl. Sci. Eng.*, **2**, 450 (1957).

13. Y. Kitamura, I. Pázsit, J. Wright, A. Yamamoto and Y. Yamane, “Calculation of the Pulsed Feynman- and Rossi-Alpha Formulae with Delayed Neutrons,” *Ann. Nucl. Energy.*, **32**, 671 (2005).

14. T. Gozani, “A Modified Procedure for the Evaluation of Pulsed Source Experiments in Subcritical Reactors,” *Nukleonik*. **4**, 348 (1962).

15. S. B. Degweker and Y. S. Rana, “Reactor Noise in Accelerator Driven Systems – II,” *Ann. Nucl. Energy.*, **34**, 463 (2007).

16. J. B. Lagrange, T. Planche, E. Yamakawa, T. Uesugi, Y. Ishi, Y. Kuriyama, B. Qin, K. Okabe and Y. Mori, “Straight Scaling FFAG Beam Line,” *Nucl. Instrum. Methods A*, **691**, 55 (2013).

17. E. Yamakawa, T. Uesugi, J. B. Lagrange, Y. Kuriyama, Y.Ishi and Y. Mori “Serpentine Acceleration in Zero-Chromatic FFAG Accelerators,” *Nucl. Instrum. Methods A*, **716**, 46 (2013).

18. T. Yagi, T. Misawa, C. H. Pyeon and S. Shiroya, “A Small High Sensitivity Neutron Detector Using a Wavelength Shifting Fiber,” *Appl. Radiat. Isot.*, **69**, 176 (2011).

19. H. Takada, K. Kosako and T. Fukahori, “Validation of JENDL High-Energy File through Analyses of Spallation Experiments at Incident Proton Energies from 0.5 to 2.83 GeV,” *J. Nucl. Sci. Technol.*, **46**, 589 (2009).

20. J. T. Goorley, M. R. James, T. E. Booth, F. B. Brown, J. S. Bull, L. J. Cox, J. W. Durkee, J. S. Elson and M. L. Fensin, R. A. Forster, J. S. Hendricks, H. G. Hughes, R. C. Jonhs, B. C. Kiedrowski, R. L. Martz, S. G. Mashnik, G. W. McKinney, D. B. Pelowitz, R. E. Prael, J. E. Sweezy, L. S. Warters, T. Wlicox and A. J. Zukaitis, “Initial MCNP6 Release Overview - MCNP6 Version 1.0,” Los Alamos National Laboratory, LA-UR-13-22934

(2013).

21.K. Okumura, T. Kugo, K. Kaneko and K. Tsuchihashi, “SRAC2006: A Comprehensive Nuetronics Calculation Code System,” JAEA-DATA/Code 2007-004, Japan Atomic Energy Agency, Japan (2007).

22. K. Shibata, O. Iwamoto, T. Nakagawa, N. Iwamoto, A. Ichihara, S. Kunieda, S. Chiba, N. Otuka and J. Katakura, “JENDL-4.0: A New Library for Nuclear Science and Technology,” *J. Nucl. Sci. Technol.*, **48**, 1 (2011).

23. G. Chiba, Y. Nagaya and T. Mori, “On Effective Delayed Neutron Fraction Calculations with Iterated Fission Probability,” *J. Nucl. Sci. Technol.*, **48**, 1163 (2011).

CHAPTER 4

1. Y. Nauchi and T. Kameyama, “Proposal of Direct Calculation of Kinetic Parameters β_{eff} and Λ Based on Continuous Energy Monte Carlo Method,” *J. Nucl. Sci. Technol.*, **42**, 503 (2005).

2. R. K. Meulekamp and S. C. van der Marck, “Calculating the Effective Delayed Neutron Fraction with Monte Carlo,” *Nucl. Sci. Eng.*, **152**, 142 (2006).

3. Y. Nagaya, G. Chiba, T. Mori, D. Irwanto and K. Nakajima, “Comparison of Monte Carlo Calculation Method for Effective Delayed Neutron Fraction,” *Ann. Nucl. Energy*, **37**, 1308 (2010).

4. Y. Nauchi, and T. Kameyama, “Development of Calculation Technique for Iterated Fission Probability and Reactor Kinetic Parameters using Continuous-Energy Monte Carlo Method,” *J. Nucl. Sci. Technol.*, **47**, 977 (2010).

5. G. Chiba, Y. Nagaya and T. Mori, “On Effective Delayed Neutron Fraction Calculations

with Iterated Fission Probability," *J. Nucl. Sci. Technol.*, **48**, 1163 (2011).

6. M. M. Bretsher, "Perturbation Independent Methods for Calculating Research Reactor Kinetic Parameters," ANL/RERTR/TM30, Argonne National Laboratory (1997).
7. G. Chiba, "Calculation of Effective Delayed Neutron Fraction using a Modified k-Ratio Method," *J. Nucl. Sci. Technol.*, **46**, 399 (2009).
8. Z. Zhong, A. Talamo and Y. Gohar. "Monte Carlo and Deterministic Computational Methods for the Calculation of the Effective Delayed Neutron Fraction," *Computer Phys. Com.*, **184**, 1660 (2013).
9. C. Berglöf, M. Fernández-Ordóñez, D. Villamarín, V. Bécares, E. M. González-Romero, V. Bournos, I. Serafimovich, S. Mazanik, Y. Fokov. "Spatial and Source Multiplication Effects on the Area Ratio Reactivity Determination Method in a Strongly Heterogeneous Subcritical System," *Nucl. Sci. Eng.*, **166**, 134 (2010).
10. C. Jammes, B. Geslot, R. Rosa, G. Imei and P. Fougeras, "Comparison of Reactivity Estimations Obtained from Rod-Drop and Pulsed Neutron Source Experiments," *Ann. Nucl. Energy*, **32**, 1131 (2005).
11. P. Ravetto, M. M. Rostagno, G. Bianchini, M. Carta and A. D'Angelo, "Application of the Multipoint Method to the Kinetics of Accelerator-Driven Systems," *Nucl. Sci. Eng.*, **148**, 79 (2004).
12. A. Gandini, "ADS Subcriticality Evaluation based on the Generalized Reactivity Concept," *Ann. Nucl. Energy*, **31**, 813 (2004).
13. A. Gandini, "The Physics of Subcritical Multiplying Systems," *J. Nucl. Sci. Technol.*, **39**, 673 (2002).
14. K. Okumura, T. Kugo, K. Kaneko and K. Tsuchihashi, "SRAC2006: A Comprehensive Nuetronics Calculation Code System," JAEA-DATA/Code 2007-004, Japan Atomic Energy Agency, Japan (2007).

15. J. T. Goorley, M. R. James, T. E. Booth, F. B. Brown, J. S. Bull, L. J. Cox, J. W. Durkee, J. S. Elson and M. L. Fensin, R. A. Forster, J. S. Hendricks, H. G. Hughes, R. C. Jonhs, B. C. Kiedrowski, R. L. Martz, S. G. Mashnik, G. W. McKinney, D. B. Pelowitz, R. E. Prael, J. E. Sweezy, L. S. Warters, T. Wlicox and A. J. Zukaitis, "Initial MCNP6 Release Overview - MCNP6 Version 1.0," Los Alamos National Laboratory, LA-UR-13-22934 (2013).
16. K. Shibata, O. Iwamoto, T. Nakagawa, N. Iwamoto, A. Ichihara, S. Kunieda, S. Chiba, N. Otuka and J. Katakura, "JENDL-4.0: A New Library for Nuclear Science and Technology," *J. Nucl. Sci. Technol.*, **48**, 1 (2011).
17. T. Gozaini, "A Modified Procedure for the Evaluation of Pulsed Source Experiments in Subcritical Reactors," *Nukleonik*, **4**, 348 (1962).
18. T. Yagi, T. Misawa, C. H. Pyeon and S. Shiroya, "A Small High Sensitivity Neutron Detector using a Wavelength Shifting Fiber," *Appl. Radiat. Isot.*, **69**, 176 (2011).
19. J. S. Hendricks, G. W. McKinney, L. S. Waters, T. L. Roberts, H. W. Egdorf, J. P. Finch, H. R. Trellue, E. J. Pitcher, D. R. Mayo, M. T. Swinhoe, S. J. Tobin, J. W. Durkee, F. X. Gallmeier, J. C. David, W. B. Hamilton and J. Lebenhaft, "MCNPX User's Manual, version 2.5.0.," LA-UR-05-2675, Los Alamos National Laboratory (2005).
20. M. B. Chadwick, P. Obložinský, M. Herman, N. M. Greene, R. D. McKnight, D. L. Smith, P. G. Young, R. E. MacFarlane, G. M. Hale, S. C. Frankle, A. C. Kahler, T. Kawano, R. C. Little, D. G. Madland, P. Moller, R. D. Mosteller, P. R. Page, P. Talou, H. Trellue, M. C. White, W. B. Wilson, R. Arcilla, C. L. Dunford, S. F. Mughabghab, B. Pritychenko, D. Rochman, A. A. Sonzogni, C. R. Lubitz, T. H. Trumbull, J. P. Weinman, D. A. Brown, D. E. Cullen, D. P. Heinrichs, D. P. McNabb, H. Derrien, M. E. Dunn, N. M. Larson, L. C. Leal, A. D. Carlson, R. C. Block, J. B. Briggs, E. T. Cheng, H. C. Huria, M. L. Zerkle, K. S. Kozier, A. Courcelle, V. Pronyaev and S.C. van der Marck, "ENDF/B-VII.0: Next

Generation Evaluated Nuclear Data Library for Nuclear Science and Technology," *Nucl. Data Sheets*, **107**, 2931 (2006).

21. H. Takada, K. Kosako and T. Fukahori, "Validation of JENDL High-Energy File through Analyses of Spallation Experiments at Incident Proton Energies from 0.5 to 2.83 GeV," *J. Nucl. Sci. Technol.*, **46**, 589 (2009).

ACKNOWLEDGMENTS

The author would like to express his special gratitude to Professor Tsuyoshi Misawa of Kyoto University for his guidance of this research, and the encouragement and many valuable suggestions given in the course of the present research. This thesis would not have been possible without his instructions.

The author is deeply indebted to Associate Professor Cheol Ho Pyeon of Kyoto University for his generous help and guidance in the whole course of the present study and his many invaluable suggestions and discussions.

The author expresses his gratitude to Professor Hironobu Unesaki of Kyoto University for his continuous discussions and helpful suggestions in the present study.

The author expresses his gratitude to Assistant Professor Yasunori Kitamura of Kyoto University for his continuous discussions and helpful suggestions in the present study.

The author would like to thank Assistant Professors Hiroshi Shiga and Yoshiyuki Takahashi for their discussion of this study and for support throughout the experiments in this study.

The author would like to extend his gratitude and appreciation to Associate Professors Go Chiba and Willem Frederik Geert van Rooijen and Assistant Professor Tomohiro Endo. The author would like to express his thanks for being supports in his journey toward attaining a doctorate and in developing as a professional.

The author would feel a deep sense of gratitude for the scholarship assistant by the Japan Electric Association in daily life and for support by Chubu Electric Power Co., Inc. in his study.

Finally, the author would like to be grateful to all the staff at KUCA and the FFAG

accelerator for their assistance during the experiments.

LIST OF PUBLICATION

Journal

[1] **M. Yamanaka**, C. H. Pyeon, T. Yagi and T. Misawa, "Accuracy of Reactor Physics Parameters in Thorium-Loaded Accelerator-Driven System Experiments at Kyoto University Critical Assembly," *Nucl. Sci. Eng.*, **183**, 96-106 (2016).

[2] **M. Yamanaka**, C. H. Pyeon and T. Misawa, "Monte Carlo Approach of Effective Delayed Neutron Fraction by k-ratio Method with External Neutron Source, "*Nucl. Sci. Eng.*, **184**, 551-560 (2016).

[3] **M. Yamanaka**, C. H. Pyeon, S. H. Kim, Y. Kitamura, H. Shiga and T. Misawa, "Effective Delayed Neutron Fraction in Accelerator-Driven System Experiments with 100 MeV Protons at Kyoto University Critical Assembly," *J. Nucl. Sci. Technol.*, **54**, 293-300 (2017).

[4] C. H. Pyeon, H. Nakano, **M. Yamanaka**, T. Yagi and T. Misawa, "Neutron Characteristics of Solid Targets in Accelerator-Driven System with 100 MeV Protons at Kyoto University Critical Assembly," *Nucl. Technol*., **192**, 181-190 (2015).

[5] S. H. Kim, **M. Yamanaka**, M. H. Woo, J. Y Lee, C. H. Shin and C. H. Pyeon, "A Bach Size Selection Strategy by Checking Stability of Fission Source Distribution for Monte Carlo Eigenvalue Calculations," *J. Nucl. Sci. Technol.*, **54**, 301-311 (2017).

International Conferences

[1] **M. Yamanaka**, C. H. Pyeon, T. Yagi and T. Misawa, "Accuracy of Thorium-Loaded Accelerator-Driven System at Kyoto University Critical Assembly," *Proc. Int. Topl. Mtg.*

Physics of Reactors (PHYSOR2014), Kyoto, Japan, Sep. 28-Oct. 3, on CD-ROM, (2014). Atomic Energy Society of Japan.

[2] C. H. Pyeon, H. Nakano, **M. Yamanaka**, T. Yagi and T. Misawa, "Neutronic Characteristics of Solid Pb-Bi Target in Accelerator-Driven System at Kyoto University Critical Assembly, " Proc. Int. Topl. Mtg. Physics of Reactors (PHYSOR2014), Kyoto, Japan, Sep. 28-Oct. 3, (2014). Atomic Energy Society of Japan.

[3] C. H. Pyeon, **M. Yamanaka** and Y. Takahashi, "Experimental Benchmarks on Subcriticality of Accelerator-Driven System with 100 MeV Protons at Kyoto University Critical Assembly," Proc. Int. Conf. on the physics of Reactors, Unifying Theory and Experiments in the 21st Century (PHYSOR2016), Sun Valley, Idaho, May 1-5, (2016). American Nuclear Society.

Oral presentations

[1] **M. Yamanaka**, C. H. Pyeon, T. Yagi and T. Misawa, "Study on Neutronic Characteristics of Thorium-Loaded Accelerator-Driven System," *Proc. Fall Mtg. of the Atomic Energy Society of Japan*, Hachinohe, Japan, Sep. 3-5, **J32** (2013).

[2] **M. Yamanaka**, C. H. Pyeon, T. Yagi and T. Misawa, "Study on Effective Delayed Neutron Fraction in Subcriticality Measurements," *Proc. Annu. Mtg. of the Atomic Energy Society of Japan*, Tokyo, Japan, Mar. 26-28, **O04** (2014).

[3] **M. Yamanaka**, C. H. Pyeon, T. Yagi and T. Misawa, "Study on Effective Delayed Neutron Fraction in Subcriticality Measurements (2)," *Proc. Fall Mtg. of the Atomic Energy Society of Japan, Kyoto*, Japan, Sep. 8-10, **N50** (2014).

[4] **M. Yamanaka**, T. Misawa, Y. Kitamura and C. H. Pyeon, "Effective Delayed Neutron Fraction in Subcritical System with External Neutron Source," *Proc. Fall Mtg. of the Atomic Energy Society of Japan, Shizuoka*, Japan, Sep. 9-11, **A32** (2015).

[5] **M. Yamanaka**, C. H. Pyeon, Y. Kitamura and T. Misawa, “Measurements of Effective Delayed Neutron Fraction with External Neutron Source at Kyoto University Critical Assembly,” *Proc. Reactor Physics Asia Conf.* (RPHA15), Jeju, Korea, Sep. 16-18, (2015). Korean Nuclear Society.